TECHNISCHE UNIVERSITÄT WIEN

DISSERTATION

On excited states for defects in solids using coupled cluster theories.

zur Erlangung des akademischen Grades

Doktor der technischen Wissenschaften

eingereicht von

Alejandro Agustí Martínez-Soria Gallo
Matrikelnummer 11741651

ausgeführt am Institut für Theoretische Physik
der Fakultät für Physik der Technischen Universität Wien

Betreuer: Univ.-Prof. Dr. Andreas Grüneis

Wien, _____ _____
(Unterschrift Verfasser/in) (Unterschrift Betreuer/in)

Eidesstattliche Erklärung

Hiermit erkläre ich, dass ich diese Arbeit selbständig verfasst habe, dass ich die verwendeten Quellen und Hilfsmittel vollständig angegeben habe und dass ich die Stellen der Arbeit – einschließlich Tabellen, Karten und Abbildungen – die anderen Werken oder dem Internet im Wortlaut oder dem Sinn nach entnommen sind, auf jeden Fall unter Angabe der Quelle als Entlehnung kenntlich gemacht habe.

Unterschrift:

Datum:

Ort:

Acronyms

CC4S Coupled Cluster For Solids. 76

CTF Cyclops Tensor Framework. 76

BSE Bethe-Salpeter equation. 72, 74, 88, 90

BSIE basis set incompleteness error. 7, 9, 60, 62–64, 66–69, 96, 97, 99–105, 107, 109–111, 113

CBS complete basis set. 62–64, 97, 99

CC Coupled Cluster. 40, 48, 49, 58, 73

CCSD coupled cluster with singles and doubles excitations. 4–6, 46, 49–51, 57–63, 68, 73, 97–99, 101, 102, 107, 109, 110

CCSD(T) perturbative triple excitations. 49, 51, 59, 73, 110, 111

CCSDT coupled cluster with singles, doubles and triples excitations. 49, 58

CI Configuration Interaction. 40, 47, 48, 50

CISD Configuration interaction Singles and Doubles. 35

DFT Density Functional Theory. 30, 31, 72, 76, 113

EA-EOM-CC Electron Attachment Equation of motion Coupled Cluster (EOM-CC). 73

EE-EOM-CC Electron Excitation EOM-CC. 73

EE-EOM-CCSD Equation of motion coupled cluster with singles and doubles excitations (CCSD). 5, 6, 8, 74–84, 86–90, 92

EOM Equation Of Motion. 45, 46, 48, 73

EOM-CC Equation of motion Coupled Cluster. 3, 4, 47, 48, 73

FCI Full Configuration Interaction. 47

FNO frozen natural orbital. 60, 101, 102, 104, 105, 107, 109–111, 113

HF Hartree-Fock. 5, 6, 27, 30, 34, 39, 46, 51, 53, 63, 75–78, 80, 82, 83, 95, 109, 110

IP-EOM-CC Ionization Potential EOM-CC. 73

MP Møller-Plesset. 4, 38, 49

MP2 second-order Møller-Plesset perturbation theory. 7, 38, 43, 49, 56–61, 66, 69, 96, 100, 102–104, 107, 109, 110

MP3 third-order Møller-Plesset (MP). 49, 68

MP4 fourth-order MP. 49

PAW projector augmented wave. 53

ppl Particle-Particle Ladder. 7, 58, 59, 63, 66–69, 96, 97, 99, 102–105, 109

RPA Random Phase Approximation. 46, 58, 59

TD-DFT Time-Dependent Density Functional Theory. 72, 92

UCCSD Unrestricted CCSD. 6, 76, 86, 87

UEG uniform electron gas. 9, 59, 60, 95, 96

VCC Variational Coupled Cluster. 41

List of Figures

List of Tables

Contents

Part I

Prolog

Chapter 1

English abstract

The study of the electronic structure for solid state systems is central for understanding novel physical phenomena of interacting systems and for unlocking future material properties. The road to the qualitative and quantitative understanding of these condensed matter systems is however not without its challenges. Interacting electrons imply a steep combinatorial scaling of the solution space, thus requiring the need of exponentially increasing computational resources for the *exact* resolution of the behavior of interacting electrons. In this context, Density Functional Theory (DFT) remains the most successful practical method offering a delicate balance between computational resources and accuracy of the results for systems up to several thousands of atoms. The achievements of DFT notwithstanding, it fails to deliver consistently accurate outcomes for some physical properties in simple systems. Truncated coupled cluster theory seeks to offer systematically accurate ground-state energies at a moderate computational cost for weakly-correlated systems composed of some tens of atoms.

Defects in solids present an attractive breeding ground for testing electronic structure theories due to their resemblance to a molecule embedded in an effective crystal field. Additionally, properties of extended systems are highly influenced by both the type and concentration of defects embedded within them. This dependence of bulk material properties on the defect electronic structure is also given by the dynamics and spectrum of the electronic excited state manifold of the defects. Therefore, a robust and accurate methodol-

ogy perform both ground-state and excited-state calculations of the electrons in solid-state defects is of paramount importance for both practical applications and theoretical development.

In this thesis, we implement, develop and apply coupled cluster based methodologies to calculate the ground state and excited states of defects embedded in solids. These excited states are based on the Equation Of Motion Coupled Cluster (EOM-CC) corpus of theories. Our implementation of EOM-CC theory is applied to study F-centers in alkaline earth oxides employing a periodic supercell approach with plane wave basis set and the Projector Augmented Wave (PAW) theory.

The second part of this thesis deals with a different challenge, namely the basis set problem. All wavefunctions inherit from the Coulomb interaction sharp features at coalescence points, these features are called cusps. In order to resolve these cusps, one needs to devote effort both in treating many body correlation and refining the basis set employed in the many body correlation. In this domain, we present a basis set correction scheme for the coupled cluster singles and doubles (CCSD) method. We test this approach on the Uniform Electron Gas (UEG) and on a series of molecular systems where we show the effectiveness of the scheme.

Chapter 2

Deutsche Zusammenfassung

Die Untersuchung der elektronischen Struktur von Festkörpersystemen ist von zentraler Bedeutung für das Verständnis neuartiger physikalischer Phänomene von wechselwirkenden Systemen und für die Erschließung künftiger Materialeigenschaften. Der Weg zum qualitativen und quantitativen Verständnis dieser Systeme aus kondensierter Materie ist jedoch nicht frei von Herausforderungen. Wechselwirkende Elektronen implizieren eine steile kombinatorische Skalierung des Lösungsraums und erfordern daher exponentiell steigende Rechenressourcen für die exakte Beschreibung des Verhaltens der wechselwirkenden Elektronen. In diesem Zusammenhang ist die Dichtefunktionaltheorie (DFT) nach wie vor die erfolgreichste praktische Methode, die ein Gleichgewicht zwischen Rechenaufwand und Genauigkeit der Ergebnisse für Systeme mit bis zu mehreren Tausend Atomen bietet. Ungeachtet der Errungenschaften der DFT liefert sie für einige physikalische Eigenschaften in einfachen Systemen keine gleichbleibend genauen Ergebnisse. Die sogenannte Coupled Cluster Theorie (CC) versucht, systematisch genauere Grundzustandsenergien zu moderaten Rechenkosten für schwach korrelierte Systeme zu liefern, die aus einigen Dutzend Atomen bestehen.

Defekte in Festkörpern sind nützlich für die Überprüfung elektronischen Strukturtheorien, da sie einem in ein effektives Kristallfeld eingebetteten Molekül ähneln. Darüber hinaus werden die Eigenschaften von ausgedehnten Systemen stark beeinflusst von der Art und Konzentration der in ihnen vorhandenen Defekte. Diese Abhängigkeit der Eigenschaften

von Festkörpern von der elektronischen Defektstruktur ist auch durch die Dynamik und das Spektrum der elektronischen angeregten Zustandsmannigfaltigkeit der Defekte gegeben. Daher ist eine robuste Methodik erforderlich, die akkurate Grundzustands- und Anregungszustandenergien der Elektronen in Festkörperdefekten liefert.

In dieser Arbeit implementieren, entwickeln und verwenden wir CC basierte Methoden zur Berechnung der Grundzustand- und angeregter Zustandsenergie von in Festkörpern eingebetteten Defekten. Die Berechnung dieser angeregten Zustände basiert auf der Equation Of Motion Coupled Cluster (EOM-CC) Theorie. Unsere Implementierung der EOM-CC-Theorie wird zur Untersuchung von F-Zentren in Erdalkalioxiden verwendet. Die Methode basisert auf einem periodischen Superzellenansatz mit Ebenenwellenbasisfunktionen in Kombination mit der Projector Augmented Wave (PAW) Methode.

Der zweite Teil der Arbeit befasst sich mit einer anderen Herausforderung, nämlich dem Basissatzkonvergenzproblem. Alle Wellenfunktionen erben von der Coulomb-Wechselwirkung einen Knick am Koaleszenzpunkt, diese Knicks werden Cusps genannt. Um diese Cusps aufzulösen muss man sich sowohl mit der Behandlung der Vielkörperkorrelation als auch mit der Verfeinerung des in dieser Korrelation verwendeten Basissatzes beschäftigen. In diesem Bereich, stellen wir ein Verfahren zur Korrektur des Basissatzes für die Coupled Cluster Singles and Doubles (CCSD) Methode vor. Wir testen diesen Ansatz an dem homogenen Elektronengas und an einer Reihe von molekularen Systemen, wo wir die Wirksamkeit des Schemas zeigen.

A mi madre *Lourdes*, y a mi padre *Luis*:

descansa, para no estorbar a la montaña
descansa, com pedra inert sense labor
descansa, com fa la terra sense por
descansa, y olvida, que no saluda ya el mañana

Part II

Theoretical introduction

In this section we will present some of the main methodologies used throughout the text and in the presented publications.

Although we try to make its presentation as self-contained as possible, a thorough theoretical introduction is outside the scope of this thesis and we refer to other complementary works like [173, 78, 125].

Chapter 3

Second quantization

3.1 One-body functions as orbitals

Most of this work is written in the language of second quantization. The algebra of the second quantization is based on the set of objects of one-body operators $\mathcal{F}_1 = \{\hat{c}_i \mid i \in I\}$, a map $\dagger : \mathcal{F} \to \mathcal{F}$ and a vacuum state $|\ \rangle$, where $\mathcal{F}$ is the many-body *Fock space* and $\dagger$ is the *dagger* super-operator [189]. Additionally, I is a suitable index set that defines the quantum mechanical representation of the particles in their one-body representation.
Every element in $\mathcal{F}_1$ represents the destruction of an electron, whereas $\mathcal{F}_1^\dagger = \{\hat{x}^\dagger \mid \hat{x} \in \mathcal{F}_1\}$ represents the creation of a particle. Note that formally $\hat{x}^\dagger$ is just a helpful notation for the function application $\dagger(\hat{x})$.
The size of the set $\mathcal{F}_1$ can be infinite, however in practice it is finite, i.e., it will be given by the size of the one-body functions that we are considering in each system. These one-body wave functions are commonly referred to as **orbitals**.
To motivate this rather abstract discussion we consider the following example. Let $\mathrm{SPD} = \{\varphi_{nlm} \mid n, l, m \in \mathbb{Z}\}$ be the set of orbitals that solve the Schrödinger equation for the Hydrogen atom.
Accordingly, in this case $I = \mathbb{Z}^3$ with the well-known n, l, m constraints and

$$\mathcal{F}_1 = \{\hat{c}_{nlm} \mid n, l, m \in \mathbb{Z}\}\,.$$

We can obtain the set of orbitals SPD from $\mathcal{F}_1$ by the following projection

$$\phi_{nlm}(\mathbf{r}) = \langle \mathbf{r} | \hat{c}^\dagger_{nlm} | \ \rangle .$$

Analogously one can define a basis of orbitals based on a plane wave representation or on a possibly discrete real-space representation.

3.2 Operator representation

We will use a notation for operators that is similar to the covariant and contravariant notation in the context of relativistic theories. This notation facilitates reading and writing of complicated expressions but bears not the same connotations as in said theories, since we do not concern ourselves with metric properties.
As it is often done in the literature, we define a notation akin to the *Einstein Notation*, for instance, the following operator definition

$$\begin{aligned}\hat{O} &= \sum_{a_1 \cdots a_u} \sum_{a_1 \cdots a_d} o^{a_1 \cdots a_u}_{a_1 \cdots a_d} \hat{c}^\dagger_{a_1} \cdots \hat{c}^\dagger_{a_u} \hat{c}_{a_1} \cdots \hat{c}_{a_d} \\ &= o^{a_1 \cdots a_u}_{a_1 \cdots a_d} \hat{c}^{a_1} \cdots \hat{c}^{a_u} \hat{c}_{a_1} \cdots \hat{c}_{a_d}\end{aligned}$$

showcases the main conventions that we are going to use throughout the text. We will sum over repeated indices and the indices belonging to creation operators will be placed in the super-index part of the tensor coefficient expression. Thus, in this last expression for $\hat{O}$ we have u creation operators and d annihilation operators, which are placed as super-index and sub-index respectively in the coefficient tensor name o and also in the one-body operators $\hat{c}$, i.e., $\hat{c}^k = \hat{c}^\dagger_k$.
Additionally, the concept of the n-bodyness of an operator is of relevance. A one-body wavefunction is represented by the Hilbert space vector

$$|p\rangle = \hat{c}^p | \ \rangle$$

where $| \ \rangle$ is the already mentioned vacuum state. An operator $\hat{O}_1$ having a one-body char-

acter can be defined as an operator for which there exist $|p\rangle$ and $|q\rangle$ for which $\langle p|\,\hat{O}_1\,|q\rangle \neq 0$. As it is readily seen, this definition depends highly on the choice of $|\ \rangle$ object. A one-body operator is one that only allows for such elements different from 0. Most one-body operators in this text will conserve the particle number operator $\hat{N}$ and will have the following form:

$$\hat{O}_1 = o_q^p \hat{c}^p \hat{c}_q.$$

This definition of one-body operators admits a simple generalization to n-body operators. Thus, $\hat{N}$ conserving two-body operators have the form

$$\hat{O}_2 = o_{rs}^{pq} \hat{c}^p \hat{c}^q \hat{c}_s \hat{c}_r$$

and an $\hat{N}$ conserving n-body operator is thus given by

$$\hat{O}_n = o_{s_1 \cdots s_n}^{p_1 \cdots p_n} \hat{c}^{p_1} \cdots \hat{c}^{p_n} \hat{c}_{s_n} \cdots \hat{c}_{s_1}.$$

Notice that this definition does discriminate between operators that might have mixed n-bodyness. Specifically, operators such as $\hat{c}^a$ or $\hat{c}^p \hat{c}_q + \hat{c}^p \hat{c}^q \hat{c}_s \hat{c}_r$ have a one-body and two-body character but are not purely one-body or two-body. Nevertheless, we are only interested in developing a sound working definition of this concept.

Chapter 4

The electronic many-body problem

The electronic many-body problem, as already stated in the introduction, consists in computing observables of a system of electrons. These observables might be the ground-state energy, photo-luminescence spectra, critical temperatures and a host of other properties. Of course a way of calculating these properties comes about by solving the many-electron Schrödinger equation, thus obtaining the wavefunction of the system. With this wavefunction, one can go about to calculate all physical observables. Methodologies that find approximations to the wavefuncion of the system directly are fittingly called *Wavefunction based methods*.

In the language that we have hitherto introduced, the electronic Hamiltonian can be written as

$$\hat{H} = h_q^p \hat{c}^p \hat{c}_q + \frac{1}{4} V_{rs}^{pq} \hat{c}^p \hat{c}^q \hat{c}_s \hat{c}_r \tag{4.1}$$

where the one-body operator coefficients h_q^p are given by the kinetic energy of the electrons and the electron-nucleus interaction coulombic potential. This is, in terms of the orbitals ψ_p and ψ_q we can write

$$h_q^p = -\frac{1}{2} \int^{\infty} \psi_p^{\dagger}(\mathbf{r}) \nabla^2 \psi_q(\mathbf{r}) \, \mathrm{d}\mathbf{r} - \sum_{I \in \mathrm{Ions}} \int^{\infty} \psi_p^{\dagger}(\mathbf{r}) \frac{Z_I}{|\mathbf{r} - \mathbf{R}_I|} \psi_q(\mathbf{r}) \, \mathrm{d}\mathbf{r}$$

where Ions is the set of ions of the system, $\mathbf{R}_I$ is the position of the I-th ion and Z_I its atomic charge. Throughout this work we employ atomic units ($m_e = \hbar = 1$) unless stated otherwise.

Furthermore, the electron-electron interaction V_{rs}^{pq} is given by

$$V_{rs}^{pq} = \int_0^\infty \int_0^\infty \psi_p^\dagger(\mathbf{r}_1)\,\psi_r(\mathbf{r}_1)\,\frac{1}{|\mathbf{r}_1 - \mathbf{r}_2|}\psi_q^\dagger(\mathbf{r}_2)\,\psi_s(\mathbf{r}_2)\,\mathrm{d}\mathbf{r}_2\mathrm{d}\mathbf{r}_1 \tag{4.2}$$

It is worth noting that whenever $q = r$ and $q = s$ then V_{pq}^{pq} represents the coulombic interaction of two charge densities ρ_p and ρ_q, i.e.,

$$V_{pq}^{pq} = \int_0^\infty \int_0^\infty \frac{|\rho_p(\mathbf{r_1})|^2\,|\rho_q(\mathbf{r_2})|^2}{|\mathbf{r}_1 - \mathbf{r}_2|}\mathrm{d}\mathbf{r}_2\mathrm{d}\mathbf{r}_1 \tag{4.3}$$

Chapter 5

Hartree-Fock approximation

One of the most straightforward approximations to solve the Schrödinger equation for the electronic wavefunction of the Hamiltonian (4.1) is the *Hartree-Fock* approximation.
It consists in finding the best approximation to the electronic wavefunction that can be represented by a single Slater determinant, oftentimes denoted as $|0\rangle$ [71, 72, 53, 54].
A single Slater determinant containing N electrons in the orbital basis $\{\hat{c}_a\}$ can be written like

$$|\Psi_{i_1\dots i_N}\rangle = \hat{c}^{i_1}\cdots\hat{c}^{i_N}\,|\;\rangle \tag{5.1}$$

where we have defined implicitly the Slater determinant $\Psi_{i_1\dots i_N}$ composed of N orbitals.
We can easily calculate the energy of a determinant making use of the zero-temperature and single-reference *Wick's theorem* [191, 131, 61]. In this context, the energy of $\Psi_{i_1\dots i_N}$ is given by computing the expectation value of (4.1), i.e.

$$E_{\Psi_{i_1\dots i_N}} = E^1_{\Psi_{i_1\dots i_N}} + E^2_{\Psi_{i_1\dots i_N}} = \langle\Psi_{i_1\dots i_N}|\,\hat{H}\,|\Psi_{i_1\dots i_N}\rangle \tag{5.2}$$

where the one-body part for the energy is given by

$$E^1_{\Psi_{i_1\dots i_N}} = \langle\;|\,\hat{c}_{i_N}\dots\hat{c}_{i_1}f^p_q\hat{c}^p\hat{c}_q\hat{c}^{i_1}\dots\hat{c}^{i_N}\,|\;\rangle \tag{5.3}$$

$$= \mathcal{C}\left\{\hat{c}_i,\hat{c}^p\right\}\mathcal{C}\left\{\hat{c}_q,\hat{c}^j\right\}\delta\left(i,j\in\{i_1\dots i_N\}\right)\delta_{ij}f^p_q \tag{5.4}$$

where the $\delta(\ldots)$ functions pose restrictions for the indices, in this case, that the i and j indices have to be one of the occupied electronic indices. Likewise, we have introduced implicitly the *Wick contraction* operator $\mathcal{C}\{a, b\}$ [191] which in this work is given by the difference between the product operator and its normal order, i.e.,

$$\mathcal{C}\left\{\hat{a}, \hat{b}\right\} = \langle\ |\, \hat{a}\hat{b} - \left\{\hat{a}\hat{b}\right\} |\ \rangle\,.$$

From now on we will consider our orbital basis $\left\{\hat{c}_p\right\}$ to be orthonormal. Thus, in this case one finds that

$$\mathcal{C}\left\{\hat{c}_p, \hat{c}^q\right\} = \delta_p^q$$

and all further combinations are zero.

It is customary to use different letters for different types of states. In this work we use the following index conventions for the operators $\hat{c}$ and their scalar tensors:

Table 5.1: Index conventions.

Indices	Interpretation
$p, q \ldots$	general indices
$a, b \ldots h$	virtual indices
$i, j \ldots o$	occupied indices

The HF equations are found applying a variational ansatz with respect to the system orbitals $\phi_p(\mathbf{r}) = \langle \mathbf{r}|\, \hat{c}^p\, |\ \rangle$, i.e., one takes the Lagrange function

$$\mathcal{L}[i_1 \ldots i_N] = \langle \Psi_{i_1 \ldots i_N}|\, \hat{H}\, |\Psi_{i_1 \ldots i_N}\rangle + \epsilon_{pq}\left(\langle p\,|q\rangle - \delta_{pq}\right)$$

where the last term represents the orthonormality conditions of the orbital set $\{\phi_p\}$. One thus obtains the extremal points by solving the *Euler-Lagrange* equations for this problem in terms of the orbitals ϕ_p.

The well-known resulting expressions are a set of coupled linear equations where the equations depend on the solutions to be constructed. Therefore, a self-consistent approach is mostly taken for solving the equations, where a starting guess for the equations is provided, and after solving the problem another set of equations from the solution is computed. The

process is continued until convergence of relevant quantities, for instance energy and electron density.

Chapter 6

Density functional theory

Arguably the most successful theoretical framework in materials science is the Density Functional Theory.

Thomas and shortly after Fermi devised a simple non-relativistic method to calculate atomic fields and atomic properties from a purely theoretical model [177, 51]. In order to calculate an approximation for the total potential in an atom they viewed the system of electrons as forming a homogeneous cloud surrounding it. Thus, each electron is governed by the simple Hamiltonian

$$\frac{1}{2}\mathbf{p}^2 - v_{\mathrm{TF}}$$

where v_{TF} is generated by a combination of the effective Hartree-like interaction of the electrons and the nuclear potential. Since they Pauli exclusion principle had been included in this framework, the energy of the system in this TF can be written in modern terms like

$$E_{\mathrm{TF}}[n] = \langle\Phi|\,\hat{T} + \hat{V}_{\mathrm{ne}} + \hat{V}_{\mathrm{H}}\,|\Phi\rangle$$

where using the functional derivative in terms of the electron density $\mathbf{r} \mapsto n(\mathbf{r})$ one can write

$$v_{\mathrm{TF}}(\mathbf{r}) = \frac{\delta}{\delta n(\mathbf{r})}\left(\hat{V}_{\mathrm{ne}} + \hat{V}_{\mathrm{H}}\right)[n]$$

It is worth noting explicitly that both the energy coming from both $\hat{V}_{\mathrm{ne}}$ and $\hat{V}_H$ is a direct

functional of the electron density $\mathbf{r} \mapsto n(\mathbf{r})$.

Some refinements were made throughout the years by including Fock exchange and electron-electron correlation [120, 42]. However, the most general result came by the help of a formal theorem about the general relationship of the exact ground state density of a *many-body* electron system and its Hamiltonian [85]:

1. The *ground-state density* determines the Hamiltonian up to an additive constant:

$$n_{\mathrm{G}} \longrightarrow \hat{H}, \qquad E[n] = \langle \Psi_{\mathrm{G}}[n] | \, \hat{H}[n] \, | \Psi_{\mathrm{G}}[n] \rangle$$

2. The minimization of $E[n]$ gives the exact ground-state energy E_{G} and density n_{G}.

Here

$$\hat{H} = \hat{T} + \hat{V}_{\mathrm{ne}} + \hat{V}_{\mathrm{H}} + \hat{V}_{\mathrm{xc}}$$

and $\hat{V}_{\mathrm{xc}}$ is known as the exchange-correlation operator. The existence of this operator is hinted indirectly by said theorem and provides the fermionic and coulombic electronic correlation to the system, in an exact fashion.

This theorem, albeit strikingly powerful, does not deliver a constructive algorithm to instantiate neither the energy functional $n \mapsto E[n]$ nor the complete operator functional $n \mapsto \hat{H}[n]$. In particular, $\hat{V}_{\mathrm{xc}}$ is not known or only known numerically in the simplest cases [130].

Kohn and Sham developed a practical scheme in order to render the formal Density Functional Theory (DFT) theory implementable in practical situations [104, 103]. The Kohn-Sham DFT theory uses a one-body equation for the orbitals not unlike the HF equations

$$\left(\frac{1}{2}\mathbf{p}^2 + v_{\mathrm{ne}} + v_{\mathrm{H}} + v_{\mathrm{xc}} \right) \phi_i = \epsilon_i \phi_i$$

where v_{xc} represents formally the suitable spatial representation of the operator V_{xc}, i.e.,

$$v_{\mathrm{xc}}(\mathbf{r}) = \frac{\delta V_{\mathrm{xc}}[n]}{\delta n(\mathbf{r})}.$$

In practice however, v_{xc} is approximated by a choice of functional form. Kohn-Sham DFT

is however not the only formulation or solving technique for the wider DFT landscape, but represents indeed the most successful and most promising tool for the routine calculation of properties of molecules and extended systems [118, 119, 153, 39, 105, 65, 142].

Chapter 7

Many-body methods

Considering a single Slater determinant as an approximation for the exact electronic wavefunction has severe shortcomings.

The most important limitation of a single-determinant is the fact that the inter-electron correlation is missing. Of course, due to the nature of Slater determinants, a certain kind of correlation is always present, namely the fermionic correlation. In other words, the probability of finding two electrons at the same point in space *with the same spin* is zero for any determinant.

In order to go beyond fermionic correlation, a direct approach entails including more and more determinants in the representation of the wavefunction. Exactly which determinants are included in the wavefunction is the subject of many-body wavefunction-based theories. Certainly, the problem becomes intractable very soon if one considers the sizes of the Hilbert spaces involved. Namely, let us consider that we have an orbital space of size M, i.e.,

$$\{\hat{c}_1, \ldots, \hat{c}_M\}$$

and considering N electrons, we can distribute N electrons over M orbitals in

$$\frac{M!}{(M-N)!N!}$$

which represents the size of the many-body electronic Hilbert space.

As a means of an illustrative example, let us consider the size of the Hilbert space in terabytes (TB) if we consider a modest quantity of virtual orbitals per occupied, for instance 10.

Table 7.1: Size of Hilbert space for some chosen number of electrons considering 10 virtual orbitals per occupied orbital.

N	M	Size of Hilbert Space (TB)
10	100	2.52e+02
20	200	2.35e+16

Table 7.1 is quite telling. For a modest number of electrons the memory required to store a single vector in the Hilbert space becomes so large that it does not fit a single supercomputing node at the time of this writing. However, for a given system not all the vectors in the Hilbert space are going to contribute in the energies or processes that one is interested in. Thus, one of the main goals of many-body electronic structure theory involves designing methods to sample the Hilbert space in a way that is efficient and accurate, without incurring in the cost of storing all the vectors in the Hilbert space.

Chapter 8

Configuration interaction

The most straightforward approach to solving the Schrödinger equation within a given basis would be fully diagonalizing the Hamilton operator $\hat{H}$.
The full N-electron Hilbert space can be generated by electron-number conserving excitation operators

$$\{\hat{\tau}_\mu\} = \left\{1,\ \hat{c}^a\hat{c}_i,\ \hat{c}^a\hat{c}^b\hat{c}_j\hat{c}_i,\ \hat{c}^a\hat{c}^b\hat{c}^c\hat{c}_k\hat{c}_j\hat{c}_i,\ \ldots\right\}$$

acting on the Hartree-Fock determinant $|0\rangle$, where we have defined implicitly the notation $\hat{\tau}_\mu$ to denote a general excitation operator.
Using this notation, a general vector in the many-body Hilbert space can be generated using operators having the following form

$$\hat{\Psi}_i = c_i^\mu \hat{\tau}_\mu \tag{8.1}$$

which is a general linear combination of wave operators that will generate determinants once they act upon the reference determinant.
Akin to the HF equations formulation, we can also use a formal Lagrangian operator $\hat{\mathcal{L}}$ in order to find the working equations, i.e.

$$\hat{\mathcal{L}} = c_{i\mu}c_i^\nu\hat{\tau}^\mu\hat{H}\hat{\tau}_\nu + \lambda_{ij}\left(c_{i\mu}c_j^\nu\hat{\tau}^\mu\hat{\tau}_\nu - \delta_{ij}\right)$$

where the parameter space is simply

$$\{c_i^\mu, c_{i\mu}, \lambda_{ij}\}\,.$$

Notice that we have added the orthonormality condition through the λ_{ij} parameters as usual in these contexts. Thus,

$$\begin{aligned}\frac{\partial}{\partial c_{k\xi}}\hat{\mathcal{L}} &= \delta_{ik}\delta_{\mu\xi}c_i^\nu\hat{\tau}^\mu\hat{H}\hat{\tau}_\nu + \delta_{ik}\delta_{\mu\xi}\lambda_{ij}c_j^\nu\hat{\tau}^\mu\hat{\tau}_\nu \\ &= c_k^\nu\hat{\tau}^\xi\hat{H}\hat{\tau}_\nu + \lambda_{kj}c_j^\nu\hat{\tau}^\xi\hat{\tau}_\nu \\ &= \hat{\tau}^\xi\left(c_k^\nu\hat{H}\hat{\tau}_\nu + \lambda_{kj}c_j^\nu\hat{\tau}_\nu\right) \\ &= 0\end{aligned}$$

which assuming that a suitable rotation of the many-body basis renders the matrix λ_{kj} diagonal, i.e., $\lambda_{kj} = \delta_{kj}\lambda_j$, entails the usual eigenvalue equation

$$\hat{H}c_k^\nu\hat{\tau}_\nu + \lambda_k c_k^\nu\hat{\tau}_\nu = 0.$$

As we have already discussed in table 7.1, storing the whole vector is indeed only feasible for the smallest systems. A common way around this limitation is restricting the excitation order in the linear μ expansion in (8.1). This approach truncates the excitation order and diagonalizes the Hamilton operator $\hat{H}$ in a subspace of $\{\hat{\tau}\}$. These class of methods are classified acccording to their truncation order. For instance, restricting the linear expansion to singles and doubles excitations is denoted as Configuration interaction Singles and Doubles (CISD). This explicit expansion thus reads

$$\hat{\Psi} = C_0\hat{1} + C_i^a\hat{c}^a\hat{c}_i + C_{ij}^{ab}\hat{c}^a\hat{c}^b\hat{c}_j\hat{c}_i$$

and the eigenvalue equation acts in the singles and doubles excitation manifold. Even though this parametrization seems to solve many of the size explosion problems that the Hilbert space naturally creates, there are some major drawbacks to this approach. One of the main drawbacks is the lack of size-consitency of these truncated theories.

This is a central fact also in the application of coupled-cluster theories to solids and big molecules. Thus, we find it fitting to expand further on this topic. We say that a method is size-consistent if it can deliver additive energies for systems composed of non-interacting parts. As an example, let us consider two water molecules, one on Earth and the other on Mars. It is readily seen that they can not possibly be correlated by means of the electromagnetic force. Therefore, if we should calculate the energy of the system composed by these two molecules, the result should be the sum of the two isolated energies. Indeed, using a truncated CI methodology will give us all excitations up to a given truncation order o. In order to have the same accuracy in the isolated systems, we should recover the excitations to order o in a separable way. This however is not possible in the truncated CI approach due to non-vaninishing unconnected diagrams [133, 173, 196]. Nevertheless, efforts have been made to palliate this shortcoming, as in the quadratic CI theory [140] where additional terms are added to the linear ansatz presented in order to render the theory size-consistent. Other theories like Coupled Cluster, have this property formally ingrained in the explicit ansatz.

Chapter 9

Perturbation theories

Already in the early days of quantum mechanics it was clear that the exact solution of the Schrödinger equation is well beyond our technical capabilities. Thus, an attempt was made following the ideas of Rayleigh to develop a perturbative method for the solution of the quantum wave equation [157]. This general framework is therefore known as Rayleigh-Schrödinger perturbation theory.

This theory consists in solving a part of the Hamiltonian that is tractable and consider the rest as a perturbation. By series expansion of the energy and wavefunction one can find concrete expressions for the energy and wavefunction.

Let $\hat{H}$ be the original Hamiltonian and let

$$\hat{H} = \hat{H}_0 + \hat{H}_1$$

where $\hat{H}_1$ is the perturbing term and $\hat{H}_0$ the reference system that one considers solved. The main result for the energy and eigenstate expansion is given by the following equation

$$\lambda^n \left(\left(\hat{H}_0 - E_0 \right) |n\rangle + \left(\hat{H} - \hat{H}_0 - E_1 \right) |n-1\rangle - \sum_{m=0}^{n-2} E_{n-m} |m\rangle \right) = 0, \quad n \in \mathbb{N} \tag{9.1}$$

where we have used an explicit sum for sake of clarity, and λ is a coupling-strength parameter. Here, E_n is the n-th order correction to the energy and $|n\rangle$ is the n-order correction

for the eigenstate of $\hat{H}$. The cases where $n \in \{1, 2\}$ correspond to the well-known first order and second order perturbation theory, respectively.

Møller and Plesset [129] used this formalism to make a choice of $\hat{H}_0$ and therefore $\hat{H}_1$. Namely, they chose as $\hat{H}_0$ to be the one body interaction of the Hartree-Fock theory, i.e, the Fock operator $\hat{F}$. In this framework therefore the perturbation $\hat{H}_1$ is given by $\hat{H} - \hat{F}$. This partitioning of the problem entails an important form of the second-order correlation energy which reads as

$$E_2 = \frac{1}{4} \sum_{abij} \frac{V_{ij}^{ab} V_{ab}^{ij} - V_{ji}^{ab} V_{ab}^{ij}}{\epsilon_i + \epsilon_j - \epsilon_a - \epsilon_b} \tag{9.2}$$

where the denominator is simply the difference between the zeroth expectation value E_0 of the Fock operator $\hat{F}$ and the expectation value of a doubly excited determinant $\hat{c}^a \hat{c}^b \hat{c}_j \hat{c}_i \left|0\right\rangle$. This theory thus presented is known as MP2 and has seen much success in molecular and solid-state systems [68, 52, 155]. Møller-Plesset theories are size-consistent and typically applied up to third order, from which the accuracy starts to vary wildly with system and with order.

Already quite early other partitions of the perturbation have been studied. For instance, instead of considering a denominator composed of diagonal elements of the Hartree-Fock energies, one can in principle consider other kind of terms. In the so-called Epstein-Nesbet perturbation theory, diagonal terms of the full Hamiltonian are considered in lieu of the single-particle energies, which can be seen as a repartitioning of the full Hamiltonian [132, 49, 57].

Finally, the MP family of methods has been shown to be a divergent series in some systems such as the Neon atom [33]. Recent studies however suggest that this pathological behavior can be tamed. Partitioning the Hamiltonian in an optimal way renders the series better behaved in terms of convergence speed and divergence of the long tail of the series [92].

Chapter 10

Coupled cluster methods

In this section we will discuss the main characteristics of the coupled cluster methodology. All the methodologies we have seen thus far suffer from several shortcomings such as lack of dynamic correlation, size-consistency issues, or divergent behavior.
The coupled cluster family of methods strives to achieve a reasonable compromise in sorting out these shortcomings by elegantly choosing an ansatz that represents size-consistency from the outset [112, 35, 134, 10].

10.1 Ground state coupled cluster

The coupled cluster ansatz comes in exponential form

$$|\Psi_{\mathrm{CC}}\rangle = e^{\hat{T}} |0\rangle \tag{10.1}$$

where $|0\rangle$ is commonly the HF determinant or any other single determinant[41]. This determinant is generally known as the reference. The cluster operator $\hat{T}$ is given by a sum of many-body excitation operators starting from first order, i.e.

$$\hat{T} = t^{\mu}\hat{\tau}^{\mu} = t_i^a \hat{c}^a \hat{c}_i + t_{ij}^{ab} \hat{c}^a \hat{c}^b \hat{c}_j \hat{c}_i + t_{ijk}^{abc} \hat{c}^a \hat{c}^b \hat{c}^c \hat{c}_k \hat{c}_j \hat{c}_i + \dots$$

where the operator expansion would go on up to the total number of electrons N.

It is worth noting that in contrast to the CI approaches, a truncation in the cluster operator $\hat{T}$ to order o does not result in an ansatz where the excitations only go up to order o, rather to order o^k where k is a natural number such that $o^k \leq N$. Indeed, this observation comes from the fact that formally for operators

$$e^{\hat{T}} = \frac{1}{!n}\hat{T}^n.$$

While Configuration Interaction (CI) and Coupled Cluster (CC) are not order by order equivalent, they are nevertheless exact theories in the limit of full inclusion of the excitation operators up to the number of electrons. It is thus readily seen, that for a given truncation order always the CI type truncation is included in the CC ansatz. In this sense, up to second order, the relation is

$$C_i^a = t_i^a \tag{10.2}$$

$$C_{ij}^{ab} = \frac{1}{2}t_i^a t_j^b + t_{ij}^{ab}. \tag{10.3}$$

Furthermore, terms exceeding the doubles are included through the exponential super-operator from the point of view of the CI expansion, since terms like $\hat{T}_1\hat{T}_2$ or $\hat{T}_1^3$ form part of the triples coefficients C_{ijk}^{abc} in respective CI expansion.

Additionally, there are many ways of understanding the consequences of this exponential ansatz. In dealing with time-independent systems, it is somewhat natural to use the time-independent perturbation theory as outlined by Møller and Plesset. In this context, Brueckner conjectured [26, 27] that for the case of nuclear matter with many particles in a one-body self-consistent field the perturbation series converged and no *unlinked diagrams* played a role in the total correlation energy. Goldstone in turn generalized these ideas in a diagrammatic methodology [62] for closed-shell fermionic systems, recovering the results of Brueckner as a natural consequence of his framework. The diagram expansion of CC does not contain connected diagrams, which in the case of the energy coincides with being linked [122, 25].

The exponential ansatz has also the consequence that the parameters to be optimized, i.e., t^μ appear in a non-linear way in the description of the wavefunction. It is in principle pos-

sible to minimize the energy E variationally through the optimization of the t^μ amplitudes as in the CI case, i.e., optimize the expression

$$E[t^\mu] = \frac{\langle \Psi_{\mathrm{CC}} | \hat{H} | \Psi_{\mathrm{CC}} \rangle}{\langle \Psi_{\mathrm{CC}} | \Psi_{\mathrm{CC}} \rangle} = \frac{\langle 0 | e^{\hat{T}^\dagger} \hat{H} e^{\hat{T}} | 0 \rangle}{\langle 0 | e^{\hat{T}^\dagger} e^{\hat{T}} | 0 \rangle}. \tag{10.4}$$

Methods using this Variational Coupled Cluster (VCC) approach have been shown to be superior in quality as the traditional approaches that we will introduce in the following [14, 147, 116]. This is partially due to the strict variational property of being an upper-bound to the true ground-state energy. However, it is in most cases computationally unattractive in comparison to the more straightforward implementations of the traditional approaches. Further approaches exist, such as the bivariational approach of Arponen [7, 4] which makes possible the calculations of further electronic properties but incur in a noticeable increase in the complexity of the equations through the consideration of double-linked diagrams.
Traditional coupled cluster methods obtain the t-amplitudes in a projective, iterative fashion. Starting from the Schrödinger equation

$$\hat{H} e^{\hat{T}} | 0 \rangle = E e^{\hat{T}} | 0 \rangle$$

we can multiply by $e^{-\hat{T}}$ on both sides, and we obtain an equation involving the similarity transformed Hamiltonian

$$\bar{H} = e^{-\hat{T}} \hat{H} e^{\hat{T}} \tag{10.5}$$

that reads

$$\bar{H} | 0 \rangle = E | 0 \rangle . \tag{10.6}$$

The many-body determinantal space is given by

$$\begin{aligned} \mathcal{H} &= \left\{ |0\rangle , |_i^a\rangle , \left|{}_{ij}^{ab}\right\rangle , \left|{}_{ijk}^{abc}\right\rangle , \left|{}_{ijkl}^{abcd}\right\rangle , \dots \right\} \\ &= \left\{ |0\rangle , \hat{c}^a \hat{c}_i | 0 \rangle , \hat{c}^a \hat{c}^b \hat{c}_j \hat{c}_i | 0 \rangle , \hat{c}^a \hat{c}^b \hat{c}^c \hat{c}_k \hat{c}_j \hat{c}_i | 0 \rangle , \hat{c}^a \hat{c}^b \hat{c}^c \hat{c}^d \hat{c}_l \hat{c}_k \hat{c}_j \hat{c}_i | 0 \rangle , \dots \right\} , \end{aligned}$$

we can now project equation (10.6) onto the space $\mathcal{H}$ and obtain a series of equations

$$\langle 0| \bar{H} |0\rangle = E \tag{10.7}$$

$$\langle {}^{a}_{i}| \bar{H} |0\rangle = 0 \tag{10.8}$$

$$\left\langle {}^{ab}_{ij}\right| \bar{H} |0\rangle = 0 \tag{10.9}$$

$$\left\langle {}^{abc}_{ijk}\right| \bar{H} |0\rangle = 0$$

$$\ldots = 0$$

which then entail a series of non-linear coupled equations. One can readily write the equations using the rules of Wick's theorem [191, 131] using the single reference determinant as a new vacuum. The connectedness of the tensor contractions comes about by the similarity transformation. Indeed, $\bar{H}$ can be written with the help of the BCH identity as

$$\bar{H} = H + [H,T] + \frac{1}{2!}[[H,T],T] + \frac{1}{3!}[[[H,T],T],T] + \cdots$$

where in every instance of the appearing commutator disconnected terms get canceled [126]. Therefore, all terms appearing in $\bar{H}$ are connected.

In order to understand how we can solve these equations, let us look at the doubles equations (10.9) and investigate some relevant terms. In a spin-orbital basis, the doubles equations can be written as

$$\begin{aligned} 0 = {} & V_{ij}^{ab} - V_{ij}^{ba} \\ & - f_i^m t_{mj}^{ab} + f_j^m t_{mi}^{ab} - f_e^b t_{ij}^{ea} + f_e^a t_{ij}^{eb} \\ & + R_{ij}^{ab} \end{aligned}$$

where R_{ij}^{ab} represents all the rest terms that include linear and non-linear terms coupling t-amplitudes of different orders with V_{rs}^{pq}.

For the sake of this analysis, let us suppose that we are dealing with Hartree-Fock orbitals such that the one-body matrix f is diagonal, i.e.: $f_q^p = \epsilon_p \delta_{pq}$. In this case, we readily

obtain

$$\begin{aligned} 0 &= V_{ij}^{ab} - V_{ij}^{ba} \\ &- \epsilon_i t_{ij}^{ab} - \epsilon_j t_{ij}^{ab} + \epsilon_b t_{ij}^{ab} + \epsilon_a t_{ij}^{ab} \\ &+ R_{ij}^{ab} \end{aligned}$$

and taking the t-amplitudes as a common term, we obtain the equation

$$t_{ij}^{ab} \left(\epsilon_i + \epsilon_j - \epsilon_a - \epsilon_b\right) = V_{ij}^{ab} - V_{ij}^{ba} + R_{ij}^{ab} \left[t_i^a, t_{ij}^{ab}, t_{ijk}^{abc}, \ldots\right]$$

where we have written the explicit dependence of R_{ij}^{ab} on the t-amplitudes. This equation is key for solving effectively the non-linear equations, since we can choose as a first approximation to set $t_\mu = 0$ for all t-amplitudes appearing in R_{ij}^{ab}. We can therefore approximate the doubles amplitudes t_{ij}^{ab} in the next step by solving for it in equation (10.1), thus obtaining:

$$t_{ij}^{ab} = \frac{V_{ij}^{ab} - V_{ij}^{ba}}{\epsilon_i + \epsilon_j - \epsilon_a - \epsilon_b}$$

which correspond to the doubles amplitudes that appear in the MP2 theory.

Thus, following this procedure it is possible to retrieve a recursive set of diagrams up to infinite order. Surely, in general a truncation is put in place, where the orders in the t-amplitudes are restricted as well as the projections in the many-body space. Since the $\hat{T}$ operator is fermionic and thus the amplitudes t_{ij}^{ab} are antisymmetric within the upper and lower indices, it is straightforward to understand why given the definition of V_{ij}^{ab}, the object $V_{ij}^{ab} - V_{ij}^{ba}$ appears time and again. This object is called the antisymmetrized coulomb integrals and one often denotes them by W_{ij}^{ab}.

For reference, we provide the singles equations that result from purely applying Wick's theorem and that was implemented in our code [59, 83]:

$$
\begin{aligned}
0 = & f_i^b \\
& - f_i^k t_k^b f_c^b + t_i^c - t_l^c W_{ic}^{lb} f_d^k + t_{ki}^{db} \\
& + \frac{1}{2} t_{lm}^{cb} W_{ic}^{lm} + \frac{1}{2} t_{mi}^{cd} W_{cd}^{mb} \\
& - t_i^c t_l^b f_c^l - t_k^b t_m^d W_{id}^{km} - t_i^c t_m^d W_{cd}^{mb} \\
& - \frac{1}{2} t_{lm}^{cb} t_i^f W_{cf}^{lm} - \frac{1}{2} t_{mi}^{cd} t_n^b W_{cd}^{mn} \\
& + t_{li}^{cb} t_n^e W_{ce}^{ln} - t_i^c t_l^b t_n^e W_{ce}^{ln}
\end{aligned}
$$

together with the doubles equations

$$
\begin{aligned}
0 = & W_{ij}^{cd} \\
& - t_m^c W_{ij}^{md} + t_m^d W_{ij}^{mc} + t_j^e W_{ie}^{cd} - t_i^e W_{je}^{cd} \\
& - f_i^m t_{mj}^{cd} + f_j^m t_{mi}^{cd} - f_e^d t_{ij}^{ec} + f_e^c t_{ij}^{ed} \\
& + \frac{1}{2} t_{mn}^{cd} W_{ij}^{mn} + t_{nj}^{ec} W_{ie}^{nd} - t_{nj}^{ed} W_{ie}^{nc} - t_{ni}^{ec} W_{je}^{nd} + t_{ni}^{ed} W_{je}^{nc} \\
& + \frac{1}{2} t_{ij}^{ef} W_{ef}^{cd} \\
& + t_m^c t_n^d W_{ij}^{mn} - t_j^e t_n^c W_{ie}^{nd} + t_j^e t_n^d W_{ie}^{nc} + t_i^e t_n^c W_{je}^{nd} - t_i^e t_n^d W_{je}^{nc} + t_i^e t_j^f W_{ef}^{cd} \\
& - f_f^m t_{mj}^{cd} t_i^f + f_f^m t_{mi}^{cd} t_j^f + f_f^m t_{ij}^{fc} t_m^d - f_f^m t_{ij}^{fd} t_m^c \\
& + \frac{1}{2} t_{mn}^{cd} t_j^g W_{ig}^{mn} - \frac{1}{2} t_{mn}^{cd} t_i^g W_{jg}^{mn} \\
& - t_{nj}^{ec} t_o^d W_{ie}^{no} + t_{nj}^{ed} t_o^c W_{ie}^{no} + t_{ni}^{ec} t_o^d W_{je}^{no} - t_{ni}^{ed} t_o^c W_{je}^{no} - t_{mj}^{cd} t_o^f W_{if}^{mo} + t_{mi}^{cd} t_o^f W_{jf}^{mo} \\
& - t_{nj}^{ec} t_i^g W_{eg}^{nd} + t_{nj}^{ed} t_i^g W_{eg}^{nc} + t_{ni}^{ec} t_j^g W_{eg}^{nd} - t_{ni}^{ed} t_j^g W_{eg}^{nc} \\
& - \frac{1}{2} t_{ij}^{ef} t_o^c W_{ef}^{od} + \frac{1}{2} t_{ij}^{ef} t_o^d W_{ef}^{oc} \\
& + t_{ij}^{ec} t_o^f W_{ef}^{od} - t_{ij}^{ed} t_o^f W_{ef}^{oc} \\
& + \frac{1}{2} t_{ij}^{ed} t_{op}^{fc} W_{ef}^{op} - \frac{1}{2} t_{ij}^{ec} t_{op}^{fd} W_{ef}^{op} + \frac{1}{4} t_{ij}^{ef} t_{op}^{cd} W_{ef}^{op} - \frac{1}{2} t_{mi}^{cd} t_{pj}^{fg} W_{fg}^{mp} + \frac{1}{2} t_{mj}^{cd} t_{pi}^{fg} W_{fg}^{mp} \\
& - t_{ni}^{ed} t_{pj}^{gc} W_{eg}^{np} + t_{ni}^{ec} t_{pj}^{gd} W_{eg}^{np} \\
& + t_j^e t_n^c t_o^d W_{ie}^{no} - t_i^e t_n^c t_o^d W_{je}^{no} - t_i^e t_j^f t_o^c W_{ef}^{od} + t_i^e t_j^f t_o^d W_{ef}^{oc} + \frac{1}{2} t_i^e t_j^f t_{op}^{cd} W_{ef}^{op} \\
& + t_i^e t_n^d t_{pj}^{gc} W_{eg}^{np} - t_i^e t_n^c t_{pj}^{gd} W_{eg}^{np} - t_j^e t_n^d t_{pi}^{gc} W_{eg}^{np} + t_j^e t_n^c t_{pi}^{gd} W_{eg}^{np} + t_i^e t_o^f t_{pj}^{cd} W_{ef}^{op} - t_j^e t_o^f t_{pi}^{cd} W_{ef}^{op} \\
& + \frac{1}{2} t_m^c t_n^d t_{ij}^{gh} W_{gh}^{mn} \\
& - t_m^d t_o^f t_{ij}^{hc} W_{fh}^{mo} + t_m^c t_o^f t_{ij}^{hd} W_{fh}^{mo} + t_i^e t_j^f t_o^c t_p^d W_{ef}^{op}
\end{aligned}
$$

10.2 Equation of motion coupled cluster

The usual formulation of *single reference* coupled cluster theory is essentially a theory for the ground state. Indubitably, one is in general not only interested in the ground state but in excited states. The main approach of the Equation Of Motion (EOM) is to improve

on top of the coupled cluster ground state $|\Psi_{\mathrm{CC}}\rangle$ by obtaining several excited states $|\Psi_i\rangle$. For this, the methodology relies on the general equation of motion framework to obtain excited states. This framework can be used also to obtain excited states for other theories such as Random Phase Approximation (RPA) or HF [151, 152].

In this EOM framework, one can define a *linear* excitation operator that delivers us the excited states

$$|\Psi_i\rangle = \hat{R}_i \, |\Psi_{\mathrm{gs}}\rangle \, .$$

where $|\Psi_{\mathrm{gs}}\rangle = |\Psi_{\mathrm{CC}}\rangle$ is the solution of the ground state coupled-cluster calculation.

Being $\hat{R}$ a linear excitation operator, it acquires the following familiar form

$$\hat{R} = r^{\mu} \hat{\tau}_{\mu}$$

where μ, as before, is an index denoting a charge-neutral particle-hole excitation as in the CCSD case.

The name *equation of motion* is motivated by the following consideration, since $|\Psi_i\rangle$ is the i-th excited state, we can write

$$\hat{H} \, |\Psi_i\rangle = \hat{H} \hat{R}_i \, |\Psi_{\mathrm{gs}}\rangle = E_i \, |\Psi_i\rangle = E_i \hat{R}_i \, |\Psi_{\mathrm{gs}}\rangle$$

but also since $|\Psi_{\mathrm{gs}}\rangle$ is the ground state,

$$\hat{R}\hat{H} \, |\Psi_{\mathrm{gs}}\rangle = \hat{R} E_{\mathrm{gs}} \, |\Psi_{\mathrm{gs}}\rangle = E_{\mathrm{gs}} \hat{R} \, |\Psi_{\mathrm{gs}}\rangle$$

and subtracting these two equations we obtain therefrom

$$[\hat{H}, \hat{R}] \, |\Psi_{\mathrm{gs}}\rangle = (E_i - E_{\mathrm{gs}}) \hat{R} \, |\Psi_{\mathrm{gs}}\rangle = \Delta E_i \hat{R} \, |\Psi_{\mathrm{gs}}\rangle \tag{10.10}$$

which is reminiscent to the equation of motion for operators in the *Heisenberg* picture. Now we restrict the choice of the ground state to be a solution for the coupled cluster equations, i.e., $|\Psi_{\mathrm{gs}}\rangle = e^{\hat{T}} \, |0\rangle$, where $|0\rangle$ is a single Slater determinant with a virtual and an active space which we will mostly consider to be a HF determinant, but can in principle

involve any other kind of orbitals.

Now let us rewrite equation 10.10 in terms of the vacuum state $|0\rangle$:

$$[\hat{H}, \hat{R}_i]e^{\hat{T}}\,|0\rangle = (E_i - E_{\mathrm{gs}})e^{\hat{T}}\,|0\rangle$$

Now we can use the fact that any two $\hat{\tau}_\mu$ and $\hat{\tau}_\nu$ operators commute as long as they include the same amount of hole indices and particle indices and they only create particle-hole pairs. This lemma implies that $\hat{R}_i$ and $e^{\hat{T}}$ commute $[\hat{R}_i, e^{\hat{T}}] = 0$, videlicet, $\hat{T}$ and $\hat{R}_i$ excite and annihilate in the same partition of the orbital space. This in turn entails

$$\begin{aligned}
[\hat{H}, \hat{R}_i]e^{\hat{T}} &= \hat{H}e^{\hat{T}}e^{-\hat{T}}\hat{R}_i e^{\hat{T}} - \hat{R}_i e^{\hat{T}}e^{-\hat{T}}\hat{H}e^{\hat{T}} \\
&= e^{\hat{T}}\left(e^{-\hat{T}}\hat{H}e^{\hat{T}}\hat{R}_i - \hat{R}_i e^{-\hat{T}}\hat{H}e^{\hat{T}}\right) \\
&= e^{\hat{T}}[\bar{H}, \hat{R}_i]
\end{aligned}$$

where we have factored in the similarity transformed Hamiltonian $\bar{H}$. In consequence, we arrive at the following form of the equation of motion for the linear operator $\hat{R}_i$ and its energy E_i

$$[\bar{H}, \hat{R}_i]\,|0\rangle = (E_i - E_{\mathrm{gs}})\hat{R}_i\,|0\rangle = \Delta E_i \hat{R}_i\,|0\rangle \tag{10.11}$$

The commutator here has the same effect as in the ground state coupled cluster case, it removes disconnected contractions from the Wick normal products. Therefore, the equality in (10.11) is equivalent to

$$\left(\bar{H}\hat{R}_i\right)_{\mathrm{c}}|0\rangle = \Delta E_i \hat{R}_i\,|0\rangle\,, \qquad \Delta E_i = E_i - E_{\mathrm{gs}} \tag{10.12}$$

which is the final defining equation for EOM-CC.

As we have seen, EOM-CC can be interpreted as diagonalizing the similarity transformed Hamiltonian just as Full Configuration Interaction (FCI) diagonalizes the original $\hat{H}$ Hamiltonian. Since truncated CI diagonalization violates the size-extensivity in such a way that for large enough systems the correlation energy contributed by the method becomes arbi-

trarily small, it is expedient to ask the same question for the EOM-CC method. It is thus worthwhile discussing notable differences between truncated CI and EOM-CC methods. Firstly, it is intuitively understandable that the main culprits for the size-extensivity violation of a method have to do with unconnected terms in the energy expression [73, 133, 197, 196]. In fact, equation (10.12) is identical in overall form to a CI approach when restricting the equations only to connected terms. Since the EOM-CC equations do not contain such disconnected terms we can expect that the size-extensivity error be manageable at least. This is indeed the case. In order to gain a bit more intuition we further discuss the similarities between linear response CC and EOM.

In linear response CC, given a temporal disturbance of the many body Hamiltonian $\hat{H}$

$\hat{H}(t) = \hat{H} + \hat{V}e^{-i\omega t} + \hat{V}^{\dagger}e^{+i\omega t}$

one makes use of the linear Ansatz

$$\hat{T}(t) = \hat{T} + \hat{R}e^{-i\omega t} + \hat{R}^{\dagger}e^{+i\omega t}$$

which represents the linear response of the system. The Ansatz solution remains an exponential, albeit dependent on time, $|\Psi_{\mathrm{gs}}(t)\rangle = e^{\hat{T}(t)}\,|0\rangle$, this ensures for every t and truncation size-consistency. Inserting this time-dependent amplitude into the time-dependent Schrödinger equation and keeping the lowest order we recover the expression

$$e^{-\hat{T}}\hat{H}e^{\hat{T}}\hat{R}|0\rangle = (E_{\mathrm{CC}} + \omega)\hat{R}|0\rangle$$

which is identical to our EOM equation (10.12). Consequently, this means that the equations of EOM can be interpreted as the first order of a size-consistent theory, and can be expected to suffer less from size-consistency issues than a bare truncated CI. This is of course altogether due to the use of a similarity transformed Hamiltonian instead of the bare electronic Hamiltonian.

10.3 Addition of perturbative triples

When dealing with coupled cluster theories, going one order further in the truncation of the t-amplitudes incurs a steep increase of computational scaling by two orders of magnitude. However, it is highly desirable to include a higher level of correlation even if only in an approximate way, be it in many body perturbation theory [111] or in coupled cluster theories [143].

CCSD, reinterpreted as a many body resummation theory, contains all terms appearing in third-order MP (MP) and beyond these. Coupled cluster with singles, doubles and triples excitations (CCSDT) on the other hand, does not contain all diagrams from fourth-order MP (MP) but contains even a bigger class of diagrams than CCSD [183, 12].

Perturbative triple excitations (CCSD(T)) is a theory that includes the effect of triple excitations in CC in a non-iterative way [144], this is, the inclusion of these triple excitations is done in a *one-shot* fashion and includes a balanced family of fifth-order diagrams. CCSD(T) is very accurate for systems in thermochemistry inasmuch as it delivers consistently highly accurate results for a large set of molecules as compared with other many-body correlation methods [160, 43, 145].

There are several ways to motivate the main expression of the CCSD(T) energy. Let us first look at the expression for the MP2 correlation energy:

$$\Delta E(\mathrm{MP2}) = \frac{1}{E_0 - E_\mu} \langle 0| \hat{V} |\mu\rangle \langle \mu| \hat{V} |0\rangle$$

we have the reference determinant $|0\rangle$ and an arbitrary excited determinant $|\mu\rangle$. In practice however, $|\mu\rangle$ is restricted to the space of double excited determinants since the coulomb interaction $\hat{V}$ is a two body operator and the only elements that can contribute in this sum are excitation states of the form $\left|{}^{ab}_{ij}\right\rangle$ that give rise to matrix elements V_{ij}^{ab} and its complex conjugate. Formally, we can conceive the case where we have a CCSD state $|\Psi\rangle$ as a reference state, where as before

$$|\Psi\rangle = \exp\left\{t_i^a \hat{c}^a \hat{c}_i + t_{ij}^{ab} \hat{c}^a \hat{c}^b \hat{c}_j \hat{c}_i\right\} |0\rangle = c^\mu \hat{\tau}_\mu$$

where we have written also the expanded version of the exponential in order to write next

the state $|\Psi\rangle$ as a CI linear ansatz with coefficients c^{μ}.

Formally, by replacing $|0\rangle$ by $|\Psi\rangle$ in the expression for the $\Delta(\mathrm{MP2})$ energy we obtain

$$\Delta E = \frac{c_{\nu}^{\dagger} c_{\mu}}{E_0 - E_{\tau}} \langle \nu | \hat{V} | \tau \rangle \langle \tau | \hat{V} | \mu \rangle .$$

Please note that the denominator of the expression is included *ad-hoc*, since the actual denominator of the perturbation given from a direct application of Rayleigh-Schrödinger perturbation theory should involve expectation values of the reference state $|\Psi\rangle$. In principle ν and μ should run over all possible determinants, from singles to the number of electrons N since they are expanding the reference state $|\Psi\rangle$, which on account of the exponential ansatz spans the whole determinant space.

Given that the computational framework is based on a CCSD theory, one restricts the space of ν, μ to singles and doubles excitations. Within this context, contractions where τ belongs to the singles and doubles manifold represent diagrams that are already included in the iterative CCSD equations. Certainly, this method remains in the scope of adding corrections related to triples substitutions and therefore τ it is restricted to triples excitations.

It is important to note that some perturbative triples terms are already present in the CCSD correlation energy. This certainly the case since the exponential ansatz induces terms in the c_{ijk}^{abc} coefficients of the form $t_i^a t_{jk}^{bc}$, which are effectively coupling with the triple excitation manifold. It can even be shown that the leading terms in energy caused by the restriction of μ and ν to singles excitations pertain to this class of terms [140]. Therefore, one chooses to remove the singles from the μ and ν altogether and add them as a separate term.

With this in mind the, when we make use of the pertinent notation the final expression reads

$$\begin{aligned}\Delta E(\mathrm{CCSD(T)}) &= \frac{c_\mu}{E_0 - E_\tau}\left(c^\dagger_{\nu'}\left\langle\nu'\right| + c^\dagger_\nu\left\langle\nu\right|\right)\hat{V}\left|\tau\right\rangle\left\langle\tau\right|\hat{V}\left|\mu\right\rangle \\ &= c^{AB}_{IJ}\frac{\left(c^{\dagger d}_{\ l}\left\langle{}^{d}_{l}\right| + c^{\dagger ef}_{\ \ mn}\left\langle{}^{ef}_{mn}\right|\right)\hat{V}\left|{}^{abc}_{ijk}\right\rangle\left\langle{}^{abc}_{ijk}\right|\hat{V}\left|{}^{AB}_{IJ}\right\rangle}{\epsilon_i + \epsilon_j + \epsilon_k - \epsilon_a - \epsilon_b - \epsilon_c}\end{aligned}$$

This expression can be also understood from the point of view of the diagonalization of the similarity transformed Hamiltonian $\bar{H}$ [167]. It can be motivated that this expression is near to the first order in perturbation to the energy difference

$$E_{\mathrm{FCI}} - E_{\mathrm{CCSD}}.$$

This result motivates and reinforces the interpretation that this addition to the energy corrects the CCSD energy rather than being overly biased on correcting the HF reference energies, like the CCSD energy.
In conclusion, even though no rigorous derivation of the functional form of the CCSD(T) is available, its usefulness remains hitherto uncontested within its respective domain of applicability.

Chapter 11

Electronic cusp

11.1 Orbital representation

Up to this point, the orbitals ϕ_p have been treated as general functions. However, they are an essential degree of freedom to improve the quality of the calculation results in quantum chemical calculations.

In the simple case of the Hydrogen atom, the one-electron Schrödinger equation leads to radial functions of the form

$$\phi(\mathbf{r}) = Ce^{-\alpha r}$$

where C and α are constants. This simple system exemplifies quite faithfully a general problem. Namely, around the origin of the function there is a discontinuity of the derivative, which makes the approximation of this orbital by functions which are typically $\mathcal{C}^\infty$, challenging in practical terms. These approximating functions are typically Gaussian type functions

$$\phi(\mathbf{r}) = Ce^{-\alpha r^2}$$

in the case of molecular systems and plane waves in extended systems

$$\phi_{\mathbf{G}}(\mathbf{r}) = Ce^{i\mathbf{G}\cdot\mathbf{r}}.$$

In figure 11.1 we can see an elementary depiction of these orbitals.

Clearly, in order to represent a purely exponential orbital we will need infinitely many Gaussian orbitals and even more plane waves. Since this behavior of the orbital is specially important for electrons that are near the nucleus and not so active in the chemical processes, a common way around this problem in molecular systems is the usage of basis sets that are optimized to account for the effect of the core electrons in the coefficients of the valence electrons. Thus, one evades the problem of the localised core orbitals altogether. This approach is often refereed to as frozen core.

In the case of plane wave basis sets, pseudo-potentials are used that account for said difficulty of plane waves to represent sharp features of core electrons [77]. In this context, several methodologies exist which construct the effective potential in different ways [159]. The HF program used in this work as a starting point for periodic calculations, VASP [110], uses the projector augmented wave (PAW) approximation [19, 20], which maps both the orbitals and the operators to pseudised representations that ensure the smoothness of the orbitals in the whole space. This palliates part of the basis set convergence problem in the case of extended systems.

11.2 Electron-electron cusp

In section 11.1 we have discussed the fact that the choice of orbitals can hinder greatly the quality of the actual orbital representation electrons. This analysis however remains in the one-body picture of the problem.

There is however another central limitation in the representation of electronic wavefunctions that arises when we consider a system with more than one electron.

A pedagogical and somewhat simplified illustration of the physical intuition of the electron-electron cusp starts by considering the classical gravitational interaction between two point-like planets. Figure 11.2 illustrates this case schematically. Since the classical gravitational law also follows the r^{-2} law, we can safely use this case for illustrative purposes. Let us

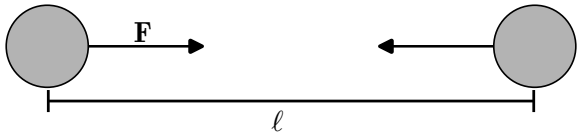

Figure 11.2: Schematic representation of two objects subjected to a attracting force F.

suppose that the bodies have a small velocity towards each other when they are separated by a distance ℓ which should be large enough (on the order of several thousands millions of kilometers). In the isolated system composed by both bodies, their total energy is a constant of motion. This energy is composed by their kinetic energy and their gravitational interaction through the $K\ell^{-1}$ potential, where K is a constant. Whenever they are as close as $1\mathring{\mathrm{A}}$, the force $\mathbf{F}$, following the r^{-2} power law, takes on ever-increasing values, and with it the kinetic energy increases in the same measure. Certainly, since the potential energy decreases in the same fashion but with a different sign, the total energy of the system stays constant. However, in terms of a classical intuition, it is not quite physical to accept that the kinetic energy actually becomes infinite. Indeed, planets are not point particles and their relative distances are never infinitesimally valued.

Quantum mechanics however allows for the interpretation that two electrons can be at the very same position at the same time, provided they exhibit a different spin degree of freedom. With this somewhat deceiving intuition, one finds that these electrons can in fact reach infinite velocities. This fact is imprinted in the *Kato cusp condition* for the electron-electron interaction [96, 97]. Indeed, the singularity of the coulomb potential is cancelled by the momentum operator acting on the many-electron wavefunction $\Psi(\mathbf{r}_1, \ldots, \mathbf{r}_N)$ as the i-th electron approaches the j-th electron. In fact, these kinds of singularities described by Kato are the only ones exhibited by electronic non-relativistic many-body Born-Oppenheimer systems. Therefore, Ψ is everywhere else throughout the configuration space continuous and allowing for continuous derivatives [97].

For two electron systems, the cusp condition is readily found by inserting $\Psi(\mathbf{r}_1, \mathbf{r}_2)$ into the two-electron Schrödinger equation, letting r_{12} decrease towards zero and finding a relation that cancels the $1/r_{12}$ singularity of the electron-electron Coulomb interaction potential. In the simple case of a singlet wave function Ψ (where the radial part is symmetric), one

finds

$$\left.\frac{\partial \Psi}{\partial r_{12}}\right|_{r_{12}\to 0} = \frac{1}{2}\Psi(r_{12} \to 0).$$

For a more general N-electronic singlet wave function the derivative at r_{ij} has in general a directional dependence in the neighbourhood of the coalescence point $r_{ij} \to 0$ and the mathematically correct expression is

$$\lim_{r_{ij}\to 0} \frac{1}{4\pi} \int \frac{\partial \Psi}{\partial r_{ij}} \mathrm{d}\Omega = \frac{1}{2}\Psi(r_{ij} \to 0),$$

where the integral integrates over the solid angle domain. For more details about this procedure we refer to the literature [78, 115, 84].

An important consequence of the cusp is that at the coalescence point $r_{ij} \to 0$ the wave function Ψ has the following form

$$\Psi(\ldots, \mathbf{r}_i, \ldots, \mathbf{r}_j, \ldots) \propto r_{ij}\eta(\mathbf{r}_1, \ldots, \hat{\mathbf{r}}_i, \ldots, \hat{\mathbf{r}}_j, \ldots, \mathbf{r}_N)$$

where η is a function not depending on r_i or r_j in an infinitesimal neighborhood of $r_{ij} \to 0$. As in the case of the orbital representation of the sharp core exponential features, we encounter again the difficulty of representing this sharp feature in said vicinity. However, in this case we are not able directly to create a pseudo-potential to take care of these intricate features for us, since the sharpness of the feature is dependent on the dynamic correlation between all electron pairs. One can however tackle this problem from the point of view of the basis set and introduce r_{ij} dependent basis functions that have the cusp r_{ij}-dependence ingrained in their *Ansatz* form. These approaches are often referred to as explicitly correlated theories such as `f12` or `r12` [107, 176, 175, 106, 8, 18].

In passing we note that similar relations exist for the interaction between the electrons and the nuclei. For our purposes however this is of no relevance.

11.3 MP2 in the Complete Basis Set limit

As a first relevant example of a theory tackling the basis set size convergence problem we discuss briefly an approach in order to obtain converged correlation energies in MP2.

In (9.2) we wrote the energy expression of MP2 using a basis of spin-orbitals. A common technique to factorize the energy denominator is by taking the *Laplace* transform

$$\frac{1}{\epsilon_a + \epsilon_b - \epsilon_i - \epsilon_j} = \int_0^\infty e^{-t(\epsilon_a+\epsilon_b-\epsilon_i-\epsilon_j)} \mathrm{d}t.$$

The previous equality allows replacing a part of the contraction by a numerical integral, which given the nature of the exponential decay of the integrand, it mostly requires around 10 points in a suitable integration grid [3, 192]

In extended systems, by further decomposing the Coulomb integrals V_{ij}^{ab} into a tensor contraction such as

$$V_{ij}^{ab} = \Gamma_i^{aG} \left(\Gamma_j^{bG}\right)^\dagger$$

one can further reduce the naive scaling of $\mathcal{O}(N^5)$ into a quartic scaling in terms of the contraction variable length N_G [156].

Alternatively in molecular systems, linear scaling methods have been developed that take advantage of local correlation domanins in molecules in order to tame the scaling fo the method [158].

Reducing the computational resources needed to obtain converged results with respect to the basis set size thus enables treating systems with more accuracy.

In particular, such methodologies can be used to develop new methodologies for different methods. These new methods base their results on the soundness of the original techniques.

11.4 Diagrammatic decomposition of the CCSD correlation energy

The CCSD equations can be understood by decomposing its terms in meaningful groupings of contractions. Their definition comes about by considering the topology of their contracted inidices. When written in a pictorial form by means of Goldstone diagrams an immediate intuitive meaning is bestowed upon them [62, 150, 6, 126, 113].

A way of identifying their meaningfulness is by interpreting the different contractions in

terms of existing approximations for the energy or the wave function. Additionally, the coupled cluster approach can be understood as an infinite resummation of many-body perturbation theory diagrams. In this sense, some perturbative theories and resummation techniques can be recovered in the framework of its equations.

Taking this into account, we will briefly discuss how the RPA fits into the CC framework. The RPA was first developed by Macke [124] and soon after by Pines and Bohm [139, 139, 22, 23] in their seminal works. As already shown in (10.1), the amplitude equations in coupled cluster consist of a series of terms involving contractions of the Coulomb integrals V_{rs}^{pq} and the t-amplitudes t_μ. A common approach to explore the accuracy and flexibility of these equations is by truncating the excitation degree of the t-amplitudes, giving rise to the truncated CC methods CCSD, CCSDT, etc. Alternatively, terms can be selectively left out, giving rise to approaches such as distinguishable coupled cluster [98] or a host of other approximations [32, 117, 138].

In order to recover the diagrammatics of the RPA, we consider non-antisymmetrized Coulomb integrals V_{rs}^{pq} together with the following contractions

$$
\begin{aligned}
0 = {} & V_{ij}^{cd} && (11.1)\\
& - f_i^m t_{mj}^{cd} + f_j^m t_{mi}^{cd} - f_e^d t_{ij}^{ec} + f_e^c t_{ij}^{ed} && (11.2)\\
& + t_{ik}^{ce} V_{ej}^{kd} && (11.3)\\
& - t_{ni}^{ed} V_{eg}^{np} t_{pj}^{gc} + t_{ni}^{ec} V_{eg}^{np} t_{pj}^{gd} && (11.4)
\end{aligned}
$$

where we have only kept contractions with particle-hole bubbles. Starting from a diagonal one-body representation of the problem where $f_q^p \propto \delta_q^p$, the iterative procedure creates RPA like terms which in the case of convergence agree with the RPA energy for parts of CC energy expression. This approach for solving for the CC amplitudes is termed direct ring coupled cluster [81, 69].

The same process can be done with the MP2 channel where only the V_{ij}^{cd} term is included in the doubles. The process is however terminated in the first iterative step, giving rise to the MP2 energy expression. Another notable channel is the ppl channel, wherein the

relevant terms are

$$0 = V_{ij}^{cd} \tag{11.5}$$
$$- f_i^m t_{mj}^{cd} + f_j^m t_{mi}^{cd} - f_e^d t_{ij}^{ec} + f_e^c t_{ij}^{ed} \tag{11.6}$$
$$+ V_{ef}^{cd} t_{ij}^{ef} \,. \tag{11.7}$$

Performing an iterative procedure in some of these channels alone is in some cases rewarding. For instance, it is known that in the high-density limit of the uniform electron gas, i.e. when $r_s \to 0$ the RPA approach just outlined becomes exact [24, 5, 56]. For real systems or intermediate regions in the UEG however there is in general a complex interplay between the different channels.

It is important to stress that replacing CCSD converged t-amplitudes t^μ into the RPA, ppl or MP2 channels will give different contributions to the correlation energy. This fact begs the question of how every contribution depends on the basis set size used for computing it.

It can be shown that most of the additional correlation energy that comes from increasing the basis set size comes from the MP2 and ppl channels and their magnitudes are of comparable absolute value but with an opposite sign [89]. Furthermore, the ppl terms of the CCSD equations are the most expensive ones to compute. We have previously discussed that methods exist and can be developed to lower the computational cost of MP2 calculations through various techniques. We can therefore motivate a method to approximate the ppl correlation energy from the MP2 by simply exploiting the relation between the MP2 and ppl channels. The interested reader can find more details in our publication [89].

11.5 The focal-point basis set correction

The rest of this chapter will present the focal-point basis set correction developed in [87] for the CCSD and CCSD(T) methods.

1. Overview

   The scheme is based on employing frozen natural orbitals (FNOs) and diagrammatically decomposed contributions to the electronic correlation energy that dominate the basis set incompleteness error (BSIE). As discussed in our work [89], the BSIE of the CCSD correlation energy is dominated by the MP2 perturbation energy and the particle-particle ladder term. Here, we derive a simple approximation to the BSIE of the particle-particle ladder term that effectively corresponds to a rescaled pair-specific MP2 BSIE, where the scaling factor depends on the spatially averaged correlation hole depth of the coupled-cluster and first-order pair wavefunctions. The evaluation of the derived expressions is simple to implement in any existing code. We will analyse the UEG and motivate therein the approach taken. Furthermore, we apply the method to coupled-cluster theory calculations of atoms and molecules using FNOs.

2. The pair-specific decomposed PPL correlation energy in the CBS limit In this section we introduce a correction to the BSIE of the CCSD correlation energy. The CCSD correlation energy of a spin-restricted system is given by

$$E_{\mathrm{c}}^{\mathrm{CCSD}} = \sum_{ij} \sum_{ab} T_{ij}^{ab} \left(2 \langle ij|V|ab\rangle - \langle ji|V|ab\rangle \right) \tag{11.8}$$

   where the first term is the *so-called* direct diagram and the negative term is the exchange diagram. T_{ij}^{ab} is computed from the CCSD singles (t_i^a) and doubles $\left(t_{ij}^{ab}\right)$ amplitudes as $T_{ij}^{ab} = t_{ij}^{ab} + t_i^a t_j^b$. t_i^a and t_{ij}^{ab} are obtained by solving the corresponding amplitude equations [12, 34, 13].

   For the sake of clarity, let us note in passing that the notation $|pq\rangle$ denotes a non-antisymmetrized state of two electrons created directly from the Dirac vacuum, i.e.,

$$\langle \mathbf{r}_1 \mathbf{r}_2 | pq \rangle = \phi_p(\mathbf{r}_1) \phi_q(\mathbf{r}_2)$$

   and it does *not* denote a *Slater* determinant. Consequently, in this notation the

integrals V_{ab}^{ij} become

$$\langle ij|V|ab\rangle = V_{ab}^{ij} = \int \mathrm{d}\mathbf{r}_1 \mathrm{d}\mathbf{r}_2 \frac{\phi_i^\dagger(\mathbf{r}_1)\phi_a(\mathbf{r}_1)\phi_j^\dagger(\mathbf{r}_2)\phi_b(\mathbf{r}_2)}{|\mathbf{r}_1 - \mathbf{r}_2|}. \tag{11.9}$$

Next, we employ the diagrammatic decomposition of the CCSD correlation energy discussed previously that is obtained by substituting the doubles amplitude in (11.8) with corresponding contributions from the right hand side of the converged amplitude equation, which is given by

$$\Delta_{ij}^{ab} t_{ij}^{ab} = \underbrace{\langle ab|V|ij\rangle}_{\text{driver/mp2}} + \underbrace{\sum_{cd} \langle ab|V|cd\rangle\, T_{ij}^{cd}}_{\text{ppl}} + \underbrace{\cdots}_{\text{rest}} \tag{11.10}$$

wherein $\Delta_{ij}^{ab} = \epsilon_i + \epsilon_j - \epsilon_a - \epsilon_b$ are the one-electron energy differences in the Hartree–Fock approximation. This yields the following correlation energy contributions [89]

$$E_{\mathrm{c}}^{\mathrm{CCSD}} = E^{\mathrm{mp2}} + E^{\mathrm{ppl}} + E^{\mathrm{rest}}, \tag{11.11}$$

where E^{mp2} corresponds to the MP2 correlation energy

$$E^{\mathrm{mp2}} = \sum_{ij} \sum_{ab} W_{ab}^{ij} \langle ab|V|ij\rangle \tag{11.12}$$

and the particle-particle ladder term is defined as

$$E^{\mathrm{ppl}} = \sum_{ij} \sum_{ab} W_{ab}^{ij} \sum_{cd} \langle ab|V|cd\rangle\, T_{ij}^{cd}. \tag{11.13}$$

We note that E^{mp2} was referred to as E^{driver} in previous related works [90, 163]. W_{ab}^{ij} is given by

$$W_{ab}^{ij} = \frac{2\langle ij|V|ab\rangle - \langle ji|V|ab\rangle}{\epsilon_i + \epsilon_j - \epsilon_a - \epsilon_b} \tag{11.14}$$

and it is the diagrams that close the CCSD correlation energy expression.

For the sake of brevity, we define E^{rest} such that it contains all remaining contributions to the CCSD correlation energy.

As discussed previously, the BSIE of the CCSD correlation energy is dominated by the BSIE in E^{mp2} and E^{ppl} [89].

The following discussion is based on the premise that the finite virtual orbital manifold is spanned by a set of canonical orbitals that needs to be augmented with additional virtual orbitals to reach the complete basis set (CBS) limit, while the occupied orbitals are fully converged to the CBS limit regardless of the approximations used in the virtual orbital space. This situation closely resembles *ab initio* calculations employing re-canonicalized frozen natural orbitals [174]. We choose the following index labels for occupied and virtual spatial orbitals

$i, j, k, \ldots$	occupied states
$a, b, c, \ldots$	virtual states in finite basis
$\alpha, \beta, \gamma, \ldots$	augmented virtual states
$\mathcal{A}, \mathcal{B}, \mathcal{C}, \ldots$	union of all virtual states.

The union of all virtual states spans the complete virtual orbital manifold. We stress that there is a difference in our notation compared to F12 literature, where α is the union of virtual states inside or outside the conventional orbital space.

The particle-particle ladder term E^{ppl} defined by Eq. (11.13) can also be expressed as

$$\epsilon_{ij}^{\text{A}} = \left\langle \Psi_{ij}^{(1)} \middle| V \middle| \Psi_{ij}^{\text{cc}} \right\rangle , \tag{11.15}$$

where

$$\left\langle \Psi_{ij}^{(1)} \right| = \sum_{ab} W_{ab}^{ij} \left\langle ab \right| , \tag{11.16}$$

and

$$\left| \Psi_{ij}^{\text{cc}} \right\rangle = \sum_{cd} T_{ij}^{cd} \left| cd \right\rangle . \tag{11.17}$$

Herein $\left|\Psi_{ij}^{(1)}\right\rangle$ refers to the linearized first order wavefunction whereas $\left|\Psi_{ij}^{\text{cc}}\right\rangle$ resembles a coupled-cluster pair wavefunction. In practice, these wavefunctions are calculated employing a finite virtual orbital basis set. Consequently, the ppl term only couples wavefunctions with the same occupied pair index. We note that the exponential CCSD pair wavefunction ansatz cannot be expressed by $\left|\Psi_{ij}^{\text{cc}}\right\rangle$ only but also depends explicitly on the HF wavefunction and other polynomials of single and double amplitudes not included in the definition of $\left|\Psi_{ij}^{\text{cc}}\right\rangle$.

We formally define the CBS limit of the linearized first-order and coupled-cluster-like pair wavefunction by

$$\left|\Psi_{ij}^{(1)\text{-cbs}}\right\rangle = \left|\Psi_{ij}^{(1)}\right\rangle + \left|\delta_{ij}^{(1)}\right\rangle \tag{11.18}$$

and

$$\left|\Psi_{ij}^{\text{cc-cbs}}\right\rangle = \left|\Psi_{ij}^{\text{cc}}\right\rangle + \left|\delta_{ij}^{\text{cc}}\right\rangle, \tag{11.19}$$

respectively. $\left|\delta_{ij}^{(1)}\right\rangle$ and $\left|\delta_{ij}^{\text{cc}}\right\rangle$ are defined such that they correct for the BSIE in the respective parent wavefunctions $\left|\Psi_{ij}^{(1)}\right\rangle$ and $\left|\Psi_{ij}^{\text{cc}}\right\rangle$. Following the notation of this article, the latter are obtained from a virtual basis set a. Already in 1985, Kutzelnigg discussed that the conventional expansion, using products of one-electron states, can not represent the wavefunction accurately at regions where the interelectronic distance approaches zero [114]. Thus, for increasing one-electron basis set sizes, the contribution of $\left|\delta_{ij}^{(1)}\right\rangle$ and $\left|\delta_{ij}^{\text{cc}}\right\rangle$ will largely be localized to the cusp region at small interelectronic distances. Substituting the above BSIE corrections into Eq. (11.15), yields the following contributions to the ppl energy in the CBS limit:

$$\epsilon_{ij}^{\text{B}} = \left\langle \delta_{ij}^{(1)} \middle| V \middle| \Psi_{ij}^{\text{cc}} \right\rangle \tag{11.20}$$

$$\epsilon_{ij}^{\text{C}} = \left\langle \Psi_{ij}^{(1)} \middle| V \middle| \delta_{ij}^{\text{cc}} \right\rangle \tag{11.21}$$

$$\epsilon_{ij}^{\text{D}} = \left\langle \delta_{ij}^{(1)} \middle| V \middle| \delta_{ij}^{\text{cc}} \right\rangle. \tag{11.22}$$

Consequently, the CBS limit formally reads

$$E^{\text{ppl-cbs}} = \sum_{ij} \left(\epsilon_{ij}^{\text{A}} + \epsilon_{ij}^{\text{B}} + \epsilon_{ij}^{\text{C}} + \epsilon_{ij}^{\text{D}} \right). \tag{11.23}$$

This work outlines an efficient approximation to $E^{\text{ppl}-\text{cbs}}$. To this end, we analyse ϵ_{ij}^{B} and ϵ_{ij}^{C} and provide suitable approximations for them in the following sections. We disregard ϵ_{ij}^{D} since it is of second-order in the BSIE of the pair wavefunctions (δ). We recall that ϵ_{ij}^{A} is evaluated in the conventional coupled-cluster calculation using the finite basis set.

3. Coupling of $\left|\delta_{ij}^{(1)}\right\rangle$ to $\left|\Psi_{ij}^{\text{cc}}\right\rangle$

We now turn to the expression for ϵ_{ij}^{B} and employ the resolution of the identity (RI)

$$\begin{aligned} \epsilon_{ij}^{\text{B}} = &\sum_{\alpha\beta} \left\langle \delta_{ij}^{(1)} \middle| \alpha\beta \right\rangle \left\langle \alpha\beta \middle| V \middle| \Psi_{ij}^{\text{cc}} \right\rangle \\ &+ \sum_{a\beta} \left\langle \delta_{ij}^{(1)} \middle| a\beta \right\rangle \left\langle a\beta \middle| V \middle| \Psi_{ij}^{\text{cc}} \right\rangle \\ &+ \sum_{\alpha b} \left\langle \delta_{ij}^{(1)} \middle| \alpha b \right\rangle \left\langle \alpha b \middle| V \middle| \Psi_{ij}^{\text{cc}} \right\rangle . \end{aligned} \tag{11.24}$$

The above equation can be interpreted as the coupling of the change of the first-order wavefunction to $|\Psi_{ij}^{\text{cc}}\rangle$. Due to $\left\langle \delta_{ij}^{(1)} \middle| ab \right\rangle = 0$, only projectors that involve at least one state from the augmented virtual basis have to be included in the RI. The orbitals ϕ_α, and ϕ_β are strongly oscillating in space, *i.e.*, they bear large wave number and/or high angular momentum number. In contrast, $|\Psi_{ij}^{\text{cc}}\rangle$ is expected to be much smoother. Following fundamental ideas of scattering theory, we replace the complicated scattering problem with a much simpler one, by means of the following approximation

$$\left|\Psi_{ij}^{\text{cc}}\right\rangle = \sum_{cd} T_{ij}^{cd} \left|cd\right\rangle \approx \left|ij\right\rangle g_{ij}^{\text{cc}}, \tag{11.25}$$

where $|ij\rangle$ is a mean-field state constructed from the Hartree–Fock orbitals of the occupied pair i and j. We stress that the left-hand-side and right-hand-side of Eq. (11.25) are orthogonal. However, this approximation is only used in the context of evaluation of matrix elements in expressions such as Eq. (11.24), which include the Coulomb interaction.

The scaling factor g_{ij}^{cc} is chosen such that the spatially averaged correlation hole depths of the correlated wavefunction and its mean-field approximation are equated after projection onto the occupied space of the same electron pair:

$$\sum_{cd} T_{ij}^{cd} \langle ij|\delta(\mathbf{r}_{12})|cd\rangle = \langle ij|\delta(\mathbf{r}_{12})|ij\rangle \, g_{ij}^{\mathsf{cc}}. \tag{11.26}$$

The appearing integrals are defined in an analogous manner to Eq. (11.9) but with the Coulomb kernel replaced by the Dirac delta function $\delta(\mathbf{r}_{12})$. When using Gaussian basis functions, this requires only minor modifications of the original integral routines (see [1]). From the above equation, we obtain an explicit expression for the pair-specific correlation hole depth scaling factor given by

$$g_{ij}^{\mathsf{cc}} = \frac{\sum_{cd} T_{ij}^{cd} \langle ij|\delta(\mathbf{r}_{12})|cd\rangle}{\langle ij|\delta(\mathbf{r}_{12})|ij\rangle}. \tag{11.27}$$

For the sake of brevity in the following paragraphs, we introduce a projection operator $\hat{g}_{ij}$ that yields an approximate mean-field state when applied to any correlated electron pair state, such that

$$|ij\rangle \, g_{ij}^{\mathsf{cc}} = \hat{g}_{ij} \left|\Psi_{ij}^{\mathsf{cc}}\right\rangle. \tag{11.28}$$

To get a better understanding of the above approximation, we now inspect the explicit expression for $\epsilon_{ij}^{\mathsf{B}}$ of a singlet state, which is given by

$$\langle \delta_{ij}|V|\psi_{ij}\rangle = \iint d\mathbf{r}_{12} d\mathbf{r}_{12} \tilde{\delta}_{ij}^{*}(\mathbf{r}_{12}, \bar{\mathbf{r}}_{12}) \frac{1}{|\mathbf{r}_{12}|} \tilde{\psi}_{ij}(\mathbf{r}_{12}, \bar{\mathbf{r}}_{12}). \tag{11.29}$$

Here, the electron-pair functions δ_{ij} and ψ_{ij} have been transformed to a real-space representation in $\mathbf{r}_{12} = \mathbf{r}_1 - \mathbf{r}_2$ and $\bar{\mathbf{r}}_{12} = \mathbf{r}_1 + \mathbf{r}_2$. Because $\tilde{\delta}_{ij}$ is largely localized around the cusp region, it effectively screens the Coulomb kernel at large interelectronic distances $|\mathbf{r}_{12}|$. $\epsilon_{ij}^{\mathrm{B}}$ is therefore dominated by contributions from short interelectronic distances. Moreover, $\tilde{\psi}_{ij}$ is a smooth function in the cusp region compared to $\tilde{\delta}_{ij}$, suggesting that

$$\tilde{\psi}_{ij}(\mathbf{r}_{12}, \bar{\mathbf{r}}_{12}) \approx \tilde{\psi}_{ij}(\mathbf{r}_{12} = 0, \bar{\mathbf{r}}_{12}) \tag{11.30}$$

is a reasonable approximation. $\tilde{\psi}_{ij}(0, \bar{\mathbf{r}}_{12})$ is the correlation hole depth as a function of $\bar{\mathbf{r}}_{12}$. The central approximation of this work is based on employing a mean field ansatz for $\tilde{\psi}_{ij}(0, \bar{\mathbf{r}}_{12})$ that is obtained by projecting $\tilde{\psi}_{ij}(0, \bar{\mathbf{r}}_{12})$ onto a corresponding zeroth-order mean-field wave function and ensuring that the spatially averaged correlation depths of the mean-field ansatz and $\tilde{\psi}_{ij}$ agree. This is achieved using the pair-specific projection operator $\hat{g}_{ij}$ defined in Eq. (11.28).

Using the mean-field approximation described above, i.e. operator $\hat{\Delta}_{ij}$, $\epsilon_{ij}^{\mathrm{B}}$ can be approximated as follows

$$\epsilon_{ij}^{\mathrm{B}} = \left\langle \delta_{ij}^{(1)} \middle| V \middle| \Psi_{ij}^{\mathrm{cc}} \right\rangle \approx \underbrace{\left\langle \delta_{ij}^{(1)} \middle| V \middle| ij \right\rangle}_{\Delta\epsilon_{ij}^{(2)}} g_{ij}^{\mathrm{cc}} \tag{11.31}$$

where $\Delta\epsilon_{ij}^{(2)}$ refers to the pair-specific BSIE correction of the MP2 correlation energy. Thus, we have shown that the $\epsilon_{ij}^{\mathrm{B}}$ contribution to the ppl term can be approximated using $\Delta\epsilon_{ij}^{(2)}$ times a scaling factor that depends on the spatially averaged correlation hole depth of $\left|\Psi_{ij}^{\mathrm{cc}}\right\rangle$.

4. Coupling of $\left|\delta_{ij}^{cc}\right\rangle$ to $\left|\Psi_{ij}^{(1)}\right\rangle$ We now focus on the coupling between the first-order wavefunction and the BSIE correction to Ψ_{ij}^{cc}. Using once more the RI we write Eq. (11.21) in the following way

$$
\begin{aligned}
\epsilon_{ij}^{\mathrm{C}} =& \sum_{\mathcal{CD}} \left\langle \Psi_{ij}^{(1)} \middle| V \middle| \mathcal{CD} \right\rangle \left\langle \mathcal{CD} \middle| \delta_{ij}^{\mathrm{cc}} \right\rangle \\
\approx& \sum_{\mathcal{CD}} \left\langle \Psi_{ij}^{(1)} \middle| \hat{g}_{ij}^{\dagger} V \middle| \mathcal{CD} \right\rangle \left\langle \mathcal{CD} \middle| \delta_{ij}^{\mathrm{cc}} \right\rangle \\
=& g_{ij}^{(1)} \sum_{\mathcal{CD}} \langle ij|V|\mathcal{CD}\rangle \left\langle \mathcal{CD} \middle| \delta_{ij}^{\mathrm{cc}} \right\rangle .
\end{aligned}
\tag{11.32}
$$

In the above equation, we have approximated the first-order state by a mean-field state that exhibits an identical spatially averaged correlation hole depth. Furthermore, the exact expression for $\left|\delta_{ij}^{\mathrm{cc}}\right\rangle$ is not accessible, as we do not intend to solve the coupled-cluster equations in the large basis set. Moreover, we note that $\langle cd|\delta_{ij}^{\mathrm{cc}}\rangle \neq 0$, which is in contrast to the BSIE of the first-order state, where $\langle cd|\delta_{ij}^{(1)}\rangle = 0$. Therefore, we approximate the orbital representation of $\left|\delta_{ij}^{\mathrm{cc}}\right\rangle$ including only the dominant contributions (driver and ppl) in the complete basis set limit of the amplitude equations as defined by Eq. (11.10):

$$
\begin{aligned}
\left\langle \mathcal{CD} \middle| \delta_{ij}^{\mathrm{cc}} \right\rangle \approx & \underbrace{\left\langle \mathcal{CD} \middle| \delta_{ij}^{(1)} \right\rangle}_{\mathrm{(I)}} \oplus \underbrace{\frac{\left\langle \gamma\zeta \middle| V \middle| \Psi_{ij}^{\mathrm{cc}} \right\rangle}{\epsilon_i + \epsilon_j - \epsilon_\gamma - \epsilon_\zeta}}_{\mathrm{(II)}} \\
& \oplus \underbrace{\frac{\left\langle c\zeta \middle| V \middle| \Psi_{ij}^{\mathrm{cc}} \right\rangle}{\epsilon_i + \epsilon_j - \epsilon_c - \epsilon_\zeta}}_{\mathrm{(III)}} \oplus \underbrace{\frac{\left\langle \gamma d \middle| V \middle| \Psi_{ij}^{\mathrm{cc}} \right\rangle}{\epsilon_i + \epsilon_j - \epsilon_\gamma - \epsilon_d}}_{\mathrm{(IV)}} \\
& \oplus \frac{\left\langle \mathcal{CD} \middle| V \middle| \delta_{ij}^{\mathrm{cc}} \right\rangle}{\epsilon_i + \epsilon_j - \epsilon_{\mathcal{C}} - \epsilon_{\mathcal{D}}} \oplus \cdots
\end{aligned}
\tag{11.33}
$$

The direct sum notation is used to emphasize the fact that γ is a subset of $\mathcal{C}$. In the following we consider only those terms defined by (I) – (IV) because they are of zeroth-order in $\delta \cdot V$, while the rest is $\mathcal{O}(\delta \cdot V)$.

We now turn to the contributions of the terms defined by (I) – (IV) to $\epsilon_{ij}^{\mathrm{C}}$. Inserting

(I) from Eq. (11.33) into the last line of Eq. (11.32) yields

$$\epsilon_{ij}^{\mathrm{C}}(\mathrm{I}) = g_{ij}^{(1)} \Delta\epsilon_{ij}^{(2)}. \tag{11.34}$$

To account for the contributions of (II) − (IV) to $\epsilon_{ij}^{\mathrm{C}}$, we again approximate $\left|\Psi_{ij}^{\mathrm{cc}}\right\rangle$ using the mean-field ansatz defined by Eq. (11.28).

Inserting the resulting approximations into the last line of Eq. (11.32) yields

$$\epsilon_{ij}^{\mathrm{C}}(\mathrm{II} - \mathrm{IV}) = g_{ij}^{(1)} \Delta\epsilon_{ij}^{(2)} g_{ij}^{\mathrm{cc}}. \tag{11.35}$$

Therefore, our final approximation to Eq. (11.21) is given by

$$\epsilon_{ij}^{\mathrm{C}} \approx \epsilon_{ij}^{\mathrm{C}}(\mathrm{I}) + \epsilon_{ij}^{\mathrm{C}}(\mathrm{II} - \mathrm{IV}) = \Delta\epsilon_{ij}^{(2)} \left(g_{ij}^{(1)} + g_{ij}^{(1)} g_{ij}^{\mathrm{cc}} \right), \tag{11.36}$$

which corresponds again to $\Delta\epsilon_{ij}^{(2)}$ scaled by a factor that depends on the correlation hole depths of $\left|\Psi_{ij}^{\mathrm{cc}}\right\rangle$ and $\left|\Psi_{ij}^{(1)}\right\rangle$.

We note that a corresponding BSIE correction in MP3 theory would have to include $\epsilon_{ij}^{\mathrm{C}}(\mathrm{I})$ only. However, in CCSD theory the BSIE of $|\Psi_{ij}^{\mathrm{cc}}\rangle$ is not well approximated using $\delta_{ij}^{(1)}$. Therefore $\epsilon_{ij}^{\mathrm{C}}(\mathrm{II} - \mathrm{IV})$ accounts for the change of $\delta_{ij}^{(1)}$ due to the most important ppl coupling terms linear in $|\Psi_{ij}^{\mathrm{cc}}\rangle$. The coupling strength of these terms is on the order of g_{ij}^{cc} and needs to be included to attain high accuracy.

5. The pair-specific PPL basis-set correction We now summarize the final approximation to the BSIE correction of the ppl energy:

$$\epsilon_{ij}^{\mathrm{B}} + \epsilon_{ij}^{\mathrm{C}} \approx \Delta\epsilon_{ij}^{(2)} \left(g_{ij}^{\mathrm{cc}} + g_{ij}^{(1)} + g_{ij}^{(1)} g_{ij}^{\mathrm{cc}} \right). \tag{11.37}$$

We stress that the contribution of $\epsilon_{ij}^{\mathrm{D}}$ defined in Eq. (11.22) has been neglected because it is not of leading order in δ. We arrive at the following approximate CBS

limit expression of the ppl energy:

$$E^{\text{ps-ppl}} = E^{\text{ppl}} + \underbrace{\sum_{ij} \Delta\epsilon_{ij}^{(2)} \left(g_{ij}^{\text{cc}} + g_{ij}^{(1)} + g_{ij}^{(1)} g_{ij}^{\text{cc}} \right)}_{\Delta\text{ps-ppl}} . \tag{11.38}$$

At this point, we note again that in the above expression the pair-specific correlation hole depth scaling factors g_{ij}^{cc} and $g_{ij}^{(1)}$ are computed in a finite basis set, whereas $\Delta\epsilon_{ij}^{(2)}$ refers to the BSIE correction of the pair-specific MP2 correlation energy.

11.6 Finite size effects

In extended systems, an additional problem in practical calculations is the size of the simulation cell. An extended system is supposed to be macroscopic in size, but this limit can only be reached in model systems and not in realistic atomistic simulations. Therefore, studying and characterizing the behaviour of properties such as the energy with respect to the system size is of paramount importance. Several techniques are used throughout the literature in order to obtain finite size corrections, from simple extrapolations of the energies to extrapolations of the electronic transition structure factor [178, 66, 121].

Part III

Defects in solids

This chapter is an adaptation of the publication found in [59].

Chapter 12

Introduction

DFT [104, 85] using approximate exchange and correlation energy density functionals is arguably the most successful ab initio approach to compute materials properties. Its application goes beyond ground state properties by providing a reference or starting point for methods that treat excited-state phenomena explicitly.

In this context, theories such as Time-Dependent Density Functional Theory (TD-DFT) [136, 153] and the GW approximation [76] are widely-used to tackle excited states in molecules and solids [161, 63]. Nonetheless, they often suffer from a strong dependence on the DFT reference calculation. In the case of TD-DFT results depend strongly on the choice of the approximate exchange and correlation density functional. Similarly, so-called non-selfconsistent G_0W_0 quasiparticle energies depend strongly on the Kohn-Sham orbital energies, whereas fully self-consistent GW calculations are not as often performed and do not necessarily improve upon the accuracy compared to G_0W_0 [67]. To compute charge neutrality preserving optical absorption energies from the electron addition and removal energies obtained in the GW framework, it is necessary to account for the exciton binding energy. Excitonic effects are often approximated using the Bethe-Salpeter equation (BSE) [154]. We note that despite the high level of accuracy and efficiency of GW BSE calculations [148], many choices and approximations have to be made in practice that are difficult to justify in a pure ab initio framework. Therefore, it seems worthwhile to explore alternative methods that are less dependent on DFT approaches.

CC [37, 38, 35] formulations are widely-used in the field of molecular quantum chemistry for both the ground state and excited states via the EOM-CC formalism [168].

Ground state CC theories such as CCSD and CCSD(T) [144, 167] have become one of the most successful methods in molecules in terms of their systematically improvable accuracy and computational efficiency. Likewise, EOM-CC methods are routinely applied to molecular systems with great success [169, 11, 137, 187, 91]. However, we stress that the computational cost of CC theories is significantly larger than that of Green's function based methods mentioned above. Nonetheless, several studies have focused on making use of these wavefunction methods also in solids to study ground and excited state properties [66, 60, 127].

While EOM type methods are well understood and benchmarked in finite systems, this is less so for periodic systems, where ongoing efforts are made towards applications in solids. Previous applications of EOM type methods have focused on electronic band structures using the Ionization Potential EOM-CC (EOM-CC) and Electron Attachment EOM-CC (EOM-CC) extensions [127, 60, 141, 60, 128] as well as its Electron Excitation EOM-CC (EOM-CC) extensions [95, 188], all of which are based on Gaussian basis sets. For local phenomena, such as defect excitation energies, several studies have been performed employing cluster models of the periodic structures [179, 166]. One of the main challenges in these calculations is to achieve a good control over the finite basis set and system size errors, which is often achieved using extrapolation techniques.

In this chapter, we study excited state properties of point defects in solids, computed on the level of EE-EOM-CC. Understanding impurities in solids is important for both theoretical and practical reasons. Lattice defects affect bulk properties of the host crystal and both the understanding of ground and excited-state properties is essential for these systems [58, 184]. Here, we focus on color centers in the alkaline earth oxide crystals MgO, CaO and SrO in the rock salt structure. Removing an oxygen atom from these systems results in so-called F-centers that can be filled by 2 (F^0), 1 (F^+) or 0 (F^{2+}) electrons. The corresponding one-electron states are stabilized by the Madelung potential of the crystal and their electron density is in general localized in the cavity formed by the oxygen vacancy. These defects are typically produced by neutron irradiation [149] or

additive colorization [46]. Much effort has been made to elucidate the exact mechanism of the luminescence of F-centers in MgO, CaO and SrO [15, 171]. The ground and excited state properties of these vacancies are of importance for a wide range of technological applications including color center lasers. Furthermore, vacancies of oxides are of general importance for understanding their surface chemistry and related properties.

In this chapter we will concentrate on the diamagnetic F^0-center. The trapped electrons can be viewed as a pseudo-atom embedded in a solid, where the optical absorption and emission between ground and low-lying excited states is characterized by the electron transfer between $1s$ into $2s$ or $2p$ one-electron states. Initial theoretical studies of these defects were already performed in the 1960s and 1970s using effective Hamiltonians [99, 195, 194]. Modern ab initio studies of the F^0 center in MgO have employed cluster approaches in combination with quantum chemical wavefunction based methods [166], fully periodic supercell approaches in combination with the GW-BSE approach [146, 180] or Quantum Monte Carlo calculations [50]. In this chapter we seek to employ a periodic supercell approach and a novel implementation of EE-EOM-CCSD theory using a plane wave basis set. In addition to the F-center in MgO, we will also study F-centers in CaO and SrO. We note that EE-EOM-CCSD theory is exact for ground and excited states of two electron systems and is therefore expected to yield very accurate results for the F^0 center in alkaline earth oxides. We will discuss different techniques to correct for finite basis set and supercell size errors and demonstrate that EE-EOM-CCSD theory can be used to compute accurate absorption and emission energies compared to experiment without the need for adjustable parameters and the ambiguity caused by the choice of the starting point.

Chapter 13

Benchmark results

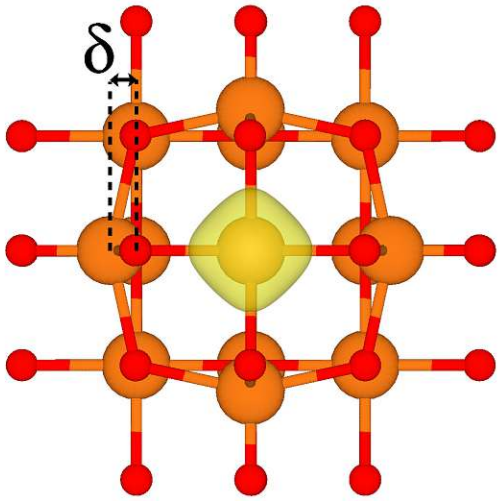

Figure 13.1: Geometry of neutral F-center in MgO. Red and orange spheres correspond to oxygen and magnesium atoms, respectively. The yellow isosurface was computed from the localized electronic states in the band gap of MgO that originates from the two trapped electrons. δ measures the displacement along the A_{1g} vibrational mode with the Mg atoms out of their equilibrium position in the bulk structure and was deliberately chosen larger for this figure to emphasize the effect of lattice relaxation.

Here, all EE-EOM-CCSD calculations of defective supercells employ a HF reference. The HF calculations are performed using the Vienna ab initio simulation package (VASP) [109]

and a plane wave basis set in the framework of the projector augmented wave (PAW)[19] method. The energy cutoff for the plane wave basis set is 900eV. The defect geometries have been relaxed on the level of DFT PBE, starting from a defective geometry with the corresponding equilibrium lattice constant (MgO: 4.257Å, CaO: 4.831Å, SrO: 5.195Å) keeping the lattice vectors and volume fixed.

In this chapter we study defective 2×2×2, 3×3×3 and 4×4×4 fcc supercells containing 15, 53, and 127 atoms, respectively. The oxygen vacancy results in an outward relaxation of the alkaline earth atoms away from the cavity created by the oxygen vacancy. This outward relaxation strongly overlaps with the vibrational mode A_{1g} and is illustrated in Fig.13.1. While the DFT PBE calculations have been carefully checked for convergence with respect to the k-point mesh used to sample the first Brillouin zone, all HF and post-HF calculations employ the Γ-point approximation.

We have implemented UCCSD and EE-EOM-CCSD in the Coupled Cluster For Solids (CC4S) code that was previously employed for the study of various ground state properties of periodic systems [66, 86]. The employed Coulomb integrals and related quantities were calculated in a completely analogue manner. Our UCCSD implementation is based on the intermediate amplitudes approach of Stanton et al. [170]. On the other hand, our EE-EOM-CCSD implementation uses intermediates for the similarity transformed Hamiltonian $e^{-\hat{T}}\hat{H}e^{\hat{T}}$ from Stanton et al.[168] and Shavitt et al.[162]. We use the Cyclops Tensor Framework (CTF) [164] for the implemented computer code, which enables an automated parallelization of the underlying tensor contractions.

The similarity transformed Hamiltonian is a non-Hermitian operator and therefore left and right eigenvectors differ in general. The diagonalization of the similarity transformed Hamiltonian is done using a generalized Davidson solver [82, 28]. This solver enables the calculation of EE-EOM-CCSD energies by approximating the left eigenvector space by the right eigenvector space. For the initial guess of the eigenvectors, we use the one-body HF excitation energies and corresponding Slater determinants. The UCCSD and EE-EOM-CCSD calculations have been performed using only a small number of active HF orbitals around the Fermi energy of the employed supercells. Most occupied orbitals at low energies

are frozen and the same applies to all unoccupied orbitals above a certain cutoff energy. The following sections summarize the benchmarks of the implemented EE-EOM-CCSD code and investigate the convergence behavior of the computed excitation energies with respect to the number of active orbitals as well as system size.

13.1 Orbital basis convergence of excited states

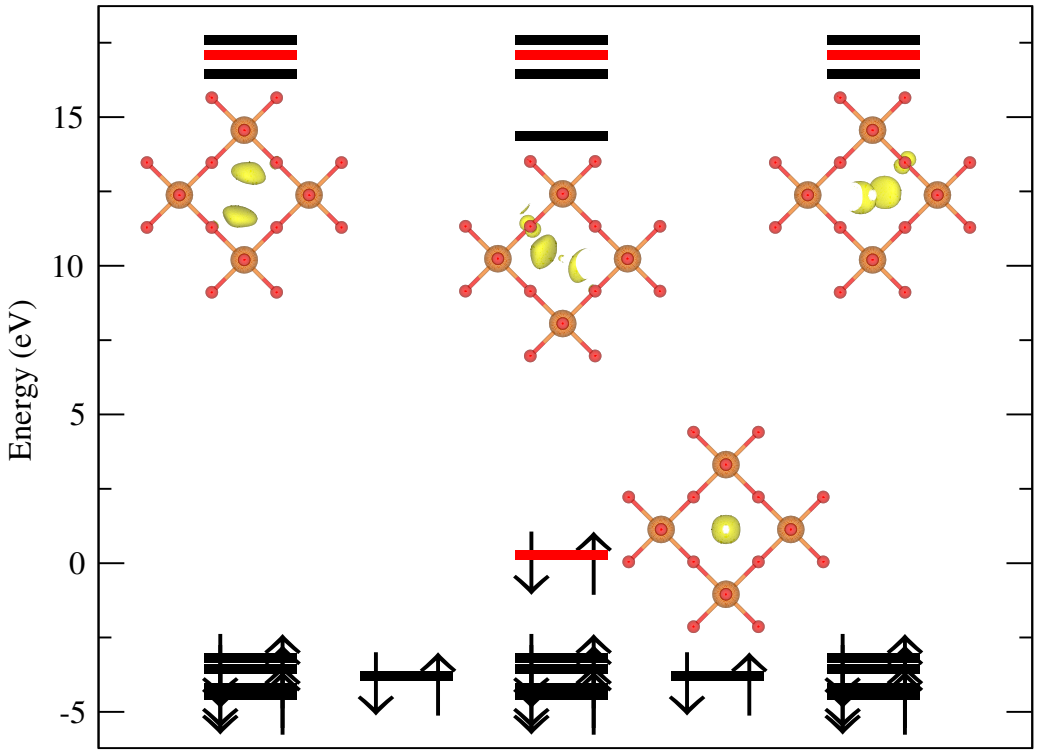

Figure 13.2: Occupied and virtual HF energy levels. The red levels correspond to defect states and the corresponding isosurfaces of the charge densities are depicted.

All presented findings in this section have been obtained for the F-center in MgO. However, the corresponding findings for CaO and SrO are qualitatively identical unless stated explicitly.

We first seek to investigate the character of the employed HF orbitals and the convergence of the computed excitation energies with respect to the canonical orbital basis set size.

The HF orbitals have been computed for a defective 2×2×2 MgO supercell containing 15 atoms. Figure 13.2 depicts the energy levels around the Fermi energy and isosurfaces of charge densities computed for the defect states. The occupied state with the highest one-electron energy corresponds to the occupied defect state and its orbital energy is located in the gap of the bulk crystal. Its charge density is well localized in the cavity created by the oxygen vacancy. In the thermodynamic limit (big supercells or dense k-meshes), the direct and fundamental gap of pristine MgO is 15.5 eV on the level of HF theory [68], which is significantly larger than the experimental gap of about 7.8 eV. The neglect of correlation effects in HF theory overestimates band gaps for a wide range of simple semiconductors and insulators. The orbital ordering between defect and bulk states depicted in Fig.13.2 is qualitatively identical to the one observed for CaO and SrO. However, we stress that in contrast to MgO, CaO and SrO exhibit an indirect band gap with a conduction band minimum at the Brillouin zone boundary.

We note that the supercells investigated in this work contain up to 127 atoms, corresponding to more than 1000 valence electrons. The computational cost of EE-EOM-CCSD theory scales as $\mathcal{O}(N^6)$, where N is some measure of the system size. In particular, the cost for some of the most important tensor algebraic operations scales as $\mathcal{O}(N_\mathrm{v}^4 N_\mathrm{o}^2)$ and $\mathcal{O}(N_\mathrm{v}^2 N_\mathrm{o}^4)$, where N_o and N_v refer to the number of occupied and virtual orbitals, respectively. Additionally, the memory footprint of our implementation scales as $\mathcal{O}(N^4)$. Due to the steep scaling of the computational cost, an explicit treatment of all electrons on the level of EE-EOM-CCSD becomes intractable and renders it necessary to freeze a large fraction of the occupied and virtual HF states. In the following we will investigate the convergence of the computed excitation energies with respect to the number of active virtual and occupied states.

We first investigate the convergence of EE-EOM-CCSD excitation energies with respect to the virtual orbital basis set. Among the 61 occupied spatial HF orbitals we keep only the four orbitals active with the highest energy. Furthermore, we only investigate many-electron excited states with r_i^a excitation amplitudes that correspond to a significant charge transfer from the occupied s-like defect state to the virtual p-like defect states as illustrated in Fig.13.2. Fig.13.3 depicts the convergence of the EE-EOM-CCSD excitation energies

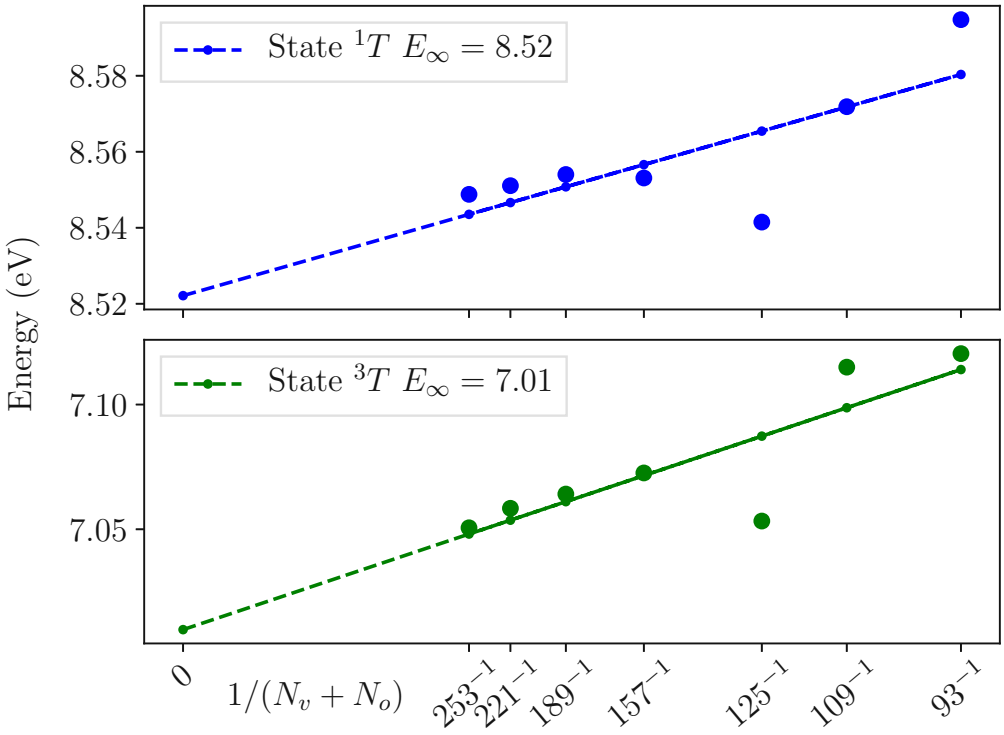

Figure 13.3: Basis set extrapolation of lowest EE-EOM-CCSD excitation energies corresponding to excitations of the F-center defect in MgO. All computed energies have been fitted against $1/(N_\mathrm{v} + N_\mathrm{o})$, where N_v and N_o is the number of virtual and occupied orbitals used. The lower and higher excitation energies correspond to a singlet-triplet and a singlet-singlet transition, respectively. This extrapolation has been obtained for a supercell composed of eight Mg and seven O atoms.

that we assign to local excitations of the F-center. In passing we note that EE-EOM-CCSD theory predicts a number of excited states that describe electronic excitations with charge transfer from the defect to bulk states, which will not be explored in this work. The electronic ground state of the neutral F-centers studied in this work is a singlet state. The lower and higher excitation energies shown in Fig.13.3 correspond to a singlet-triplet and singlet-singlet transition energy, respectively. We observe for both excitation energies a $1/(N_v + N_o)$ convergence to the complete basis set limit. This behavior is not unexpected and agrees with the convergence of ground state energies. Furthermore, we note that a similar convergence was observed for EE-EOM-CCSD exciton energies of bulk materials [188] and for excitation energies of the cytosine molecule [108]. We note that it might seem advantageous to replace HF virtual orbitals with a different type of orbitals; for example, natural orbitals, to accelerate the convergence. However, we have found that these orbitals will mostly accelerate the convergence of the ground state energy, introducing large basis set incompleteness errors in the convergence of excitation energies. In this work we will employ a $1/(N_v + N_o)$ extrapolation to approximate excitation energies in the complete basis set limit of all systems.

Fig.13.4 shows the employed basis set extrapolation for identical transitions in a larger 4×4×4 supercell. We note that the slope of the excitation energy extrapolation is significantly steeper compared to the 2×2×2 supercell shown in Fig.13.3. This can be attributed to the smaller number of virtual orbitals relative to the complete basis set size for the given plane wave cutoff energy. Therefore we ignore the first 4 points in the extrapolation for *all* systems in the 4×4×4 supercell. In the case of CaO and SrO, the basis set convergence of the excitation energies is qualitatively identical, and we employ the same orbital basis set sizes in all extrapolations.

We now investigate the convergence of the EE-EOM-CCSD excitation energies with respect to the number of active occupied orbitals, keeping a virtual orbital basis set consisting of 10 unoccupied orbitals and employing a 2×2×2 supercell only. Figure 13.5 depicts the convergence of the lowest defect excitation energy (singlet-triplet transition) with respect to the size of the active occupied orbital space. The horizontal axis at the bottom shows the number of active occupied orbitals. The horizontal axis at the top of Fig.13.5 shows

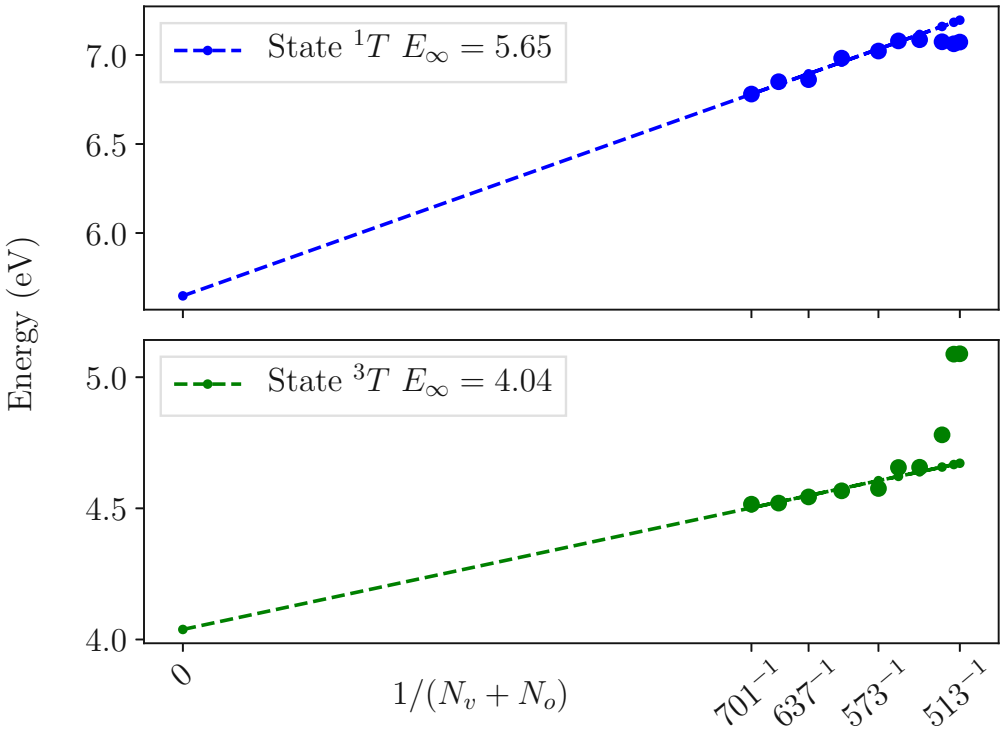

Figure 13.4: Basis set extrapolation of lowest EE-EOM-CCSD excitation energies corresponding to excitations of the F-center defect in MgO using a 4×4×4 supercell. The fit has been performed ignoring the first four data points. States, energies and fit are to be interpreted as in Fig.13.3.

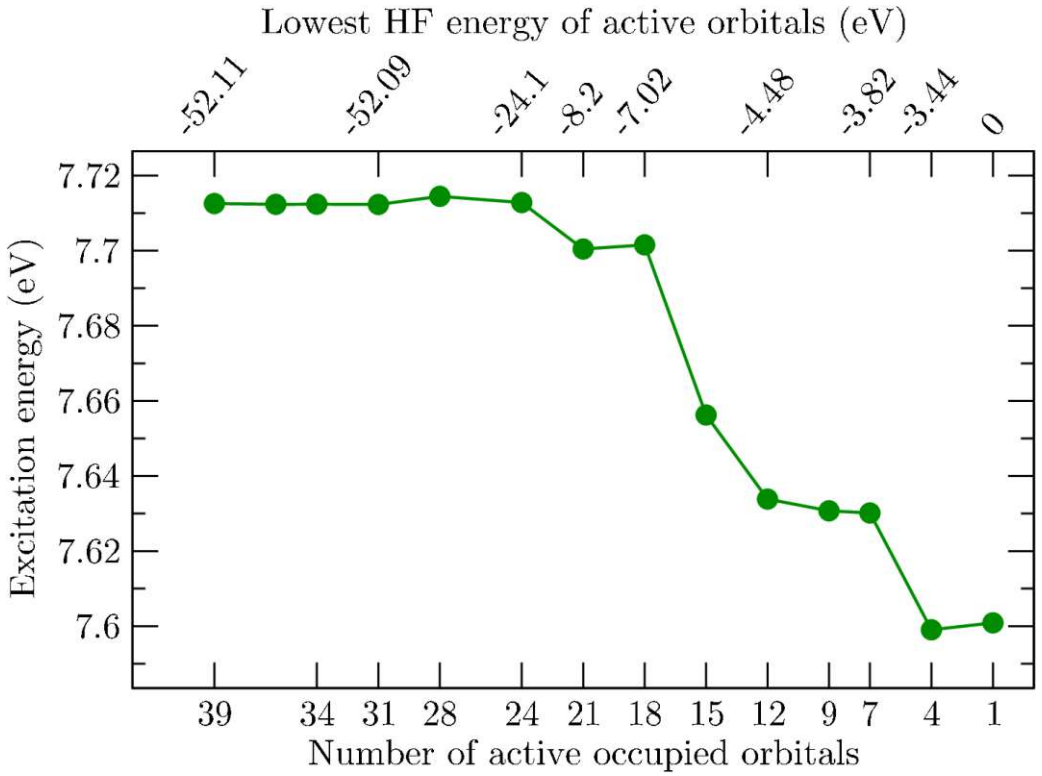

Figure 13.5: Convergence of the EE-EOM-CCSD excitation energy for the singlet-triplet transition in the F-center of MgO with respect to the number of inactive/frozen occupied orbitals in the EE-EOM-CCSD calculation. For the employed supercell the HF, calculations have been performed using 61 occupied and 10 virtual orbitals. The top horizontal axis shows the lowest HF energy of the included active occupied orbital relative to the occupied defect state. All orbitals with a lower energy have not been included in the respective EE-EOM-CCSD calculation.

the corresponding lowest HF orbital energy. Our findings demonstrate that the excitation energy increases with respect to the number of active occupied orbitals and is well converged to within a few meV using more than about 25 occupied orbitals. However, a comparison between the converged result and a minimal active occupied orbital space, consisting of the occupied defect orbital only, reveals that such a truncation introduces excitation energy errors of about 120 meV. We note that one-electron states with relative energies below -50 eV exhibit Mg $2p$ and $2s$ character and are therefore expected to be negligible for the computed excitation energies. From the above findings we conclude that the excitations studied in the present work exhibit a significantly larger error from the virtual orbital basis truncation than from the occupied orbital basis truncation. Due to the computational cost of EE-EOM-CCSD calculations we will therefore extrapolate the excitation energy to the complete basis set limit while using only 4 occupied orbitals.

13.2 System size convergence of excitation energies

Table 13.1: Convergence of the F-center's excitation energies in MgO, CaO and SrO for increasing supercell size. TDL corresponds to the extrapolated thermodynamic limit estimate of the respective excitation energies assuming a $1/N$ convergence and employing the energies of the 2×2×2 and 4×4×4 supercells. Here N stands for a measure of the system size. In this case, the number of electrons is used. All energies in eV units.

System	Supercell	^3T	^1T
MgO	2×2×2	7.009	8.522
	3×3×3	4.866	6.571
	4×4×4	4.038	5.646
	TDL	3.660	5.281
CaO	2×2×2	3.224	3.338
	3×3×3	2.951	4.025
	4×4×4	2.081	3.157
	TDL	1.936	3.134
SrO	2×2×2	2.324	2.413
	3×3×3	2.404	3.155
	4×4×4	1.332	2.351
	TDL	1.206	2.343

Having discussed basis set convergence of the computed EE-EOM-CCSD excitation energies, we now turn to the discussion of their convergence with respect to supercell size. Excitation energies are intensive quantities. However, their convergence with respect to system size can sometimes be extraordinarily slow. We have computed the F-center's singlet-triplet and singlet-singlet transition energies for three different supercell sizes containing 15, 53 and 127 atoms. Table 13.1 lists the computed excitation energies for all systems using different supercell sizes. The excitation energies have been obtained using 4 active occupied orbitals only and extrapolating to the complete basis set limit as discussed in the previous sections.

We note that the excitation energies converge monotonously for MgO with increasing supercell size, but show some non-monotonic behaviour for the other two systems studied. This can be explained by the fact that CaO and SrO exhibit a conduction band minimum at the Brillouin zone boundary. The electronic states at the conduction band minimum are therefore only accounted for when using supercells that are constructed from even-numbered multiples of the fcc unit cell. Neglecting these important states around the Fermi energy leads to a significant overestimation of the excitation energies for the excited singlet states as can be seen by comparing the results obtained for the $3\times3\times3$ supercell to findings for the $2\times2\times2$ and $4\times4\times4$ supercells.

Here, we seek to remove the remaining finite size errors of the excitation energies by performing an extrapolation to the infinite system size limit assuming a $1/N$ convergence, where N is the total number of electrons in each supercell. This approach is in agreement with procedures that are applied to ground state energy calculations [66, 121]. For the sake of consistency we employ only $2\times2\times2$ and $4\times4\times4$ supercells for the extrapolation for all three studied systems.

Our findings show that the excitation energies decrease significantly with increasing supercell size in the case of MgO. Changing the supercell size from a $2\times2\times2$ to a $4\times4\times4$ cell results in a lowering of the excitation energies by almost 3 eV. This relatively slow convergence is expected to originate from strongly delocalized excited defect states of the neutral F-center in MgO. We note in passing that the excitation energies of the F-centers in CaO and SrO exhibit a significantly faster convergence with respect to system size. We

attribute this behavior to a more localized character of the excited F-center in CaO and SrO compared to MgO that might be explained by the significantly smaller size of the cavity formed by the oxygen vacancy in MgO compared to CaO or SrO.

Chapter 14

Results and discussions

In this chapter we describe the photochemical process of absorption and emission in the F-center of alkaline earth oxides. We first discuss the energies of the electronically excited defect states as a function of the atomic displacements along the A_{1g} vibrational mode in MgO to introduce the emission model. Next, we present our results for the absorption and emission of the F-center in MgO, where problems in the interpretation of the experimentally observed luminescence band are discussed additionally. We end this chapter with a discussion of the results for CaO and SrO.

14.1 Absorption and emission process in F-centers

Our analysis of the emission process is based on a Franck-Condon [55, 40] description of the defect. This is a common approach to treat emission processes in solids and molecules [194, 123, 2].

Figure 14.1 shows the configuration coordinate diagram along an approximate A_{1g} vibrational mode for the most important EE-EOM-CCSD excited states and the UCCSD ground state singlet $^1A_{\mathrm{CC}}$. We approximate the atomic displacement along the A_{1g} mode by increasing the outward displacement of the alkaline earth atoms as depicted in Fig. 13.1, and keeping all other atomic positions of the employed 4×4×4 supercell fixed. The configuration curve has been computed only for MgO but serves as a qualitatively identical model

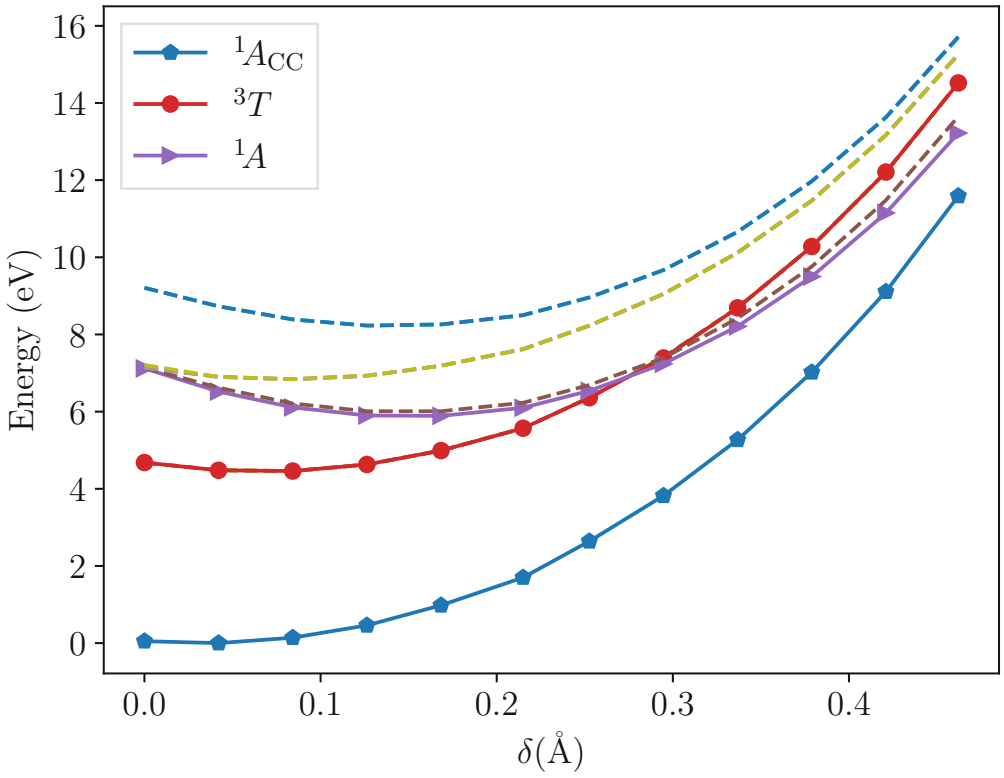

Figure 14.1: Configuration curve along the phonon A_{1g} mode for the excited states of the F-center in MgO own in Fig. 13.1). $^1A_{CC}$ curve represents the singlet UCCSD ground state e upper curves depict the EE-EOM-CCSD excited states. lines represent EE-EOM-CCSD states that do not play a role for scussion, but are included for completeness. The energies presented are energy differences between the excited energies and the UCCSD energy. calculation was done for a 4×4×4 containing 127 atoms, 4 active electrons and 64 virtual orbitals.

for CaO and SrO. Within this picture, the absorption is given by the optically allowed transition of ${}^1A_{\mathrm{CC}} \rightarrow {}^1T$ at the ground state geometry in Fig. 14.1.

Taking into account the Franck-Condon approximation, once the F-center is in the excited singlet state, a relaxation of the atoms along the ${}^1A_{1g}$ vibrational mode sets off which could induce a crossing in the configuration curve with the excited triplet state ${}^3T$. Luminescence is then achieved through the transition ${}^3T \rightarrow {}^1A_{\mathrm{CC}}$. From the above discussion and the fact that the minimum of the ${}^3T$ state is close to the minimum of the ground state, we conclude that the absorption and emission energies can therefore be well approximated using the energy differences computed in the equilibrium structure of the electronic ground state for the F-center.

14.2 MgO

The F-center in MgO was first discovered by Wertz et al. [190] in its positively charged variant (F^+-center) by electron spin resonance measurements, showing a strong localization of the electrons in oxygen vacancies. A host of experimental results followed and with it a better understanding of the absorption and luminescence mechanisms [36, 80, 184]. Experimental and theoretical studies have shown that the Mg atoms relax in an outward direction from the vacancy [182, 70].

By using a semi-empirical model, Kemp and Neeley [99] predicted an optical absorption energy of 4.73 eV in good agreement with experimental findings of 4.95 eV [36, 79]. The luminescence band of the F^+ center was measured at around 3.15 eV [30] while for the F^0 center a luminescence of 2.4 eV was predicted from temperature dependent measurements of the absorption spectrum in conjunction with a simplified Huang-Rhys model approach [79].

Using EE-EOM-CCSD in combination with the outlined extrapolation techniques yields an absorption and emission energy of 5.2 eV and 3.66 eV, respectively. Previous many-body ab initio calculations using GW-BSE [146], quantum Monte Carlo [50] methods and CASPT2 [166] agree with our results for both absorption and emission to within about 0.4 eV as summarized in Table 14.1. The calculated absorption energies are in

Table 14.1: Obtained results from this work for the absorption and emission energies of the F-centers in MgO, CaO and SrO. The EE-EOM-CCSD results are extrapolated to the complete basis set and infinite supercell size limit in order to allow for a direct comparison between theory and experiment. The GW gaps do not correspond to optical excitation energies but are included for comparison. All energies are in eV units.

System	Method	Absorption	Emission
MgO	EE-EOM-CCSD	5.28	3.66
	Exp. [193]	5.0	2.4
	QMC. [50]	5.0(1)	3.8(1)
	CASPT2 [166]	5.44	4.09
	G_0W_0@LDA0-BSE. [146]	4.95	3.4
	G_0W_0@LDA0 [146]	5.4	
	G_0W_0@PBE [180]	4.48	
	GW_0@PBE [180]	4.71	
	GW@PBE [180]	5.20	
CaO	EE-EOM-CCSD	3.13	1.93
	Exp. [17, 16]	3.02	1.93
	Exp. [193]	3.1	2.05 – 2.01
	TDDFT@B3LYP [29]	3.52	2.1
	G_0W_0@PBE [180]	3.20	
	GW_0@PBE [180]	3.53	
	GW@PBE [180]	3.87	
SrO	EE-EOM-CCSD	2.34	1.2
	Exp.[193]	2.4	

good agreement with experimental measurements of 5.0 eV. We note, however, that the GW results (excluding the exciton binding energy) obtained for different levels of self-consistency and DFT references exhibit a significant variance ranging from 4.48 eV to 5.4 eV. Consequently, GW-BSE absorption energies are strongly dependent on the DFT reference. Furthermore, we stress that a direct comparison of the computed emission energies between the quantum chemical approaches (EE-EOM-CCSD and CASPT2) and QMC or GW is complicated by the fact that the latter approaches do not consider the emission process of the de-excitation from the excited triplet states. Instead, the emission energies computed using QMC and GW-BSE correspond to the decay from the excited singlet state in its relaxed geometry along the A_{1g} mode. Nonetheless, from the results shown in Fig. 14.1, we conclude that these different emission energies are expected to agree to within the errors made by other approximations.

The measured experimental emission at 2.4 eV [46] and its interpretation is the topic of an ongoing debate. Initially, this peak has been attributed to the F-center and common interpretations have ranged from a singlet-singlet transition to a ${}^3T_{1u} \rightarrow {}^1A_{1g}$ transition [195, 193]. However, it was first suggested by Edel et al. [46, 47, 45] that this band results from a recombination process similar to recombination processes in semiconductors. Edel and coworkers argue that the three-electron vacancy F^- recombines with the F^+-center. Rinke et al. [146] have suggested that the 2.4 eV emission is produced when electrons in the defect orbitals recombine with the valence holes that can be produced by intense UV light irradiation. The creation of these holes is possibly also related to the concentration of H^- impurities that are commonly present in MgO samples, especially when these have been thermochemically reduced [64, 31, 93, 149, 172].

The presence of H^- impurities in MgO could account for the long-lived luminescence through a hopping mechanism of the electrons from H^- to H^- impurities until they encounter an F-center. However, it is not immediately clear from the ab initio calculations thus far if these states are orbital and spin triplets or otherwise as has been proposed in experimental evidence and symmetry arguments [193]. It has been noticed, however, that the strength of the 2.4 eV band is temperature dependent as well as F-center and H^- concentration dependent [172].

Typically, neutron irradiation produces mainly F^+-centers while electron irradiation or additive colorization induces mainly F-centers [46]. Rinke et al. argue that given the fact that the position of the absorption band for the F and F^+ centers are almost identical, it is to be expected that this is also the case for the emission. Even though similar luminescence peaks for these centers have been predicted in Ref. [146], no substructure in the emission band can be observed experimentally (unlike in the absorption band). Here, we propose a different interpretation of this observation. We suggest that the F-center does not in fact luminesce. Indeed, modern theoretical computations seem to agree on the fact that the 2.4 eV band does not belong to the F-center luminescence process. We stress that all theoretical results for the emission energy summarized in Table 14.1 range from 3.4 eV to 4.09 eV. Moreover, there is a strong photoconversion from F into F^+-centers [94], suggesting that before the F-center has a chance to luminesce, a conversion into F^+ happens followed by an absorption of the F^+-center since the absorption band for it is similar to the F-band. Our calculations show that the excitation energy for the singlet state in the F-center of MgO converges very slowly with respect to the system size, indicating that the optically excited state is significantly more delocalized than the ground state. This could make a photoconversion into F^+ significantly more likely and therefore corroborates our interpretation.

14.3 CaO and SrO

Historically, one of the best studied F-centers in the alkaline earth oxides is the one in CaO [195]. The identification of the F-center's charged state is made easier by the fact that, unlike for MgO, the absorption band is different for the F and F^+ centers. Furthermore, we note that the lattice constant of CaO is significantly larger than for MgO, which leads to a reduced confinement of the trapped charges and shifts the absorption band to lower energies. Early theoretical and experimental investigations have interpreted the 2.0 eV emission band to be a transition from a spin and orbital triplet $^3T_{1u}$ into the ground state singlet $^1A_{1g}$ [48, 17, 195]. However, a $^1T_{1u} \rightarrow {}^1A_{1g}$ transition is also possible at a slightly higher energy. In general, the CaO luminescence mechanism has been found to

be a combination of a singlet-singlet and a triplet-singlet transition which are activated at different temperatures [17, 16]. Since the excited triplet state lies slightly below in energy from the excited singlet state, there is a population conversion at temperatures of around 600 K. Namely, at low temperatures up to 300 K one measures a transition at around 1.98 eV, whereas as the temperature increases the excited singlet gets populated and a much more rapid luminescence gets gradually triggered at around 2 eV [17, 16].

Using EE-EOM-CCSD in combination with the outlined extrapolation techniques yields an absorption and emission energy of 3.13 eV and 1.93 eV for the F-center in CaO, respectively. To the best of our knowledge only one TD-DFT result can be found in literature for this system, predicting an absorption and emission energy of 3.52 eV and 2.1 eV, respectively. Table 14.1 also summarizes two different experimental estimates, showing that the EE-EOM-CCSD and TDDFT@B3LYP calculations agree with experiment to within 0.1 eV and 0.5 eV, respectively. We note again that GW results for the absorption energy obtained for different levels of self-consistency shows a significant variance ranging from 3.2 eV to 3.87 eV and can not be compared directly to experiment due to the neglect of the exciton binding energy.

We note that our quantum chemical results have been obtained using periodic boundary conditions, whereas previous calculations have been carried out using a cluster model approach [166, 29].

Finally, we turn to the discussion of the F-center in SrO. This system exhibits an even larger lattice constant and the absorption and emission energies are shifted to even lower energies compared to MgO and CaO. However, the F-center in SrO is qualitatively very similar to the CaO case, and the agreement of EE-EOM-CCSD in both cases with experimental values is excellent. To the best of our knowledge, there exist only experimental estimates of the absorption energy with about 2.4 eV, whereas no measurements for the emission band are known to the authors. We report the results for the singlet-triplet absorption ${}^1A_{\mathrm{CC}} \rightarrow {}^3T$ and triplet-singlet emission ${}^3T \rightarrow {}^1T$ in the infinite supercell size limit in Table 14.1. We hope that this prediction will be verified experimentally in the future.

Part IV

Basis set corrections for coupled cluster

The contents of this chapter are slightly adapted from the publication *Focal-point approach with pair-specific cusp correction for coupled-cluster theory* [87].

Chapter 15

Application to the two-electron gas

In order to assess the presented approximations, we first study a particularly simple model system – the three-dimensional UEG. The details of this model are described for instance in [163]. For the here performed analysis it is enough to study only two electrons in a homogeneous positive background. The virtual HF states are plane-waves having the following form

$$\phi_a(\mathbf{r}) = \frac{1}{\sqrt{\Omega}} e^{i\mathbf{k}_a \cdot \mathbf{r}}, \tag{15.1}$$

with HF eigenvalues being

$$\epsilon_a = \frac{1}{2}k_a^2 - \frac{1}{\Omega}\frac{4\pi}{k_a^2}. \tag{15.2}$$

Using a restricted HF reference, the ground state is thus a singlet with $\mathbf{k}_i = 0$ and therefore ϕ_i is simply a constant function. Notice that the eigenenergies are ordered with respect to the length of the corresponding momentum vector. The unit cell volume is given by Ω. This simplifies the four-index integrals to

$$\langle ii|V|a\bar{b}\rangle = \frac{1}{\Omega}\frac{4\pi}{k_a^2}\delta_{\mathbf{k}_a+\mathbf{k}_b,0}. \tag{15.3}$$

Table 15.1: BSIEs for the two-electron UEG with $r_s = 3.5$ $a.u.$. Reference energies are obtained from a calculation with 30046 virtuals. Referred to exact (ex.) is the evaluation of Eq.(15.6) for the converged amplitudes using 30046 virtuals and using N_v orbitals in the finite basis. Estimates (est.) are evaluated using Eqs.(11.31) and (11.36). The BSIE of the rest term is given in the last column and calculated between results obtained with N_v and 30046 virtual orbitals. All energies are given in mH.

N_v	ϵ^B		ϵ^C		ϵ^D	ΔE^rest
	ex.	est.	ex.	est.	ex.	
26	0.582	0.560	0.255	0.262	0.178	-0.065
56	0.343	0.332	0.157	0.162	0.076	-0.049
122	0.171	0.166	0.079	0.083	0.027	-0.029
250	0.087	0.084	0.047	0.043	0.010	-0.015
514	0.043	0.043	0.021	0.022	0.004	-0.008

Consequently, the MP2 energy expression contains only a single sum

$$E^\mathrm{mp2} = \sum_a \frac{\langle ii|V|a\bar{a}\rangle}{\epsilon_i + \epsilon_i - \epsilon_a - \epsilon_{\bar{a}}} \langle a\bar{a}|V|ii\rangle \,. \tag{15.4}$$

We use the notation $\bar{a}$ for the virtual orbital with momentum vector $-\mathbf{k}_a$. The ppl energy expression reads

$$E^\mathrm{ppl} = \sum_a \frac{\langle ii|V|a\bar{a}\rangle}{\epsilon_i + \epsilon_i - \epsilon_a - \epsilon_{\bar{a}}} \sum_c \langle a\bar{a}|V|c\bar{c}\rangle \, T_{ii}^{c\bar{c}}. \tag{15.5}$$

In a finite basis set calculation the number of virtual basis functions N_v has to be truncated. For the UEG model system, this is typically done by introducing a cutoff wave vector k_f and considering only virtual states with $|\mathbf{k}_a| < k_\mathrm{f}$. Following the ideas of the theoretical introduction, we introduce a second cutoff k_F specifying the augmented virtual states α, with $k_\mathrm{f} \leq |k_\alpha| < k_\mathrm{F}$. Hence, we can write the following four contributions to the total ppl energy

$$
\begin{aligned}
\epsilon_{ii}^{\mathrm{A}} &= \sum_{a} \frac{\langle ii|V|a\bar{a}\rangle}{\epsilon_i + \epsilon_i - \epsilon_a - \epsilon_{\bar{a}}} \sum_{c} \langle a\bar{a}|V|c\bar{c}\rangle \, t_{ii}^{c\bar{c}} \\
\epsilon_{ii}^{\mathrm{B}} &= \sum_{\alpha} \frac{\langle ii|V|\alpha\bar{\alpha}\rangle}{\epsilon_i + \epsilon_i - \epsilon_\alpha - \epsilon_{\bar{\alpha}}} \sum_{c} \langle \alpha\bar{\alpha}|V|c\bar{c}\rangle \, t_{ii}^{c\bar{c}} \\
\epsilon_{ii}^{\mathrm{C}} &= \sum_{a} \frac{\langle ii|V|a\bar{a}\rangle}{\epsilon_i + \epsilon_i - \epsilon_a - \epsilon_{\bar{a}}} \sum_{\gamma} \langle a\bar{a}|V|\gamma\bar{\gamma}\rangle \, t_{ii}^{\gamma\bar{\gamma}} \\
\epsilon_{ii}^{\mathrm{D}} &= \sum_{\alpha} \frac{\langle ii|V|\alpha\bar{\alpha}\rangle}{\epsilon_i + \epsilon_i - \epsilon_\alpha - \epsilon_{\bar{\alpha}}} \sum_{\gamma} \langle \alpha\bar{\alpha}|V|\gamma\bar{\gamma}\rangle \, t_{ii}^{\gamma\bar{\gamma}}.
\end{aligned}
\tag{15.6}
$$

We stress that one important feature of the UEG model consists in the fact, that enlarging the basis set does not alter the occupied and virtual orbitals. We now examine the proposed approximations numerically. We choose the union of all virtual states to be a very large number of 30046 states, which can be considered a good approximation to the CBS limit for the present system. In the following we gradually increase the number of virtual states in the finite basis and evaluate the approximate expressions for $\epsilon_{ii}^{\mathrm{B}}$ and $\epsilon_{ii}^{\mathrm{C}}$ in Eqs. (11.31) and (11.36) and compare them to the exact result in Eq. (15.6). The results for increasing numbers of virtual states are given in Table (15.1). The contribution of $\epsilon_{ii}^{\mathrm{B}}$ is roughly twice as large as $\epsilon_{ii}^{\mathrm{C}}$.

We find that both energy contributions can be approximated with remarkable accuracy using the presented expressions. Although the approximations made for $\epsilon_{ii}^{\mathrm{B}}$ and $\epsilon_{ii}^{\mathrm{C}}$ differ, we can not observe any significant differences in the accuracy of both terms. The term $\epsilon_{ii}^{\mathrm{D}}$, for which no approximation was introduced, converges considerably faster, when compared to the other two contributions $\epsilon_{ii}^{\mathrm{B}}$ and $\epsilon_{ii}^{\mathrm{C}}$. Hence, the BSIE of the ppl contribution can be reduced by a large portion successfully. It appears that the remaining deviation is roughly in the same order of magnitude as the rest contribution. Therefore, it is a reasonable approximation to neglect both contributions from $\epsilon_{ii}^{\mathrm{D}}$ and ΔE^{rest}.

For the above analysis, we have employed the fully converged CCSD amplitudes expanded in a basis of 30046 virtual states.

The amplitudes have been partitioned according to the cutoff k_{f} into sets corresponding to $t_{ii}^{\alpha\bar{\alpha}}$ and $t_{ii}^{a\bar{a}}$, which have been used to compute $\epsilon_{ii}^{\mathrm{B}}$ and $\epsilon_{ii}^{\mathrm{C}}$.

However, in practice and for the following benchmark systems, we employ only CCSD amplitudes that have been calculated using a finite virtual orbital basis set. However, we find only small differences between the results when using (i) virtual and augmented virtuals and (ii) only virtuals in finite basis amplitudes.

Chapter 16

Computational details

In the following sections we present results obtained for a set of benchmark systems including 107 molecules and atoms. We employ aug-cc-pVXZ basis sets for first-row elements and aug-cc-pV(X+d)Z basis sets for second-row elements [44, 100]. These basis sets will be denoted as AVXZ throughout this work. We obtained the reference energies using the quantum chemistry package PSI4 [135]. We have modified the code such that the E^{ppl} contribution is extracted from the calculation as described in [88]. For the CBS limit estimates we use AV5Z and AV6Z energies and the extrapolation formula $E_X = E_{\mathrm{CBS}} + a/X^3$, with the basis set cardinal number X. This formula is used to get CBS estimates of all three individual terms: E^{mp2}, E^{ppl}, and E^{rest}. We use unrestricted Hartree–Fock orbital functions and corresponding CCSD implementations for all open-shell systems. All correlation energy calculations in this work used the frozen core approximation.

In addition, (F12*) calculations are performed using TURBOMOLE [181, 9, 8, 75] and the AVDZ, AVTZ, and AVQZ basis sets. We employ default settings, however, we use the RI basis aug-cc-pV5Z developed by Hättig [74] in all calculations. We note that these large RI basis sets are employed for all types of auxiliary functions in the TURBOMOLE implementation, *i.e.* `$cbas`, `$jkbas`, and `$cabs`. All results in the main text employ $\gamma = 1.0$ in the parametrization of the correlation factor. Further results using a different γ parameter can be found in the supplement information.

The derived approximate BSIE corrections to the ppl term were computed using our

own coupled-cluster code cc4s, LIBINT2 [185] and CTF [164]. In these calculations, the Hartree–Fock ground state wave function was obtained with the NWChem package [186] and interfaced to cc4s as described in [59]. We stress that the employed basis set correction defined by Eq. (11.38) depends on the pair specific MP2 BSIE correction $\Delta\epsilon_{ij}^{(2)}$ and the correlation hole depth scaling factors $g_{ij}^{cc}/g_{ij}^{(1)}$.

These terms need to be computed using a consistent set of occupied orbitals. In practice this is complicated for states that belong to a degenerate set, which allows for arbitrary unitary rotations among the degenerate subspace. This is particularly problematic for the way the estimate for $\Delta\epsilon_{ij}^{(2)}$ is obtained in this work, as it involves the results from separate MP2 calculations with different basis sets. In this work, we avoid arbitrary unitary rotations among degenerate sets of orbitals by introducing point charges far away from the molecules and atoms that break corresponding symmetries, lifting all possibly problematic degeneracies. These point charges are sufficiently far away to ensure that all computed correlation energies change by a numerically negligible small amount.

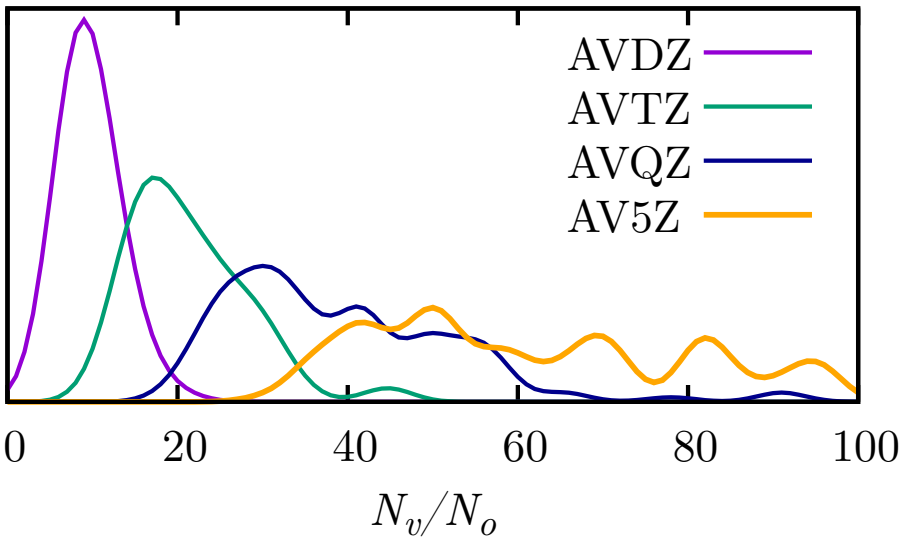

Figure 16.1: Distribution of the number of virtual orbitals per occupied for all 107 studied systems when employing an atom-centered AVXZ basis set. Gaussian function was used to smear the data.

For the newly introduced basis set correction scheme we construct frozen natural orbitals (FNOs) on the level of second-order perturbation theory [165, 101, 174]. We truncate the virtual space used for the CCSD calculations by choosing only N_v FNOs with the largest occupation number, where $N_v = X_{\mathrm{no}} \times \max\left(N_{o,\alpha}, N_{o,\beta}\right)$ with $X_{\mathrm{no}} \in [12, 16, 20, 24, 28, 32]$. $N_{o,\alpha}$ and $N_{o,\beta}$ refer to the number of occupied spin-up and spin-down orbitals, respectively. We stress that we use large basis sets (AVQZ and AV5Z) for the construction of FNOs. Therefore, the number of virtual orbitals, N_v, is defined differently than for conventional quantum chemical calculations. In conventional calculations with atom-centered basis sets, the total number of orbitals is independent of the number of occupied orbitals but depends only on the atomic species for a chosen basis set. Yet, we seek to compare the BSIEs of correlation energies calculated using both approaches. To provide an estimate for which cardinal number in the AVXZ basis set family corresponds on average to which number of virtual orbitals per occupied orbital, Fig. 16.1 depicts N_v/N_o for all studied atomic and molecular systems employing conventional AVXZ (X=D,T,Q,5) basis sets. We find that AVDZ and AVTZ roughly correspond to $X_{\mathrm{no}} = 12$ and $X_{\mathrm{no}} = 20$, respectively. Later, it will be numerically verified that our choice of fixed number of virtuals per occupied leads to a well-balanced energy description for different reactants.

We have calculated the correlation energies of in total 107 molecules and atoms. Thereupon we evaluated 26 closed-shell reaction energies (REc), 39 open-shell reaction energies (REo), 44 atomization energies (AE), 16 electron affinities (EA), and 22 ionization potentials (IP). This benchmark set is a subset of the one studied by Knizia *et al.* [102]. We had to exclude a number of molecules from their benchmark set as some of the molecules have been too large to be treated with our workflow. For some other molecules, we were not able to converge to a common HF ground state with neither of the three packages `NWChem`, `TURBOMOLE`, and `PSI4`. These molecules have also been excluded from our benchmark. A detailed list of the calculated molecules and corresponding reactions can be found in the supplementary information of [87].

Chapter 17

Results

This chapter presents results for molecular systems and is organized as follows. In section 17.1 we assess the convergence of the diagrammatically decomposed CCSD correlation energy contributions, confirming that the BSIEs in the total energy are dominated by the MP2 and ppl terms. In section 17.2 we show that this behavior persists for most quantities computed from the total energies including reaction energies, atomization energies, ionization potentials and electron attachment energies.
In addition, we explore the accuracy of the derived approximate correction to the BSIE of the ppl term for all investigated quantities. In section 17.3 we assess the accuracy of the corrected total CCSD energies and related quantities using two practical settings for the introduced focal-point approach and the respective BSIE corrections to the ppl term. These settings correspond to natural orbital basis set sizes that are similar to AVDZ and AVTZ basis sets. The obtained results are compared to conventional CCSD and CCSD(F12*) approaches. Section 17.4 discusses our findings for the (T) and (T*) correlation energy contributions using FNOs.

17.1 Total energies

We begin the analysis of the molecular systems by presenting results for the basis set errors of the diagrammatically decomposed correlation energy contributions for 107 molecules

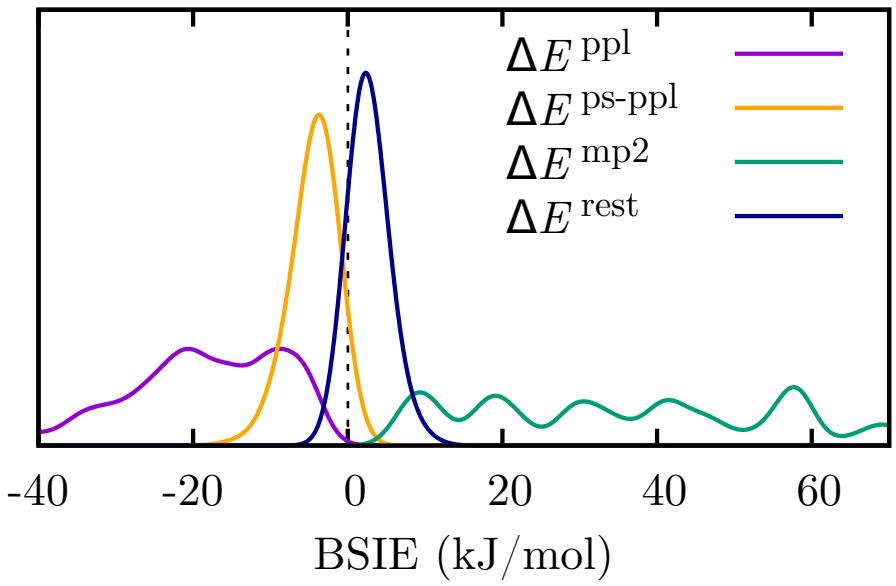

Figure 17.1: Distribution of the basis set incompleteness error (BSIE) of various investigated energy channels (MP2, ppl and rest) including the corrected ppl energy ($\Delta E^{\text{ps-ppl}}$) for 107 studied systems. The energies were calculated using 16 frozen natural orbitals per occupied orbital and are referenced to [56] values. The same Gaussian function was used to smear the data points.

and atoms. Fig. 17.1 depicts the BSIEs of the ppl (ΔE^{ppl}), MP2 (ΔE^{mp2}) and rest (ΔE^{rest}) contributions. Furthermore, the BSIEs of the ppl energies corrected according to Eq. (11.38) are also depicted ($\Delta E^{\text{ps-ppl}}$). The BSIEs are estimated using reference values obtained from a [56] extrapolation. The correlation energies are evaluated using a Hartree–Fock reference wave function and 16 FNOs per occupied orbital to approximate the virtual orbital manifold. This basis set size is on average between AVDZ and AVTZ, as can be seen in Fig. 16.1. For the construction of the FNOs, the one-particle reduced density matrix at the level of MP2 was calculated in an AV5Z basis set. Our findings show that MP2 energies calculated using 16 FNOs per occupied orbital exhibit by far the largest BSIEs when compared to the other contributions. In contrast to MP2, E^{rest} is significantly better converged. This analysis reveals that E^{rest} can already be well approximated using a smaller number of natural orbitals than required for E^{ppl} and E^{mp2}. However, adding the basis set correction to E^{ppl} as defined in Eq. (11.38), significantly reduces the remaining BSIE such that $\Delta E^{\text{ps-ppl}}$ becomes comparable to ΔE^{rest} for all studied systems. This demonstrates impressively that the approximation derived in the theoretical introduction can transfer its accuracy from the uniform electron gas model system to real atoms and molecules.

17.2 Energy differences

More decisive than well converged total energies is the question of how the proposed correction scheme works for energy differences. Therefore, we analyse the BSIEs for the different channels (E^{ppl}, E^{mp2}, and E^{rest}) for REc, REo, and AEs. The results are summarized in Table 17.1 for increasing numbers of FNOs as well as for the basis sets AVDZ-AV6Z. The MP2 contribution shows the largest BSIE followed by the ppl contribution. This is in accordance with the findings for the total energies, discussed in the previous section. We stress that only in the case of REc, the BSIE of E^{rest} and E^{ppl} is of comparable magnitude. Furthermore, we note that the computed errors using FNOs for some systems become larger again or do not reduce significantly for $X_{\text{no}} > 24$. We attribute this behavior to not sufficiently well converged FNOs. When approaching $X_{\text{no}} > 24$, one would require even

bigger basis sets than the employed AV5Z for the construction of the FNOs. Generally, it is not expected that the errors are significantly smaller than when using all possible virtual orbitals in the AV5Z basis set.

Especially for the large basis sets, the BSIE of the rest contribution is remarkably small; the rms deviation for AV5Z is only around 0.3 kJ/mol and lower. A similar high accuracy can be attained when using only a comparably small number of 20 FNOs per occupied orbital, which achieves rms deviations of around 0.5 kJ/mol for the reaction energies and 1 kJ/mol for atomization energies.

For REo and AEs the ppl contribution converges significantly slower with respect to the basis set size compared to E^{rest}. Furthermore, the BSIE cannot be diminished considerably with a finite number of FNOs. This behavior changes when taking the proposed correction into account. Compared to the uncorrected ppl contribution, the BSIE of the corrected ppl contribution is reduced by a factor of four and more, when using only 20 FNOs per occupied or less. For REc the correction has no significant effect.

In summary, rms deviations of the rest contributions (ΔE^{rest}) and corrected ppl ($\Delta E^{\text{ps-ppl}}$) contributions are on the scale of 1 kJ/mol when using 20 FNOs per occupied orbital. Reaching a similar accuracy by employing conventional basis set calculations would require a [34] extrapolation.

Table 17.1: BSIE of correlation energy contributions to REc, REo and AEs. Shown are the rms deviations to the [56] reference. Results have been obtained using 12-32 FNOs per occupied orbitals (X_{no}), [23]-[45] extrapolations, and for different conventional basis sets ranging from AVDZ up to AV6Z.

	REc (kJ/mol)				REo (kJ/mol)				AEs (kJ/mol)			
	ΔE^{mp2}	ΔE^{ppl}	ΔE^{rest}	$\Delta E^{\mathrm{ps\text{-}ppl}}$	ΔE^{mp2}	ΔE^{ppl}	ΔE^{rest}	$\Delta E^{\mathrm{ps\text{-}ppl}}$	ΔE^{mp2}	ΔE^{ppl}	ΔE^{rest}	$\Delta E^{\mathrm{ps\text{-}ppl}}$
X_{no}=12	6.396	1.850	1.212	1.199	28.325	8.811	1.513	1.986	39.350	14.985	2.783	2.257
X_{no}=16	4.576	1.302	0.822	0.931	20.556	6.509	0.783	1.502	28.230	11.118	1.437	1.321
X_{no}=20	2.978	0.877	0.437	0.739	15.771	5.224	0.489	1.390	22.094	8.941	1.005	0.949
X_{no}=24	2.240	0.540	0.338	0.667	12.429	4.130	0.308	1.257	17.231	7.115	0.650	0.723
X_{no}=28	2.289	0.626	0.299	0.536	9.416	3.114	0.242	1.284	14.024	5.930	0.600	0.664
X_{no}=32	2.476	0.649	0.516	0.485	7.241	2.398	0.392	1.325	11.494	4.903	0.559	0.627
AVDZ	15.207	2.400	3.468	-	43.096	10.296	5.200	-	67.192	21.166	12.269	-
AVTZ	6.981	1.767	2.040	-	20.598	5.675	2.544	-	27.203	9.567	4.153	-
AVQZ	3.212	1.077	0.653	-	8.945	2.666	0.624	-	11.866	4.321	0.831	-
AV5Z	1.885	0.640	0.288	-	4.553	1.370	0.300	-	6.122	2.257	0.274	-
AV6Z	1.092	0.371	0.164	-	2.636	0.793	0.177	-	3.541	1.306	0.158	-
[23]	5.420	1.708	2.049	-	11.576	3.901	2.852	-	11.131	4.941	2.534	-
[34]	2.007	0.842	0.815	-	1.393	0.662	1.468	-	1.237	0.708	1.845	-
[45]	0.730	0.262	0.148	-	0.719	0.237	0.400	-	0.458	0.172	0.416	-

17.3 Benchmarking a practical focal-point approach

Based on the findings in the previous sections we now define and assess a practical focal-point approach to compute total CCSD energies. For an even-tempered composition we combine extrapolated MP2 energies with CCSD calculations employing FNOs. We introduce the following two compositions:

$$\begin{aligned} E^{\mathrm{FPa}} =& E^{\mathrm{mp2}}([34]) + E^{\mathrm{rest}}(12) + E^{\mathrm{ppl}(12)} \\ =& E^{\mathrm{ccsd}}(12) - E^{\mathrm{mp2}}(12) + E^{\mathrm{mp2}}([34]) \end{aligned} \tag{17.1}$$

and

$$\begin{aligned} E^{\mathrm{FPb}} =& E^{\mathrm{mp2}}([45]) + E^{\mathrm{rest}}(20) + E^{\mathrm{ppl}(20)} \\ =& E^{\mathrm{ccsd}}(20) - E^{\mathrm{mp2}}(20) + E^{\mathrm{mp2}}([45]). \end{aligned} \tag{17.2}$$

$E^{\mathrm{mp2}}(X_{\mathrm{no}})$, $E^{\mathrm{ccsd}}(X_{\mathrm{no}})$, $E^{\mathrm{rest}}(X_{\mathrm{no}})$ and $E^{\mathrm{ppl}}(X_{\mathrm{no}})$ refer to the corresponding correlation energy contributions calculated employing X_{no} FNOs per occupied orbital. $E^{\mathrm{mp2}}([34])$ and $E^{\mathrm{mp2}}([45])$ refer to MP2 correlation energies obtained from a [34] and [45] extrapolation, respectively. For the first ansatz (E^{FPa}) we construct the FNOs using an AVQZ calculation, whereas for the second ansatz (E^{FPb}) the AV5Z basis set is used. In this section we will explore benchmark results obtained using both approaches with and without the introduced Δps-pplcorrection that depends on the respective pair-specific extrapolated MP2 energies and correlation hole depths. The corresponding BSIEs are summarized in Table 17.2.

Table 17.2: CCSD valence correlation energy basis set incompleteness error for closed-shell reaction (REc), open-shell reactions (REo), atomization energies (AEs), ionization potentials (IPs), and electron affinities (EAs). Reference is obtained from a [56] extrapolation. Two different variants of the focal-point approximation are used with and without correction. Details are found in the main text.

	REc (kJ/mol)		REo (kJ/mol)		AEs (kJ/mol)		IPs (kJ/mol)		EAs (kJ/mol)	
	max	rms	max	rms	max	rms	max	rms	max	rms
FPa	4.823	1.905	15.403	7.130	24.223	11.786	10.244	3.301	15.384	5.414
FPb	2.828	1.029	10.998	5.445	16.660	8.461	6.837	2.652	9.203	3.766
FPa+ Δps-ppl	7.248	2.541	8.836	3.024	9.017	2.400	3.359	1.520	5.666	1.603
FPb+ Δps-ppl	3.253	1.102	2.424	1.049	3.491	0.848	1.475	0.733	3.062	0.828
[23]	15.637	5.814	33.638	10.460	26.000	8.443	8.814	4.366	6.170	3.033
[34]	6.222	2.031	4.545	1.938	3.965	1.874	1.993	0.828	1.772	0.895
[45]	1.137	0.438	1.864	0.650	1.302	0.532	0.213	0.112	0.181	0.113
(F12*) @ AVDZ	9.859	3.163	14.625	4.274	11.957	5.821	8.375	4.632	7.059	4.720
(F12*) @ AVTZ	3.838	1.434	5.946	1.657	3.834	1.520	2.685	1.393	1.810	1.189
(F12*) @ AVQZ	2.233	0.869	1.727	0.719	1.795	0.532	0.898	0.543	1.015	0.472

The uncorrected focal-point approaches E^{FPa} and E^{FPb} yield only satisfying BSIEs for the closed-shell reaction energies. Here, FPa achieves the quality of the [34] result, although the CCSD calculation is performed with a significantly smaller virtual space of only 12 FNOs per occupied orbital. For the open-shell reactions and other properties, the focal-point method performs significantly worse with rms deviations between 3-12 kJ/mol and a maximum error of around 25 kJ/mol.

The focal-point approaches including the Δps-ppl correction yield significantly more consistent BSIEs for all studied energy differences. The rms deviations are 1.5-3 kJ/mol and around 1 kJ/mol for FPa and FPb, respectively. For the FPb+Δps-ppl approach the maximum deviation is below 4 kJ/mol for all considered reactions.

We note that for the closed-shell reactions the corrected focal-point results show larger rms deviations and larger maximum errors than the uncorrected variants. We attribute this to fortuitous error cancellation between the individual energy contributions to the CCSD correlation energy. This is only visible when the Δps-ppl-correction is insignificant as it is the case for the closed-shell reaction energies (see Sec. 17.2). Correcting for the BSIE in the ppl term, reduces this error compensation, causing slightly larger BSIEs for closed-shell reaction energies. However, the results for REc obtained including the Δps-ppl correction are of comparable size to open-shell reactions and other properties.

The extrapolation using the AVDZ and AVTZ basis sets shows large maximum errors of up to 30 kJ/mol and the rms deviation ranges from 3 to 10 kJ/mol. The [34] extrapolation yields satisfying results with rms deviations of around 2 kJ/mol, for IPs and EAs already below 1 kJ/mol. Although the [45] extrapolation yields the best statistical results, a CCSD calculation with the large AV5Z basis set is only possible for small systems. We stress that more sophisticated extrapolation techniques were already tested for the original version of the employed benchmark set. Results can be found in the supplement of Ref. [102]. Knizia *et al.* conclude that "[...] in our benchmark set there are only few systems where using either extrapolation scheme makes a noteworthy difference". Thus, the corrected FPa ansatz is to be preferred over [23] extrapolation and the corrected FPb seems to be superior compared with the [34] extrapolation. We stress that in both cases larger HF and MP2 calculations have to be performed in order to obtain the final result.

For comparison, CCSD(F12*) results are also given for three different basis sets. The F12 results obtained using the AVQZ basis set reach almost the quality of the [45] extrapolation, with rms deviations well below 1 kJ/mol. For the (F12*)@AVTZ results, the rms deviations are only around 1.5 kJ/mol, whereas (F12*)@AVDZ yields results that show rms deviations with about 3-5 kJ/mol. We note that (F12*)@AVTZ yields results with smaller rms deviations than the [34] extrapolation.

We note that the size of the virtual space in the CCSD calculation for (F12*)@AVDZ and FPa+Δps-ppl is similar. The same is true for (F12*)@AVTZ and FPb+Δps-ppl. However, the FPa and FPb approaches require HF and MP2 calculations using the AVQZ and AV5Z basis sets, respectively. Therefore, the entire computational cost of the proposed focal-point approaches depends strongly on the efficiency of the employed HF and MP2 algorithms. Further statistical analysis of the test set using HF and conventional CCSD is provided in the supplementary information.

17.4 Perturbative triples contribution

Having assessed the introduced focal-point approach for the CCSD method, we now turn to the discussion of BSIEs in the perturbative triples contribution to the CCSD(T) energies calculated using FNOs. In addition to the conventional approach of computing the (T) contribution, we will also explore the (T*) approximation, which approximates the CBS limit of (T) by rescaling the finite basis set result with a factor estimated on the level of MP2 theory as outlined in Ref. [102]. In this work, the scaling factor corresponds to $E^{\mathrm{mp2}}([45])/E^{\mathrm{mp2}}(X_{\mathrm{no}})$. The results are summarized in Table 17.3. The rms deviations for the AVDZ are 2-8 kJ/mol and even with the corrected values, denoted as (T*), the errors are within the range of 2-3 kJ/mol. With increasing cardinal numbers the deviations reduce considerably. AVQZ results show deviations of up to 1 kJ/mol, reducing even further for the (T*) correction where they do not surpass 0.5 kJ/mol. As it is apparent from the presented data, the usage of FNOs together with the (T*) ansatz seems to be highly effective. Already 12 FNOs per occupied orbital suffice to reduce the rms deviations to 0.7 kJ/mol and lower. When using 20 FNOs instead, this deviation reduces smoothly

Table 17.3: BSIE of the (T) contribution to closed-shell reaction (REc), open-shell reactions (REo), atomization energies (AEs), ionization potentials (IPs), and electron affinities (EAs). Shown are the rms deviations to the [56] reference.

	REc (kJ/mol)		REo (kJ/mol)		AEs (kJ/mol)		IPs (kJ/mol)		EAs (kJ/mol)	
	(T)	(T*)	(T)	(T*)	(T)	(T*)	(T)	(T*)	(T)	(T*)
X_{no}=12	0.914	0.522	1.925	0.456	2.881	0.633	0.808	0.387	1.378	0.710
X_{no}=16	0.583	0.385	1.175	0.316	1.765	0.350	0.522	0.252	0.877	0.415
X_{no}=20	0.418	0.265	0.808	0.255	1.336	0.259	0.381	0.177	0.679	0.333
X_{no}=24	0.292	0.203	0.616	0.227	0.989	0.236	0.298	0.122	0.506	0.207
X_{no}=28	0.268	0.183	0.487	0.241	0.824	0.209	0.260	0.110	0.421	0.166
X_{no}=32	0.206	0.233	0.397	0.244	0.699	0.192	0.223	0.092	0.364	0.129
AVDZ	1.976	3.231	5.176	3.216	8.176	2.826	3.139	2.364	4.330	2.676
AVTZ	1.055	0.823	1.485	0.997	2.165	0.450	0.862	0.432	1.275	0.566
AVQZ	0.509	0.269	0.667	0.433	0.913	0.153	0.366	0.185	0.571	0.277
AV5Z	0.270	0.135	0.303	0.231	0.425	0.087	0.179	0.088	0.296	0.151
AV6Z	0.157	0.078	0.191	0.134	0.246	0.049	0.103	0.050	0.171	0.087
[23]	0.888	-	0.705	-	0.570	-	0.232	-	0.170	-
[34]	0.255	-	0.188	-	0.133	-	0.066	-	0.121	-
[45]	0.035	-	0.088	-	0.093	-	0.024	-	0.040	-

below 0.35 kJ/mol.

We stress that computing the (T*) scaling factor using a [56] extrapolation instead of [45] extrapolation has almost no effect (0.05 kJ/mol in the rms BSIEs).

Considering the findings for the BSIEs listed in Tabs. 17.2 and 17.3 in combination, shows that it is possible to obtain CCSD(T) correlation energy estimates of REc, REo, AEs, IPs and EAs with a root-mean-square deviation from the CBS limit below 4 kJ/mol using 12 FNOs per occupied orbital only. Employing 20 FNOs per occupied orbital reduces the rms BSIE to around 1 kJ/mol for all computed energy differences. A detailed summary of all computed energies and BSIEs can be found in the supplement information.

Part V

Summary and conclusions

Quantum material science has the potential to become an increasingly vital part of the engineering landscape of the future. It could open the door to the tailoring of material properties guided by a deep understanding of the quantum mechanical description of the material. The inherent combinatorial scaling of the many-body problem precludes an exact solution of the wavefunction of the system, rendering its exact quantum mechanical description unattainable. DFT is considered as the most successful theoretical framework since it circumvents the problem of dimensionality by instead framing the many-body problem around the electronic three-dimensional density. Notwithstanding the overwhelming success of approximate DFT, limits exist to the applicability of modern state-of-the-art exchange-correlation functionals[21].

Accurate quantum chemical theories such as coupled cluster can assist in providing insight in the limitations of approaches such as approximate theories. This thesis attests to the fact that routine coupled cluster calculations are possible for a variety of systems ranging from defects embedded in solids to molecules and the uniform electron gas.

This thesis has been structure in three main parts. First, we presented a concise overview of the theoretical corpus needed to grasp the main pillars of ab initio many-body physics. The focal-point basis set correction for CCSD is also introduced in this section in order to set the stage for the last part of this thesis.

In the second part of the thesis, we present calculations of the F-center in the alkaline earth oxides crystals MgO, CaO and SrO. The excellent agreement with experiment and past theoretical works shows that computing excited states of simple solid state defects is indeed attainable within the framework of EE-EOM-CCSD. This study opens the door for further study of other defects embedded in semiconductors where weak correlation is to be expected.

The third part of this thesis is concerned with basis set corrections analyzing the electron-electron cusp. This tackles a hindrance in any quantum mechanical calculation where a basis set is used, namely the basis set incompleteness error. We present results making use of FNOs for a range molecules showing a rapid convergence of the BSIE for open-shell reaction energies, atomization energies, electron affinities and ionization potentials.

Part VI

Publications

1. Coupled cluster finite temperature simulations of periodic materials via machine learning
   Herzog, Basile and **Gallo, Alejandro** *and Hummel, Felix and Badawi, Michael and Bučko, Tomáš and Lebègue, Sébastien and Grüneis, Andreas and Rocca, Dario*
   2023, American Chemical Society (ACS) 10.26434/chemrxiv-2023-mvsxn

2. Formation energies of silicon self-interstitials using periodic coupled cluster theory
   Salihbegović, Faruk and **Gallo, Alejandro** *and Grüneis, Andreas*
   2023, American Physical Society 10.1103/PhysRevB.108.115125

3. Coupled cluster theory for the ground and excited states of two-dimensional quantum dots
   Salihbegović, Faruk and **Gallo, Alejandro** *and Grüneis, Andreas*
   2022, American Physical Society (APS) 10.1103/physrevb.105.115111

4. A periodic equation-of-motion coupled-cluster implementation applied to F-centers in alkaline earth oxides
   Gallo, Alejandro *and Hummel, Felix and Irmler, Andreas and Grüneis, Andreas*
   2021, AIP Publishing 10.1063/5.0035425

5. Focal-point approach with pair-specific cusp correction for coupled-cluster theory
   Irmler, Andreas and **Gallo, Alejandro** *and Grüneis, Andreas*
   2021, AIP Publishing 10.1063/5.0050054

6. Surface science using coupled cluster theory via local Wannier functions and in-RPA-embedding: The case of water on graphitic carbon nitride
   Schäfer, Tobias and **Gallo, Alejandro** *and Irmler, Andreas and Hummel, Felix and Grüneis, Andreas*
   2021, AIP Publishing 10.1063/5.0074936

7. Duality of Ring and Ladder Diagrams and Its Importance for Many-Electron Perturbation Theories

Irmler, Andreas and ***Gallo, Alejandro*** *and Hummel, Felix and Grüneis, Andreas*

2019, American Physical Society (APS) 10.1103/physrevlett.123.156401

8. Protecting a Diamond Quantum Memory by Charge State Control

Pfender, Matthias and Aslam, Nabeel and Simon, Patrick and Antonov, Denis and Thiering, Gergő and Burk, Sina and Fávaro de Oliveira, Felipe and Denisenko, Andrej and Fedder, Helmut and Meijer, Jan and Garrido, Jose A. and Gali, Adam and Teraji, Tokuyuki and Isoya, Junichi and Doherty, Marcus William and Alkauskas, Audrius and ***Gallo, Alejandro*** *and Grüneis, Andreas and Neumann, Philipp and Wrachtrup, Jörg*

2017, American Chemical Society (ACS) 10.1021/acs.nanolett.7b01796

Part VII

Bibliography

Bibliography

[1] Reinhart Ahlrichs. "A simple algebraic derivation of the Obara–Saika scheme for general two-electron interaction potentials". In: *Phys. Chem. Chem. Phys.* 8.26 (2006), p. 3072. ISSN: 1463-9084. DOI: 10.1039/b605188j.

[2] Audrius Alkauskas, Matthew D. McCluskey, and Chris G. Van de Walle. "Tutorial: Defects in semiconductors—Combining experiment and theory". en. In: *Journal of Applied Physics* 119.18 (18 May 12, 2016), p. 181101. ISSN: 0021-8979. DOI: 10.1063/1.4948245.

[3] Jan Almlöf. "Elimination of energy denominators in Møller—Plesset perturbation theory by a Laplace transform approach". In: *Chemical Physics Letters* 181 (4 1991), pp. 319–320. DOI: 10.1016/0009-2614(91)80078-C.

[4] J. S. Arponen, R. F. Bishop, and E. Pajanne. "Extended coupled-cluster method. I. Generalized coherent bosonization as a mapping of quantum theory into classical Hamiltonian mechanics". In: *Physical Review A* 36 (6 1987), pp. 2519–2538. DOI: 10.1103/PhysRevA.36.2519.

[5] J. S. Arponen, R. F. Bishop, and E. Pajanne. "Extended coupled-cluster method. II. Excited states and generalized random-phase approximation". In: *Physical Review A* 36 (6 1987), pp. 2539–2549. DOI: 10.1103/PhysRevA.36.2539.

[6] Jouko Arponen. "Diagrams are theoretical physicist's best friends". In: *A Festschrift in Honour of the 65th Birthdays of John W Clark, Alpo J Kallio, Manfred L Ristig and Sergio Rosati* (UMIST, Manchester, UK). World Scientific, Sept. 2001, pp. 57–64. DOI: 10.1142/9789812799760_0002.

[7] Jouko Arponen. "Variational principles and linked-cluster exp S expansions for static and dynamic many-body problems". In: *Annals of Physics* 151 (2 1983), pp. 311–382. DOI: 10.1016/0003-4916(83)90284-1.

[8] Rafał A. Bachorz et al. "The MP2-F12 method in the TURBOMOLE program package". In: *J. Comput. Chem.* 32.11 (2011), pp. 2492–2513. DOI: https://doi.org/10.1002/jcc.21825.

[9] Sree Ganesh Balasubramani et al. "TURBOMOLE: Modular program suite for *ab initio*quantum-chemical and condensed-matter simulations". In: *J. Chem. Phys.* 152 (18 2020), p. 184107. DOI: 10.1063/5.0004635.

[10] R J Bartlett. "Many-Body Perturbation Theory and Coupled Cluster Theory for Electron Correlation in Molecules". In: *Annual Review of Physical Chemistry* 32 (1 1981), pp. 359–401. DOI: 10.1146/annurev.pc.32.100181.002043.

[11] Rodney J. Bartlett. "Coupled-cluster theory and its equation-of-motion extensions". In: *Wiley Interdisciplinary Reviews: Computational Molecular Science* 2 (1 2012), pp. 126–138. DOI: 10.1002/wcms.76.

[12] Rodney J. Bartlett and Monika Musiał. "Coupled-cluster theory in quantum chemistry". In: *Rev. Mod. Phys.* 79 (1 Feb. 2007), pp. 291–352. DOI: 10.1103/RevModPhys.79.291.

[13] Rodney J. Bartlett and Monika Musiał. "Coupled-cluster theory in quantum chemistry". en. In: *Reviews of Modern Physics* 79 (1 Feb. 2007), pp. 291–352. DOI: 10.1103/revmodphys.79.291.

[14] Rodney J. Bartlett and Jozef Noga. "The expectation value coupled-cluster method and analytical energy derivatives". en. In: *Chemical Physics Letters* 150 (1-2 Sept. 1988), pp. 29–36. DOI: 10.1016/0009-2614(88)80392-0.

[15] R.H. Bartram and A.M. Stoneham. "On the luminescence and absence of luminescence of F centers". en. In: *Solid State Communications* 17 (12 Dec. 1975), pp. 1593–1598. DOI: 10.1016/0038-1098(75)91003-0.

[16] J.B. Bates and R.F. Wood. “High temperature luminescence spectra from F-centers in CaO”. en. In: *Solid State Communications* 17 (2 July 1975), pp. 201–203. DOI: 10.1016/0038-1098(75)90042-3.

[17] J.B. Bates and R.F. Wood. “Luminescence spectrum of the f-center in CaO”. en. In: *Physics Letters A* 49 (5 Oct. 1974), pp. 389–390. DOI: 10.1016/0375-9601(74)90283-7.

[18] Florian A. Bischoff et al. “Assessment of basis sets for F12 explicitly-correlated molecular electronic-structure methods”. en. In: *Molecular Physics* 107 (8-12 Apr. 2009), pp. 963–975. DOI: 10.1080/00268970802708942.

[19] P. E. Blöchl. “Projector augmented-wave method”. en. In: *Physical Review B* 50 (24 Dec. 1994), pp. 17953–17979. DOI: 10.1103/physrevb.50.17953.

[20] Peter E. Blöchl, Clemens J. Först, and Johannes Schimpl. “Projector augmented wave method:ab initio molecular dynamics with full wave functions”. en. In: *Bulletin of Materials Science* 26 (1 Jan. 2003), pp. 33–41. DOI: 10.1007/bf02712785.

[21] Mihail Bogojeski et al. “Quantum chemical accuracy from density functional approximations via machine learning”. en. In: *Nature Communications* 11 (1 Oct. 2020). DOI: 10.1038/s41467-020-19093-1.

[22] David Bohm and David Pines. “A Collective Description of Electron Interactions: III. Coulomb Interactions in a Degenerate Electron Gas”. In: *Physical Review* 92 (3 1953), pp. 609–625. DOI: 10.1103/PhysRev.92.609.

[23] David Bohm and David Pines. “A Collective Description of Electron Interactions. I. Magnetic Interactions”. In: *Physical Review* 82 (5 1951), pp. 625–634. DOI: 10.1103/PhysRev.82.625.

[24] David Bohm and David Pines. “Screening of Electronic Interactions in a Metal”. In: *Physical Review* 80 (5 1950), pp. 903–904. DOI: 10.1103/PhysRev.80.903.2.

[25] Baird H. Brandow. “Linked-Cluster Expansions for the Nuclear Many-Body Problem”. In: *Reviews of Modern Physics* 39 (4 1967), pp. 771–828. DOI: 10.1103/RevModPhys.39.771.

[26] K. A. Brueckner. "Many-Body Problem for Strongly Interacting Particles. II. Linked Cluster Expansion". In: *Physical Review* 100 (1 1955), pp. 36–45. DOI: 10.1103/PhysRev.100.36.

[27] K. A. Brueckner and C. A. Levinson. "Approximate Reduction of the Many-Body Problem for Strongly Interacting Particles to a Problem of Self-Consistent Fields". In: *Phys. Rev.* 97 (5 Apr. 1955), pp. 1344–1352. DOI: 10.1103/PhysRev.97.1344.

[28] Marco Caricato, Gary W. Trucks, and Michael J. Frisch. "A Comparison of Three Variants of the Generalized Davidson Algorithm for the Partial Diagonalization of Large Non-Hermitian Matrices". en. In: *Journal of Chemical Theory and Computation* 6 (7 July 2010), pp. 1966–1970. DOI: 10.1021/ct100111w.

[29] Javier Carrasco et al. "Optical absorption and luminescence energies of F centers in CaO fromab initioembedded cluster calculations". en. In: *The Journal of Chemical Physics* 125 (7 Aug. 2006), p. 074710. DOI: 10.1063/1.2337292.

[30] Y. Chen, J. L. Kolopus, and W. A. Sibley. "Luminescence of the F^+ Center in MgO". en. In: *Physical Review* 186 (3 Oct. 1969), pp. 865–870. DOI: 10.1103/physrev.186.865.

[31] Y. Chen et al. "Charge and mass transfer involving hydrogen in MgO crystals thermochemically reduced at high temperatures". en. In: *Physical Review B* 27 (2 Jan. 1983), pp. 1276–1282. DOI: 10.1103/physrevb.27.1276.

[32] Ove Christiansen, Henrik Koch, and Poul Jørgensen. "The second-order approximate coupled cluster singles and doubles model CC2". en. In: *Chemical Physics Letters* 243 (5-6 Sept. 1995), pp. 409–418. DOI: 10.1016/0009-2614(95)00841-q.

[33] Ove Christiansen et al. "On the inherent divergence in the Møller-Plesset series. The neon atom — a test case". en. In: *Chemical Physics Letters* 261 (3 Oct. 1996), pp. 369–378. DOI: 10.1016/0009-2614(96)00974-8.

[34] J. Cizek and J. Paldus. "Correlation problems in atomic and molecular systems III. Rederivation of the coupled-pair many-electron theory using the traditional quantum chemical methodst". In: *Int. J. Quantum Chem.* 5.4 (1971), pp. 359–379. DOI: 10.1002/qua.560050402.

[35] Jiří Čížek. "On the Correlation Problem in Atomic and Molecular Systems. Calculation of Wavefunction Components in Ursell-Type Expansion Using Quantum-Field Theoretical Methods". en. In: *The Journal of Chemical Physics* 45 (11 Dec. 1966), pp. 4256–4266. DOI: 10.1063/1.1727484.

[36] F. P. Clarke. "Irradiation damage in single crystals of magnesium oxide". en. In: *Philosophical Magazine* 2 (17 May 1957), pp. 607–627. DOI: 10.1080/14786435708242703.

[37] F. Coester and H. Kümmel. "Short-range correlations in nuclear wave functions". In: *Nuclear Physics* 17 (1960), pp. 477–485. DOI: 10.1016/0029-5582(60)90140-1.

[38] F. Coester and H. Kümmel. "Time dependent theory of scattering of nucleons by nuclei". en. In: *Nuclear Physics* 9 (2 Jan. 1958), pp. 225–236. DOI: 10.1016/0029-5582(58)90394-8.

[39] Aron J. Cohen, Paula Mori-Sánchez, and Weitao Yang. "Insights into Current Limitations of Density Functional Theory". en. In: *Science* 321 (5890 Aug. 2008), pp. 792–794. DOI: 10.1126/science.1158722.

[40] Edward Condon. "A Theory of Intensity Distribution in Band Systems". en. In: *Physical Review* 28 (6 Dec. 1926), pp. 1182–1201. DOI: 10.1103/physrev.28.1182.

[41] T. Daniel Crawford and Henry F. Schaefer. "An Introduction to Coupled Cluster Theory for Computational Chemists". In: *Reviews in Computational Chemistry*. John Wiley & Sons, Inc., Jan. 2007, pp. 33–136. ISBN: 9780470125915. DOI: 10.1002/9780470125915.ch2.

[42] P. A. M. Dirac. "Note on Exchange Phenomena in the Thomas Atom". en. In: *Mathematical Proceedings of the Cambridge Philosophical Society* 26 (3 July 1930), pp. 376–385. DOI: 10.1017/s0305004100016108.

[43] Alexander G. Donchev et al. "Quantum chemical benchmark databases of gold-standard dimer interaction energies". en. In: *Scientific Data* 8 (1 Feb. 10, 2021). ISSN: 2052-4463. DOI: 10.1038/s41597-021-00833-x.

[44] Thom H. Dunning, Kirk A. Peterson, and Angela K. Wilson. "Gaussian basis sets for use in correlated molecular calculations. X. The atoms aluminum through argon revisited". en. In: *J. Chem. Phys.* 114 (21 June 2001), pp. 9244–9253. DOI: 10.1063/1.1367373.

[45] P Edel. "Photoluminescence of additively coloured magnesium oxide. II. Transient features in circular polarisation and optically detected magnetic resonance". In: *Journal of Physics C: Solid State Physics* 15 (7 Mar. 1982), pp. 1569–1580. DOI: 10.1088/0022-3719/15/7/022.

[46] P Edel et al. "Photoluminescence properties of additively coloured MgO. I. Effects of uniaxial stress and ODMR". In: *Journal of Physics C: Solid State Physics* 12 (23 Dec. 1979), pp. 5245–5253. DOI: 10.1088/0022-3719/12/23/028.

[47] P. Edel. "Colouir centres in oxides. Origin of the luminescence excited in the F absorption band in MgO". en. In: *Le Journal de Physique Colloques* 41 (C6 July 1980), pp. C6–531–C6–532. ISSN: 0449-1947. DOI: 10.1051/jphyscol:19806139.

[48] P. Edel, Y. Merle D'Aubigné, and R. Louat. "Couplage Jahn-Teller dans le niveau excite des centres F dans CaO: Effet des contraintes uniaxiales". fr. In: *Journal of Physics and Chemistry of Solids* 35 (1 Jan. 1974), pp. 67–70. DOI: 10.1016/0022-3697(74)90012-2.

[49] Paul S. Epstein. "The Stark Effect from the Point of View of Schroedinger's Quantum Theory". en. In: *Physical Review* 28 (4 Oct. 1926), pp. 695–710. DOI: 10.1103/physrev.28.695.

[50] Elif Ertekin, Lucas K. Wagner, and Jeffrey C. Grossman. "Point-defect optical transitions and thermal ionization energies from quantum Monte Carlo methods: Application to theF-center defect in MgO". en. In: *Physical Review B* 87 (15 Apr. 2013). DOI: 10.1103/physrevb.87.155210.

[51] E. Fermi. "Eine statistische Methode zur Bestimmung einiger Eigenschaften des Atoms und ihre Anwendung auf die Theorie des periodischen Systems der Elemente". In: *Zeitschrift fuer Physik* 48 (1-2 Jan. 1928), pp. 73–79. DOI: 10.1007/BF01351576.

[52] Reinhold F. Fink. "Why does MP2 work?" en. In: *The Journal of Chemical Physics* 145 (18 Nov. 2016), p. 184101. DOI: 10.1063/1.4966689.

[53] V. Fock. "Näherungsmethode zur Lösung des quantenmechanischen Mehrkörperproblems". de. In: *Zeitschrift für Physik* 61 (1-2 Jan. 1930), pp. 126–148. DOI: 10.1007/bf01340294.

[54] V.A. Fok. "Проблема многих тел в квантовой механике". ru. In: *Uspekhi Fizicheskih Nauk* 16 (7 1936), pp. 943–954. DOI: 10.3367/ufnr.0016.193607g.0943.

[55] J. Franck and E. G. Dymond. "Elementary processes of photochemical reactions". en. In: *Transactions of the Faraday Society* 21 (February 1926), p. 536. DOI: 10.1039/tf9262100536.

[56] David L. Freeman. "Coupled-cluster expansion applied to the electron gas: Inclusion of ring and exchange effects". en. In: *Physical Review B* 15 (12 June 1977), pp. 5512–5521. DOI: 10.1103/physrevb.15.5512.

[57] David L. Freemen. "Many-body perturbation theory applied to molecules: Analysis and correlation energy calculation for Li2, N2, and H3". en. In: *The Journal of Chemical Physics* 64 (6 1976), p. 2641. DOI: 10.1063/1.432518.

[58] J. Friedel. "Structure des centres colorés". In: *Le Journal de Physique Colloques* 28 (C4 Aug. 1967), pp. C4–3–C4–9. DOI: 10.1051/jphyscol:1967401.

[59] Alejandro Gallo et al. "A periodic equation-of-motion coupled-cluster implementation applied to F-centers in alkaline earth oxides". en. In: *The Journal of Chemical Physics* 154 (6 Feb. 2021), p. 064106. DOI: 10.1063/5.0035425.

[60] Yang Gao et al. "Electronic structure of bulk manganese oxide and nickel oxide from coupled cluster theory". en. In: *Physical Review B* 101 (16 Apr. 2020). DOI: 10.1103/physrevb.101.165138.

[61] Michel Gaudin. "Une démonstration simplifiée du théorème de wick en mécanique statistique". In: *Nuclear Physics* 15 (1960), pp. 89–91. DOI: 10.1016/0029-5582(60)90285-6.

[62] J. Goldstone. "Derivation of the Brueckner many-body theory". en. In: *Proceedings of the Royal Society of London. Series A. Mathematical and Physical Sciences* 239 (1217 Feb. 1957), pp. 267–279. DOI: 10.1098/rspa.1957.0037.

[63] Dorothea Golze, Marc Dvorak, and Patrick Rinke. "The GW Compendium: A Practical Guide to Theoretical Photoemission Spectroscopy". In: *Frontiers in Chemistry* 7 (July 2019). DOI: 10.3389/fchem.2019.00377.

[64] R. Gonzalez, Y. Chen, and K. L. Tsang. "Diffusion of deuterium and hydrogen in doped and undoped MgO crystals". en. In: *Physical Review B* 26 (8 Oct. 1982), pp. 4637–4645. DOI: 10.1103/physrevb.26.4637.

[65] Stefan Grimme and Mirko Waletzke. "A combination of Kohn–Sham density functional theory and multi-reference configuration interaction methods". In: *The Journal of Chemical Physics* 111 (13 Oct. 1999), pp. 5645–5655. DOI: 10.1063/1.479866.

[66] Thomas Gruber et al. "Applying the Coupled-Cluster Ansatz to Solids and Surfaces in the Thermodynamic Limit". In: *Physical Review X* 8 (2 2018). DOI: 10.1103/PhysRevX.8.021043.

[67] Manuel Grumet et al. "Beyond the quasiparticle approximation: Fully self-consistent GW calculations". en. In: *Physical Review B* 98 (15 Oct. 2018). DOI: 10.1103/physrevb.98.155143.

[68] Andreas Grüneis, Martijn Marsman, and Georg Kresse. "Second-order Møller–Plesset perturbation theory applied to extended systems. II. Structural and energetic properties". en. In: *The Journal of Chemical Physics* 133 (7 Aug. 2010), p. 074107. DOI: 10.1063/1.3466765.

[69] Andreas Grüneis et al. "Making the random phase approximation to electronic correlation accurate". In: *The Journal of Chemical Physics* 131 (15 2009). DOI: 10.1063/1.3250347.

[70] L.E. Halliburton, D.L. Cowan, and L.V. Holroyd. "Lattice distortion around the F+ center in MgO". en. In: *Solid State Communications* 12 (5 Mar. 1973), pp. 393–396. DOI: 10.1016/0038-1098(73)90780-1.

[71] Hartree. "An investigation into the existence of zero-point energy in the Rock-Salt Lattice by an X-Ray Diffraction Method". en. In: *Proceedings of the Royal Society of London. Series A, Containing Papers of a Mathematical and Physical Character* 118 (779 Mar. 1928), pp. 334–350. DOI: 10.1098/rspa.1928.0055.

[72] D. R. Hartree. "The Wave Mechanics of an Atom with a Non-Coulomb Central Field. Part II. Some Results and Discussion". en. In: *Mathematical Proceedings of the Cambridge Philosophical Society* 24 (1 Jan. 1928), pp. 111–132. DOI: 10.1017/s0305004100011920.

[73] J. Hata. "A note on exclusion-principle-violating diagrams". In: *Chemical Physics Letters* 13 (4 1972), pp. 361–364. DOI: 10.1016/0009-2614(72)80100-3.

[74] Christof Hättig. "Optimization of auxiliary basis sets for RI-MP2 and RI-CC2 calculations: Core–valence and quintuple-ζ basis sets for H to Ar and QZVPP basis sets for Li to Kr". In: *Phys. Chem. Chem. Phys.* 7 (1 2005), pp. 59–66. DOI: 10.1039/B415208E.

[75] Christof Hättig, David P. Tew, and Andreas Köhn. "Communications: Accurate and efficient approximations to explicitly correlated coupled-cluster singles and doubles, CCSD-F12". en. In: *J. Chem. Phys.* 132 (23 June 2010), p. 231102. DOI: 10.1063/1.3442368.

[76] Lars Hedin. "New Method for Calculating the One-Particle Green's Function with Application to the Electron-Gas Problem". In: *Physical Review* 139 (3A 1965), A796–A823. DOI: 10.1103/PhysRev.139.A796.

[77] Volker Heine. "The pseudopotential concept". In: (1970). DOI: 10.1016/S0081-1947(08)60069-7.

[78] Trygve Helgaker, Poul Jørgensen, and Jeppe Olsen. *Molecular Electronic-Structure Theory*. John Wiley & Sons, Ltd, Aug. 2000. ISBN: 9781119019572. DOI: 10.1002/9781119019572.

[79] B Henderson, R D King, and A M Stoneham. "The temperature dependence of the F band in magnesium oxide". In: *Journal of Physics C: Solid State Physics* 1 (3 June 1968), pp. 586–593. DOI: 10.1088/0022-3719/1/3/305.

[80] Brian Henderson. "Anion vacancy centers in alkaline earth oxides". en. In: *Critical Reviews in Solid State and Materials Sciences* 9 (1 Aug. 1980), pp. 1–60. DOI: 10.1080/10408438008243569.

[81] Thomas M. Henderson and Gustavo E. Scuseria. "The connection between self-interaction and static correlation: a random phase approximation perspective". en. In: *Molecular Physics* 108.19-20 (19-20 Oct. 2010), pp. 2511–2517. DOI: 10.1080/00268976.2010.507227.

[82] K. Hirao and H. Nakatsuji. "A generalization of the Davidson's method to large nonsymmetric eigenvalue problems". In: *Journal of Computational Physics* 45 (2 Feb. 1982), pp. 246–254. DOI: 10.1016/0021-9991(82)90119-X.

[83] So Hirata. "Tensor Contraction Engine: Abstraction and Automated Parallel Implementation of Configuration-Interaction, Coupled-Cluster, and Many-Body Perturbation Theories". en. In: *The Journal of Physical Chemistry A* 107 (46 Nov. 2003), pp. 9887–9897. DOI: 10.1021/jp034596z.

[84] M. Hoffmann-Ostenhof, T. Hoffmann-Ostenof, and H. Stremnitzer. "Electronic wave functions near coalescence points". In: *Physical Review Letters* 68 (26 June 1992), pp. 3857–3860. DOI: 10.1103/PhysRevLett.68.3857.

[85] P. Hohenberg and W. Kohn. "Inhomogeneous Electron Gas". In: *Physical Review* 136 (3B Nov. 1964), B864–B871. DOI: 10.1103/PhysRev.136.B864.

[86] Felix Hummel, Theodoros Tsatsoulis, and Andreas Grüneis. "Low rank factorization of the Coulomb integrals for periodic coupled cluster theory". en. In: *The Journal of Chemical Physics* 146 (12 Mar. 2017), p. 124105. DOI: 10.1063/1.4977994.

[87] Andreas Irmler, Alejandro Gallo, and Andreas Grüneis. "Focal-point approach with pair-specific cusp correction for coupled-cluster theory". en. In: *The Journal of Chemical Physics* 154 (23 June 17, 2021), p. 234103. ISSN: 0021-9606. DOI: 10.1063/5.0050054.

[88] Andreas Irmler and Andreas Grüneis. "Particle-particle ladder based basis-set corrections applied to atoms and molecules using coupled-cluster theory". en. In: *J. Chem. Phys.* 151 (10 Sept. 2019), p. 104107. DOI: 10.1063/1.5110885.

[89] Andreas Irmler et al. “Duality of Ring and Ladder Diagrams and Its Importance for Many-Electron Perturbation Theories”. en. In: *Physical Review Letters* 123 (15 Oct. 2019). DOI: 10.1103/physrevlett.123.156401.

[90] Andreas Irmler et al. “Duality of Ring and Ladder Diagrams and Its Importance for Many-Electron Perturbation Theories”. en. In: *Phys. Rev. Lett.* 123 (Oct. 2019).

[91] Maxim V. Ivanov, Felix H. Bangerter, and Anna I. Krylov. “Towards a rational design of laser-coolable molecules: insights from equation-of-motion coupled-cluster calculations”. en. In: *Physical Chemistry Chemical Physics* 21 (35 2019), pp. 19447–19457. DOI: 10.1039/c9cp03914g.

[92] Peter J. Knowles. “Perturbation-adapted perturbation theory”. en. In: *The Journal of Chemical Physics* 156 (1 Jan. 3, 2022), p. 011101. ISSN: 0021-9606. DOI: 10.1063/5.0079853.

[93] B. T. Jeffries et al. “Luminescence in thermochemically reduced MgO: The role of hydrogen”. en. In: *Physical Review B* 25 (3 Feb. 1982), pp. 2077–2080. DOI: 10.1103/physrevb.25.2077.

[94] Lawrence A. Kappers and Eugene B. Hensley. “$F^+ \leftrightarrow F$ Center Conversions in Magnesium Oxide”. en. In: *Physical Review B* 6 (6 Sept. 1972), pp. 2475–2477. DOI: 10.1103/physrevb.6.2475.

[95] Hideki Katagiri. “Equation-of-motion coupled-cluster study on exciton states of polyethylene with periodic boundary condition”. In: *The Journal of Chemical Physics* 122.22 (2005), p. 224901. DOI: 10.1063/1.1929731.

[96] Tosio Kato. “Fundamental properties of Hamiltonian operators of Schrödinger type”. In: *Transactions of the American Mathematical Society* 70 (2 Feb. 1951), pp. 195–195. DOI: 10.1090/S0002-9947-1951-0041010-X.

[97] Tosio Kato. “On the eigenfunctions of many-particle systems in quantum mechanics”. In: *Communications on Pure and Applied Mathematics* 10 (2 1957), pp. 151–177. DOI: 10.1002/cpa.3160100201.

[98] Daniel Kats and Frederick R. Manby. “Communication: The distinguishable cluster approximation”. en. In: *The Journal of Chemical Physics* 139.2 (2 July 2013), p. 021102. DOI: 10.1063/1.4813481.

[99] James C. Kemp and Victor I. Neeley. “Wave Functions forFCenters in MgO”. en. In: *Physical Review* 132 (1 Oct. 1963), pp. 215–223. DOI: 10.1103/physrev.132.215.

[100] Rick A. Kendall, Thom H. Dunning, and Robert J. Harrison. “Electron affinities of the first-row atoms revisited. Systematic basis sets and wave functions”. en. In: *J. Chem. Phys.* 96 (9 May 1992), pp. 6796–6806. DOI: 10.1063/1.462569.

[101] Wim Klopper et al. “Multiple basis sets in calculations of triples corrections in coupled-cluster theory”. In: *Theor. Chem. Acc.* 97 (1997), pp. 1432–2234. DOI: 10.1007/s002140050250.

[102] Gerald Knizia, Thomas B. Adler, and Hans-Joachim Werner. “Simplified CCSD(T)-F12 methods: Theory and benchmarks”. In: *J. Chem. Phys.* 130 (2009), p. 054104. DOI: 10.1063/1.3054300.

[103] W. Kohn and L. J. Sham. “Quantum Density Oscillations in an Inhomogeneous Electron Gas”. In: *Physical Review* 137 (6A Mar. 1965), A1697–A1705. DOI: 10.1103/PhysRev.137.A1697.

[104] W. Kohn and L. J. Sham. “Self-Consistent Equations Including Exchange and Correlation Effects”. In: *Physical Review* 140 (4A Nov. 1965), A1133–A1138. DOI: 10.1103/PhysRev.140.A1133.

[105] Walter Kohn and C. David Sherrill. “Editorial: Reflections on fifty years of density functional theory”. en. In: *The Journal of Chemical Physics* 140 (18 May 2014), 18A201. DOI: 10.1063/1.4870815.

[106] Liguo Kong, Florian A. Bischoff, and Edward F. Valeev. “Explicitly Correlated R12/F12 Methods for Electronic Structure”. EN. In: *Chemical Reviews* 112.1 (1 Jan. 2012), pp. 75–107. DOI: 10.1021/cr200204r.

[107] Liguo Kong, Florian A. Bischoff, and Edward F. Valeev. "Explicitly Correlated R12/F12 Methods for Electronic Structure". In: *Chem. Rev.* 112.1 (2012), pp. 75–107. DOI: 10.1021/cr200204r.

[108] Karol Kowalski and Marat Valiev. "Asymptotic Extrapolation Scheme for Large-Scale Calculations with Hybrid Coupled Cluster and Molecular Dynamics Simulations". en. In: *The Journal of Physical Chemistry A* 110 (48 Dec. 2006), pp. 13106–13111. DOI: 10.1021/jp064266p.

[109] G. Kresse and J. Furthmüller. "Efficiency of ab-initio total energy calculations for metals and semiconductors using a plane-wave basis set". In: *Computational Materials Science* 6 (1 July 1996), pp. 15–50. DOI: 10.1016/0927-0256(96)00008-0.

[110] G. Kresse and D. Joubert. "From ultrasoft pseudopotentials to the projector augmented-wave method". In: *Physical Review B* 59 (3 1999), pp. 1758–1775. DOI: 10.1103/PhysRevB.59.1758.

[111] R. Krishnan and J. A. Pople. "Approximate fourth-order perturbation theory of the electron correlation energy". en. In: *International Journal of Quantum Chemistry* 14 (1 July 1978), pp. 91–100. DOI: 10.1002/qua.560140109.

[112] Hermann G. Kümmel. "A biography of the coupled cluster method". en. In: *Recent Progress in Many-Body Theories*. World Scientific, Dec. 2001, pp. 334–348. DOI: 10.1142/9789812777843_0040.

[113] Werner Kutzelnigg. "How many-body perturbation theory (MBPT) has changed quantum chemistry". en. In: *International Journal of Quantum Chemistry* 109 (15 2009), pp. 3858–3884. DOI: 10.1002/qua.22384.

[114] Werner Kutzelnigg. "r 12-Dependent terms in the wave function as closed sums of partial wave amplitudes for large l". en. In: *Theor. Chim. Acta* 68 (6 Dec. 1985), p. 445. DOI: 10.1007/bf00527669.

[115] Werner Kutzelnigg and Wim Klopper. "Wave functions with terms linear in the interelectronic coordinates to take care of the correlation cusp. I. General theory". In: *The Journal of Chemical Physics* 94 (3 Feb. 1991), pp. 1985–2001. DOI: 10.1063/1.459921.

[116] Simen Kvaal. "Variational formulations of the coupled-cluster method in quantum chemistry". In: *Molecular Physics* 111 (9-11 May 2013), pp. 1100–1108. DOI: 10.1080/00268976.2013.812254.

[117] Yoon S. Lee, Stanislaw A. Kucharski, and Rodney J. Bartlett. "A coupled cluster approach with triple excitations". en. In: *The Journal of Chemical Physics* 81 (12 Dec. 1984), pp. 5906–5912. DOI: 10.1063/1.447591.

[118] M. Levy. "Universal variational functionals of electron densities, first-order density matrices, and natural spin-orbitals and solution of the v-representability problem". In: *Proceedings of the National Academy of Sciences* 76 (12 Dec. 1979), pp. 6062–6065. DOI: 10.1073/pnas.76.12.6062.

[119] Mel Levy. "Electron densities in search of Hamiltonians". In: *Physical Review A* 26 (3 Sept. 1982), pp. 1200–1208. DOI: 10.1103/PhysRevA.26.1200.

[120] H. W. Lewis. "Fermi-Thomas Model with Correlations". In: *Physical Review* 111 (6 Sept. 1958), pp. 1554–1557. DOI: 10.1103/PhysRev.111.1554.

[121] Ke Liao and Andreas Grüneis. "Communication: Finite size correction in periodic coupled cluster theory calculations of solids". In: *J. Chem. Phys.* 145.14 (Oct. 2016), p. 141102. ISSN: 0021-9606. DOI: 10.1063/1.4964307.

[122] Ingvar Lindgren. "A coupled-cluster approach to the many-body perturbation theory for open-shell systems". en. In: *International Journal of Quantum Chemistry* 14 (S12 1978), pp. 33–58. DOI: 10.1002/qua.560140804.

[123] Yuchen Ma, Michael Rohlfing, and Adam Gali. "Excited states of the negatively charged nitrogen-vacancy color center in diamond". en. In: *Physical Review B* 81 (4 Jan. 2010). DOI: 10.1103/physrevb.81.041204.

[124] W. Macke. "Über die Wechselwirkungen im Fermi-Gas, Polarisationserscheinungen, Correlationsenergie, Elektronenkondensation". In: *Z. Naturforsch.* 5a (8 1950), pp. 192–208. DOI: 10.1515/zna-1950-0402.

[125] Richard M. Martin. *Electronic Structure: Basic Theory and Practical Methods*. Cambridge University Press, 2004. ISBN: 9780521782852.

[126] Devin A. Matthews. "Diagrams in coupled-cluster theory: Algebraic derivation of a new diagrammatic method for closed shells". In: 2019. ISBN: 9780128136515. DOI: 10.1016/B978-0-12-813651-5.00010-3.

[127] James McClain et al. "Gaussian-based coupled-cluster theory for the ground state and band structure of solids". In: *Journal of Chemical Theory and Computation* 13 (3 Jan. 2017), pp. 1209–1218. DOI: 10.1021/acs.jctc.7b00049.

[128] James McClain et al. "Spectral functions of the uniform electron gas via coupled-cluster theory and comparison to the GW and related approximations". en. In: *Physical Review B* 93 (23 June 2016), p. 235139. DOI: 10.1103/physrevb.93.235139.

[129] Chr. Møller and M. S. Plesset. "Note on an Approximation Treatment for Many-Electron Systems". en. In: *Physical Review* 46 (7 1934), pp. 618–622. DOI: 10.1103/physrev.46.618.

[130] Paula Mori-Sánchez and Aron J. Cohen. "Exact Density Functional Obtained via the Levy Constrained Search". en. In: *The Journal of Physical Chemistry Letters* 9 (17 Sept. 2018), pp. 4910–4914. DOI: 10.1021/acs.jpclett.8b02332.

[131] Debashis Mukherjee. "Normal ordering and a Wick-like reduction theorem for fermions with respect to a multi-determinantal reference state". In: *Chemical Physics Letters* 274 (5-6 1997), pp. 561–566. DOI: 10.1016/S0009-2614(97)00714-8.

[132] R. K. Nesbet. "Configuration interaction in orbital theories". en. In: *Proceedings of the Royal Society of London. Series A. Mathematical and Physical Sciences* 230 (1182 June 1955), pp. 312–321. DOI: 10.1098/rspa.1955.0134.

[133] Marcel Nooijen, K. R. Shamasundar, and Debashis Mukherjee. "Reflections on size-extensivity, size-consistency and generalized extensivity in many-body theory". en. In: *Molecular Physics* 103 (15-16 Aug. 2005), pp. 2277–2298. DOI: 10.1080/00268970500083952.

[134] J. Paldus and J. Čížek. "Time-Independent Diagrammatic Approach to Perturbation Theory of Fermion Systems". In: Elsevier, 1975, pp. 105–197. DOI: 10.1016/s0065-3276(08)60040-4.

[135] Robert M. Parrish et al. “Psi4 1.1: An Open-Source Electronic Structure Program Emphasizing Automation, Advanced Libraries, and Interoperability”. In: *J. Chem. Theory Comput.* 13.7 (2017), pp. 3185–3197. DOI: 10.1021/acs.jctc.7b00174.

[136] M. Petersilka, U. J. Gossmann, and E. K. U. Gross. “Excitation Energies from Time-Dependent Density-Functional Theory”. en. In: *Physical Review Letters* 76 (8 Feb. 1996), pp. 1212–1215. DOI: 10.1103/physrevlett.76.1212.

[137] Piotr Piecuch et al. “Communication: Existence of the doubly excited state that mediates the photoionization of azulene”. In: *The Journal of Chemical Physics* 138.20 (2013), p. 201102. DOI: 10.1063/1.4808014.

[138] Piotr Piecuch et al. “Efficient computer implementation of the renormalized coupled-cluster methods: The R-CCSD[T], R-CCSD(T), CR-CCSD[T], and CR-CCSD(T) approaches”. en. In: *Computer Physics Communications* 149 (2 Dec. 2002), pp. 71–96. DOI: 10.1016/s0010-4655(02)00598-2.

[139] David Pines and David Bohm. “A Collective Description of Electron Interactions: II. Collective”. In: *Physical Review* 85 (2 1952), pp. 338–353. DOI: 10.1103/PhysRev.85.338.

[140] John A. Pople, Martin Head-Gordon, and Krishnan Raghavachari. “Quadratic configuration interaction. A general technique for determining electron correlation energies”. In: *The Journal of Chemical Physics* 87 (10 1987), pp. 5968–5975. DOI: 10.1063/1.453520.

[141] Artem Pulkin and Garnet Kin-Lic Chan. “First-principles coupled cluster theory of the electronic spectrum of transition metal dichalcogenides”. en. In: *Physical Review B* 101 (24 June 2020). DOI: 10.1103/physrevb.101.241113.

[142] O. Gunnarsson R. O. Jones. “The density functional formalism, its applications and prospects”. In: *Reviews of Modern Physics* 61 (3 1989), pp. 689–746. DOI: 10.1103/RevModPhys.61.689.

[143] Krishnan Raghavachari. “An augmented coupled cluster method and its application to the first-row homonuclear diatomics”. en. In: *The Journal of Chemical Physics* 82 (10 May 1985), pp. 4607–4610. DOI: 10.1063/1.448718.

[144] Krishnan Raghavachari et al. “A fifth-order perturbation comparison of electron correlation theories”. en. In: *Chemical Physics Letters* 157 (6 1989), pp. 479–483. DOI: 10.1016/s0009-2614(89)87395-6.

[145] Jan Řezáč and Pavel Hobza. “Describing Noncovalent Interactions beyond the Common Approximations: How Accurate Is the “Gold Standard,” CCSD(T) at the Complete Basis Set Limit?” en. In: *Journal of Chemical Theory and Computation* 9 (5 May 2013), pp. 2151–2155. DOI: 10.1021/ct400057w.

[146] Patrick Rinke et al. “First-Principles Optical Spectra forFCenters in MgO”. en. In: *Physical Review Letters* 108 (12 Mar. 2012). DOI: 10.1103/physrevlett.108.126404.

[147] James B. Robinson and Peter J. Knowles. “Quasi-variational coupled cluster theory”. In: *The Journal of Chemical Physics* 136 (5 2012). DOI: 10.1063/1.3680560.

[148] Michael Rohlfing and Steven G. Louie. “Electron-hole excitations and optical spectra from first principles”. en. In: *Physical Review B* 62 (8 2000), pp. 4927–4944. DOI: 10.1103/physrevb.62.4927.

[149] G. H. Rosenblatt et al. “Luminescence of F and F^+ centers in magnesium oxide”. en. In: *Physical Review B* 39 (14 May 1989), pp. 10309–10318. DOI: 10.1103/physrevb.39.10309.

[150] P. J. Rossky and Martin Karplus. “The enumeration of Goldstone diagrams in many-body perturbation theory”. en. In: *The Journal of Chemical Physics* 64 (4 Feb. 1976), pp. 1596–1603. DOI: 10.1063/1.432387.

[151] D. J. Rowe. “Equations-of-Motion Method and the Extended Shell Model”. In: *Reviews of Modern Physics* 40 (1 1968), pp. 153–166. DOI: 10.1103/RevModPhys.40.153.

[152] D.J. Rowe. “An interpretation of time-dependent Hartree-Fock theory”. In: *Nuclear Physics* 80 (1 1966), pp. 209–222. DOI: 10.1016/0029-5582(66)90837-6.

[153] Erich Runge and E. K. U. Gross. "Density-Functional Theory for Time-Dependent Systems". en. In: *Physical Review Letters* 52 (12 Mar. 1984), pp. 997–1000. DOI: 10.1103/physrevlett.52.997.

[154] E. E. Salpeter and H. A. Bethe. "A Relativistic Equation for Bound-State Problems". en. In: *Physical Review* 84 (6 Dec. 1951), pp. 1232–1242. DOI: 10.1103/physrev.84.1232.

[155] Tobias Schäfer, Benjamin Ramberger, and Georg Kresse. "Laplace transformed MP2 for three dimensional periodic materials using stochastic orbitals in the plane wave basis and correlated sampling". In: *The Journal of Chemical Physics* 148 (6 Feb. 2018). DOI: 10.1063/1.5016100.

[156] Tobias Schäfer, Benjamin Ramberger, and Georg Kresse. "Quartic scaling MP2 for solids: A highly parallelized algorithm in the plane wave basis". en. In: *The Journal of Chemical Physics* 146 (10 Mar. 2017), p. 104101. DOI: 10.1063/1.4976937.

[157] E. Schrödinger. "Quantisierung als Eigenwertproblem". de. In: *Annalen der Physik* 385 (13 1926), pp. 437–490. DOI: 10.1002/andp.19263851302.

[158] Martin Schütz, Georg Hetzer, and Hans-Joachim Werner. "Low-order scaling local electron correlation methods. I. Linear scaling local MP2". In: *J. Chem. Phys.* 111.13 (1999), pp. 5691–5705. DOI: 10.1063/1.479957.

[159] Peter Schwerdtfeger. "The Pseudopotential Approximation in Electronic Structure Theory". en. In: *ChemPhysChem* 12 (17 Dec. 2011), pp. 3143–3155. DOI: 10.1002/cphc.201100387.

[160] Gustavo E. Scuseria and Timothy J. Lee. "Comparison of coupled-cluster methods which include the effects of connected triple excitations". en. In: *The Journal of Chemical Physics* 93 (8 Oct. 1990), pp. 5851–5855. DOI: 10.1063/1.459684.

[161] Michiel J. van Setten et al. "GW100: Benchmarking G0W0 for Molecular Systems". en. In: *Journal of Chemical Theory and Computation* 11 (12 Dec. 2015), pp. 5665–5687. DOI: 10.1021/acs.jctc.5b00453.

[162] Isaiah Shavitt and Rodney J. Bartlett. *Many – Body Methods in Chemistry and Physics*. Cambridge University Press, 2009. ISBN: ['9780511596834']. DOI: 10.1017/cbo9780511596834.

[163] James J. Shepherd, Thomas M. Henderson, and Gustavo E. Scuseria. "Coupled cluster channels in the homogeneous electron gas". In: *J. Chem. Phys.* 140.12 (2014), p. 124102. DOI: 10.1063/1.4867783.

[164] Edgar Solomonik et al. *A Massively Parallel Tensor Contraction Framework for Coupled-Cluster Computations*. 12. Aug. 2014, pp. 3176–3190. DOI: 10.21236/ada614387.

[165] Carlos Sosa et al. "Selection of the reduced virtual space for correlated calculations. An application to the energy and dipole moment of H2O". en. In: *Chem. Phys. Lett.* 159 (2-3 July 1989), pp. 148–154. DOI: 10.1016/0009-2614(89)87399-3.

[166] Carmen Sousa and Francesc Illas. "On the accurate prediction of the optical absorption energy of F-centers in MgO from explicitly correlated ab initio cluster model calculations". en. In: *The Journal of Chemical Physics* 115 (3 July 2001), pp. 1435–1439. DOI: 10.1063/1.1381011.

[167] John F. Stanton. "Why CCSD(T) works: a different perspective". en. In: *Chemical Physics Letters* 281 (1-3 Dec. 1997), pp. 130–134. DOI: 10.1016/s0009-2614(97)01144-5.

[168] John F. Stanton and Rodney J. Bartlett. "The equation of motion coupled-cluster method. A systematic biorthogonal approach to molecular excitation energies, transition probabilities, and excited state properties". en. In: *The Journal of Chemical Physics* 98 (9 May 1993), pp. 7029–7039. DOI: 10.1063/1.464746.

[169] John F. Stanton and Jürgen Gauss. "Theoretical study of electronically excited cis- and trans-glyoxal". en. In: *Spectrochimica Acta Part A: Molecular and Biomolecular Spectroscopy* 53 (8 July 1997), pp. 1153–1162. DOI: 10.1016/s1386-1425(96)01866-5.

[170] John F. Stanton et al. "A direct product decomposition approach for symmetry exploitation in many-body methods. I. Energy calculations". en. In: *The Journal of Chemical Physics* 94 (6 Mar. 1991), pp. 4334–4345. DOI: 10.1063/1.460620.

[171] A. M. Stoneham. "The theory of defects in solids". en. In: *Contemporary Physics* 20 (5 Sept. 1979), pp. 535–545. DOI: 10.1080/00107517908210920.

[172] G. P. Summers et al. "Luminescence from oxygen vacancies in MgO crystals thermochemically reduced at high temperatures". en. In: *Physical Review B* 27 (2 Jan. 1983), pp. 1283–1291. DOI: 10.1103/physrevb.27.1283.

[173] Attila Szabo and Neil S. Ostlund. *Modern quantum chemistry: introduction to advanced electronic structure theory*. Courier Corporation, 2012.

[174] Andrew G. Taube and Rodney J. Bartlett. "Frozen Natural Orbitals: Systematic Basis Set Truncation for Coupled-Cluster Theory". In: *Collect. Czech. Chem. Commun.* 70 (2005), pp. 837–850. DOI: 10.1135/cccc20050837.

[175] Seiichiro Ten-no and Jozef Noga. "Explicitly correlated electronic structure theory from R12/F12 ansatze". In: *WIREs Comput. Mol. Sci.* 2.1 (2012), pp. 114–125. DOI: 10.1002/wcms.68.

[176] David P. Tew and Wim Klopper. "Open-shell explicitly correlated F12 methods". In: *Molecular Physics* 108 (3-4 2010), pp. 315–325. DOI: 10.1080/00268970903449388.

[177] L. H. Thomas. "The calculation of atomic fields". In: *Mathematical Proceedings of the Cambridge Philosophical Society* 23 (05 Jan. 1927). DOI: 10.1017/S0305004100011683.

[178] Mihm Tina N. et al. "A shortcut to the thermodynamic limit for quantum many-body calculations of metals". En. In: *Nature Computational Science* 1 (12 Dec. 16, 2021). ISSN: 2662-8457. DOI: 10.1038/s43588-021-00165-1.

[179] Paul Tiwald et al. "Ab initio perspective on the Mollwo-Ivey relation for F centers in alkali halides". In: *Physical Review B* 92 (14 Oct. 2015). DOI: 10.1103/PhysRevB.92.144107.

[180] Sergio Tosoni et al. “Prediction of optical properties ofFcenters in oxides from quasi-particle excitations”. en. In: *Physical Review B* 85 (11 Mar. 2012). DOI: 10.1103/physrevb.85.115114.

[181] *TURBOMOLE V7.5 2020, a development of University of Karlsruhe and Forschungszentrum Karlsruhe GmbH, 1989-2007, TURBOMOLE GmbH, since 2007; available from* https://www.turbomole.org. https://www.turbomole.org. 2007.

[182] Wesley P. Unruh and J. W. Culvahouse. “Electron-Nuclear Double Resonance of-FCenters in MgO”. en. In: *Physical Review* 154 (3 Feb. 1967), pp. 861–866. DOI: 10.1103/physrev.154.861.

[183] Miroslav Urban et al. “Towards a full CCSDT model for electron correlation”. en. In: *The Journal of Chemical Physics* 83 (8 Oct. 1985), pp. 4041–4046. DOI: 10.1063/1.449067.

[184] John M. Vail. “Theory of electronic defects: Applications to MgO and alkali halides”. en. In: *Journal of Physics and Chemistry of Solids* 51 (7 Jan. 1990), pp. 589–607. DOI: 10.1016/0022-3697(90)90139-7.

[185] E. F. Valeev. *Libint: A library for the evaluation of molecular integrals of many-body operators over Gaussian functions*. http://libint.valeyev.net/. 2020.

[186] M. Valiev et al. “NWChem: A comprehensive and scalable open-source solution for large scale molecular simulations”. In: *Comput. Phys. Commun.* 181.9 (2010), pp. 1477–1489. ISSN: 0010-4655. DOI: https://doi.org/10.1016/j.cpc.2010.04.018.

[187] Marta L. Vidal et al. “New and Efficient Equation-of-Motion Coupled-Cluster Framework for Core-Excited and Core-Ionized States”. en. In: *Journal of Chemical Theory and Computation* 15.5 (5 May 2019), pp. 3117–3133. DOI: 10.1021/acs.jctc.9b00039.

[188] Xiao Wang and Timothy C. Berkelbach. “Excitons in Solids from Periodic Equation-of-Motion Coupled-Cluster Theory”. en. In: *Journal of Chemical Theory and Computation* 16 (5 May 2020), pp. 3095–3103. DOI: 10.1021/acs.jctc.0c00101.

[189] Steven Weinberg. “The Quantum Theory of Fields, Volume 1 - Foundations”. In: (2005).

[190] John E. Wertz et al. “Electron Spin Resonance ofFCenters in Magnesium Oxide; Confirmation of the Spin of Magnesium-25”. en. In: *Physical Review* 107 (6 Sept. 1957), pp. 1535–1537. DOI: 10.1103/physrev.107.1535.

[191] G. C. Wick. “The Evaluation of the Collision Matrix”. In: *Physical Review* 80 (2 1950), pp. 268–272. DOI: 10.1103/PhysRev.80.268.

[192] Angela K. Wilson and Jan Almlöf. “Møller-Plesset correlation energies in a localized orbital basis using a Laplace transform technique”. en. In: *Theoretica Chimica Acta* 95 (1-2 Jan. 1997), pp. 49–62. DOI: 10.1007/bf02329241.

[193] T. M. Wilson and R. F. Wood. “Electronic structure of the F center in the alkaline earth oxides”. In: *Le Journal de Physique Colloques* 37 (C7 Dec. 1976), pp. C7–190–C7–196. DOI: 10.1051/jphyscol:1976743.

[194] T. M. Wilson and R. F. Wood. “Electronic structure of theFcenter in SrO”. en. In: *Physical Review B* 16 (10 Nov. 1977), pp. 4594–4598. DOI: 10.1103/physrevb.16.4594.

[195] R.F. Wood and T.M. Wilson. “Electronic structure of the F-center in CaO and MgO”. en. In: *Solid State Communications* 16 (5 Mar. 1975), pp. 545–548. DOI: 10.1016/0038-1098(75)90420-2.

[196] Robert Yaris. “Linked-Cluster Theorem and Unitarity”. en. In: *The Journal of Chemical Physics* 41 (8 Oct. 1964), pp. 2419–2421. DOI: 10.1063/1.1726280.

[197] Robert Yaris. “Time-Dependent Perturbation—Variation Method”. en. In: *The Journal of Chemical Physics* 39 (10 Nov. 1963), pp. 2474–2477. DOI: 10.1063/1.1734050.